Journal of Pyrotechnics

Issue 19, Summer 2004

Direct Editorial Concerns and Subscription Requests to:

Journal of Pyrotechnics, Inc.
Bonnie Kosanke, Publisher
1775 Blair Road
Whitewater, CO 81527, USA
(970) 245-0692 (Voice and FAX)
email: bonnie@jpyro.com

CAUTION

The experimentation with, and the use of, pyrotechnic materials can be dangerous; it is felt to be important for the reader to be duly cautioned. Without the required training and experience no one should ever experiment with or use pyrotechnic materials. Also, the amount of information presented in this Journal is not a substitute for necessary training and experience.

A major effort has been undertaken to review all articles for correctness. However, it is possible that errors remain. It is the responsibility of the reader to verify any information herein before applying that information in situations where death, injury, or property damage could result.

Table of Contents

Issue 19 Summer 2004

If you want to receive titles and/or abstracts for future issues by email, send a note to bonnie@jpyro.com. You will then receive this information about two weeks before the next issue is ready to mail.

Publication Frequency

The *Journal of Pyrotechnics* appears approximately twice annually, typically in mid-summer and mid-winter.

Subscriptions

Anyone purchasing a copy of the Journal will be given the opportunity to receive future issues on an approval basis. Any issue not desired may be returned in good condition and nothing will be owed. So long as issues are paid for, future issues will automatically be sent. In the event that no future issues are desired, this arrangement can be terminated at any time by informing the publisher. Additional discounts are available for payment in advance for issues of the *Journal of Pyrotechnics*. Contact the publisher for more information.

Back issues of the Journal will be kept in print permanently as reference material.

Metal Monochloride Emitters in Pyrotechnic Flames — Ions or Neutrals?

Barry Sturman
6 Corowa Court, Mount Waverley, Victoria 3149, Australia

ABSTRACT

Twelve English-language books on pyrotechnics were surveyed for the authors' views on the nature of the metal monochlorides that are associated with the emission of colored light in pyrotechnic flames. Three of the ten authors stated that the emitters were metal chloride ions (MCl^+), five that they were neutral metal chloride molecules (MCl), and two took no clear position. A study of the references cited in these books establishes that the emitters are neutral monochlorides. The idea that they are MCl^+ ions is traced to a book published in 1965, which cited only one reference (published in 1949), and that reference clearly stated that the emitters are neutral molecules.

Keywords: colored flame, emitter, spectra, monochloride, ion, neutral

Introduction

A survey of 12 English-language books on pyrotechnics published since the early 1960s revealed a difference of opinion as to the nature of the metal-chlorine species that contribute to the colours of pyrotechnic flames containing chlorine (Cl) and barium (Ba), calcium (Ca), copper (Cu), or strontium (Sr). Some authors stated that the emitters are neutral monochlorides, MCl, while others indicated that the emitters are singly-charged positive monochloride ions, MCl^+. This review traces the development of this difference of opinion and attempts to establish which of the two points of view is correct by analyzing the information in the references cited in the books. Accordingly, this review has three main parts. It begins with a summary of the positions presented in the 12 books, followed by a summary of the information contained in the references cited in those books. Finally, there is a discussion of that information and of some additional material from more recent publications.

Results of the Book Survey

The following quotes show what each author wrote:

1. Ellern 1961[1]

"Except for the line spectra of the substances usable for colored lights, there is very little literature available on the theoretical aspects and quantitative relations of colored flames. Dr D. Hart [2] refers to the red flame as due to molecular bands in the red region, caused by molecular strontium oxide and chloride, and diluted with other lines and bands from incandescent particles. He refers to the green flame as being due to bright blue (*sic*) bands from copper and barium chloride in the 4000 to 5000 and 5000 to 5500 angstrom region." (p 81)

"Barrow and Caldin [3] have measured the luminous intensities of flare compositions at constant temperature". (p 98)

2. Shidlovskiy 1964 (English translation 1974)[4]

"At high temperatures, strontium chloride dissociates, forming strontium monochloride and splitting off free chlorine:

$$2\ SrCl_2 \leftrightarrow 2\ SrCl + Cl_2$$" (p 182)

"In practice, red flare compositions are formulated only on the basis of the emission of strontium oxide or strontium monochloride, the emission of the latter being more intense, and in addition, closer to the extreme red portion of the

spectrum. This accounts for the effort to introduce chlorine into all the formulations of red flare compositions." (p 183)

"Barium chloride dissociates in a flame, forming barium monochloride and splitting off free chlorine:

$2\ BaCl_2 \leftrightarrow 2\ BaCl + Cl_2$" (p 184)

"The emission spectrum of BaCl consists of numerous bands in the green portion of the spectrum." (p 185)

"The production…of an adequate, pure green flame can be achieved in practice only by using the emission of barium monochloride. Hence, compounds containing chlorine must of necessity be introduced into green flare compositions." (p 185)

"Blue flames are obtained mostly on the basis of cuprous chloride CuCl…The blue emission of cuprous chloride can be obtained only in the reducing zone of the flame and at temperatures not in excess of 1000-1200 °C." (p 186)

"A description of the formulas and technology of German signal-flare compositions used during World War II is given by Eppig.[5]" (p 186)

3. Cackett 1965[6]

"Spectra of illuminating and coloured signal flames are composed of three distinct elements. There is a general temperature continuum derived from the thermal excitation of solid and gaseous products of combustion and which is the main source of the white light that is always present. Next, there are complex systems of band spectra derived from molecular emitters such as ionized oxides and chlorides" (p 30)

"Blue flames rely for their colour on the band-system of $CuCl^+$ ranging from 4200 Å to 4600 Å and to weaker systems in the blue-green and green regions which are simultaneously developed" (p 32)

"All red signal compositions rely on the formation of $SrCl^+$ and SrO^+ ions in the flame to produce their characteristic spectral bands. In practice attention is focussed on developing the $SrCl^+$ ions to a maximum as the SrO^+ ions are always present in the flames." (p 53)

"Green signal compositions, that have really good green flames, are difficult to produce because of the unsaturated hue which is the result of diluting the $BaCl^+$ spectral band with white temperature-continuum and with orange and red spectral bands from BaO^+ and from strontium salts as impurities." (p 56).

4. Ellern 1968[7]

"Color in a flame, as used in pyrotechnics, results from the spectra of excited gaseous metal atoms, molecules or ions [8,9]. Salts of a certain limited number of metals are vaporized and the gaseous molecules or their first partial dissociation products lead to band spectra. On further splitting to neutral atoms of the metal, atomic lines are produced, and eventually metal ions create ionic spectral lines. The latter are undesirable for color production in the flame. So-called C-type chemiluminescence, wherein a small number of molecules emit an abnormally large amount of radiation, plays an important part in the colored emission of red or green flares. An excellent discussion of the mechanisms of pyrotechnic color production is found in reports by Douda.[10,11,12]" (p 97).

5. Lancaster 1972,[13] 1992,[14] and 1998[15]

"Strontium monochloride, barium monochloride and cuprous chloride are the three compounds required for the color production and the excess of chlorine has to be present to ensure their formation".[13] (p 60)

This statement was repeated in the two subsequent editions of this book.[14,15]

6. McLain 1980[16]

"Green flares derive their color from the $BaCl_2$ emission band. As the temperature rises, the BaO^+ emission band increasingly contributes colors in the orange-to-red portion of the spectrum" (p 89)

"Blue is the most difficult color to achieve and bleaches severely when intensity is raised. The blue color comes from the $CuCl^+$ emission band." (p 89)

7. Shimizu 1981[17]

"The important emitters of firework flames are molecules with the exception of Na atoms. The molecules are produced in quite different forms from the original colour producing materials mixed into the composition. The chemical combination of the emitters are relatively simple and in general are outside the ordinary valency law. For example, they are written as SrCl, BaCl, CuCl, etc. and not $SrCl_2$, $BaCl_2$, $CuCl_2$ etc."(p 57)

Pages 59–61 show flame spectra of Sr, Ba, Ca and Cu with and without Cl_2 or HCl. Atomic lines and molecular bands are identified. Figure 47 on page 63 shows the relevant molecular emission bands in relation to the CIE chromaticity diagram.

8. Shimizu 1974[18] (English translation 1983)[19]

"Strontium spectra:

"Strontium salts (carbonate, nitrate, oxalate, etc.) yield the strontium line (4607 Å)…, the SrOH band (5995–6130 Å)…, and the SrCl band (α = 6170–6230Å; β = 6270–6350Å; γ = 6400–6460Å)". (p 75)

"The strontium line is a fairly intense purple-blue. The SrOH band is an intense red-orange, and it is very important for a red colored flame. Chlorine or hydrogen chloride in the flame lowers the intensity of the SrOH band, because the molecule SrOH is changed into SrCl. The α and β bands in the SrCl band are bright red and are the most important components of a good red flame. The γ band is very weak and not important. Chlorine or hydrogen chloride in the flame strengthens the SrCl band. Generally hydrogen chloride has a greater effect than chlorine. If the flame has no chlorine or hydrogen chloride, there will be no SrCl band." (p 76)

"Barium spectra:

"Barium salts (carbonate, nitrate, oxalate, chloride etc.) give the following: barium lines at 5535.5 Å (weak yellow-green), 5778 Å (very weak yellow), and 6100 Å (weak orange)…; BaO band at 4854–6330 Å (very complicated shape, ranging from greenish-blue to red); and the BaCl band at 5505 Å to about 5350 Å (deep green). There are three intense bands: α (5110–5150 Å), β(5245–5280 Å) and γ (5305–5330 Å) …The barium lines are so weak that they have hardly any effect on the flame color. The BaO band is the most important white light source for illumination. It is reduced by the presence of chlorine or hydrogen chloride in the flame, by changing BaO into BaCl. The BaCl band is the most important green light source, but it is only present if chlorine or hydrogen chloride are in the flame. As with strontium, the effect of hydrogen chloride is greater than that of chlorine." (p 76)

"Copper Spectra

"Copper salts (sulfate, arsenite, Paris green, etc.) and powdered copper metal give a purple-blue band (4026–4058,4071–4105, 4123–4164, 4201–4219, 4229–4252, 4269–4277, 4290–4323*, 4340–4343, 4355–4399*, 4417–4432, 4438–4481*, 4496–4513, 4526–4560* Å. … There is also a band from blue to yellow-green (4590–4608, 4630–4658, 4678–4698, 4724–4747, 4769–4781, 4801–4838, 4850–4863, 4888–4928, 4950–4966, 4989–5037, 5056–5074, 5092–5120, 5151–5169, 5190–5225, 5263–5304,5285–5429, 5503–5531, and 5628 Å ...). There is another band at 5263–5531 Å.… The group of purple-blue bands is the most important factor in the production of a blue flame. The asterisks (*) denote the most intense bands. The group of bands from blue to yellow-green is very weak and unimportant. These two groups comprise the CuCl band and become very clear when chlorine or hydrogen chloride are in the flame. The CuCl band appears weaker at temperatures of 2500 °K (2227 °C) and higher because of the decomposition of the CuCl molecule. The other band (5263–5531 Å) comes from CuOH molecules. This is visible when there is no excess chlorine or hydrogen chloride in the flame, and it appears as a weak green color, detracting from a blue flame. Generally our blue flames had a red tip. This is attributable to the copper atom or CuO … the red emissions are very weak and not noteworthy." (p 76)

"Calcium spectra

"Calcium salts such as calcium carbonate give a CaOH band and a CaCl band. The CaOH band… has two portions: an intense red (6105–6270 Å) and intense yellow-green (5500–5580 Å). The CaCl band has four parts: weak red (6294–6360 Å), intense red-orange (6030–6078 Å),

intense orange (5915–5986 Å), and slightly weak yellow (5803–5838 Å). The CaOH band occurs in flames in which no chlorine or hydrogen chloride is present. It is not used by itself for producing colored flames. The CaCl band is used as an orange light source. Chlorine or hydrogen chloride intensify the CaCl bands." (p 77)

These quotes were taken from Chapter 7, which consists of 40 pages entirely devoted to colored flames. There are 4 pages of flame spectra. Figure 49 on page 823 shows the relevant molecular emission bands in relation to the CIE chromaticity diagram.

9. Conkling 1985[20]

"The best flame emission in the red region of the visible spectrum is produced by molecular strontium monochloride, SrCl…The SrCl molecule emits a series of bands in the 620–640 nanometer region – the "deep red" portion of the visible spectrum… Strontium monohydroxide, is another substantial emitter in the red and orange-red regions[10,17]. The emission spectrum of a red flare is shown in Figure 7.1…the primary emitting species are SrCl and SrOH molecules in the vapor state".[21]

"Pyrotechnic compositions containing a barium compound and a good chlorine source can generate barium monochloride, BaCl, in the flame and the emission of green light will be observed. BaCl –an unstable species at room temperature – is an excellent emitter in the 505–535 nanometer region of the visible spectrum –the 'deep green' portion [10,17] ... The emission spectrum of a green flare was shown in Figure 4.1 … molecular BaCl in the vapor state, typically the primary emitter of green light".[21]

"The best flame emission in the blue region of the visible spectrum (435-480 nanometers) is obtained from copper monochloride, CuCl. Flame emission from this molecular species yields a series of bands in the region from 428–452 nanometers, with additional peaks between 476-488 nanometers.[10,17]"

10. Akhavan 1998[22]

"Red light is produced by adding strontium compounds to the pyrotechnic mixture. At high temperatures the strontium compound breaks apart and reacts with the chlorine from the oxidizer [i.e. perchlorate (ClO_4^-) molecule] to form $SrCl^+$ as shown in Reaction 8.1.

$$KClO_4 \rightarrow KCl + 2O_2$$

$$KCl \rightarrow K^+ + Cl^-$$

$$Cl^- + Sr^{2+} \rightarrow SrCl^+$$

"It is the $SrCl^+$ molecule which emits light in the red region of the electromagnetic spectrum, ie. 600–690 nm. Green light is produced by adding barium compounds to the pyrotechnic mixture. Green light is emitted from the $BaCl^+$ molecule at 505-535 nm. Blue light is achieved by reacting copper compounds with potassium perchlorate to form $CuCl^+$ which emits light in the blue region of the visible electromagnetic spectrum, ie. 420–460 nm". (p 156)

11. Russell 2000[23]

"Under the influence of heat, oxidisers such as potassium perchlorate decompose into the chloride and oxygen.… At higher temperatures (>2500 °C) the KCl ionises and the chlorine that is liberated reacts with fragments from barium compounds to form light-emitting species such as BaCl in accordance with…

$$KCl \rightarrow K^+ + Cl^-$$

$$Cl^- + Ba^{2+} \rightarrow BaCl^+$$

The main species responsible for the green color of barium flames is BaCl, while contributions are also made from BaO and BaOH as shown in Table 8.1." (p.70)

(This table, on page 71, shows Ba, Ba^+, BaOH, BaO, and BaCl).

"Reference to Table 8.1 shows that in the absence of chlorine-containing species the visible emission is dominated by BaOH, in spite of the fact that the equilibrium concentration of BaOH is many orders of magnitude smaller than that of BaO. The reason for this is that the hydroxide is formed directly in an excited state in a process know as chemiluminescence, as shown by reaction…

$$Ba + OH \rightarrow [BaOH]^* \rightarrow BaOH + h\nu$$

"Here, [BaOH]* is the excited molecule that releases energy … that corresponds to the green region of the visible spectrum." (p 72)

"Strontium chloride has a melting point of 870 °C and exerts a considerable vapour pressure above this temperature. The boiling point of $SrCl_2$ is 1250 °C and at temperatures above this it dissociates forming strontium monochloride and chlorine…

$$2\ SrCl_2 \leftrightarrow 2\ SrCl + Cl_2$$

"At still higher temperatures (the following) reaction …predominates:

$$2\ SrCl + O_2 \leftrightarrow 2\ SrO + Cl_2$$

"An excess of chlorine... causes a shift to the left and an improvement in the flame saturation of strontium monochloride. Table 8.3 shows the main emission bands/lines for a red star." (p 73)

(This Table, on page 73, shows Sr, SrOH, SrCl, and SrO.)

"The main species responsible for the blue colour in copper flames is cuprous chloride, CuCl… In order to produce a good blue, the temperature must be controlled to ensure that the largest possible amount of vaporised CuCl is present in the flame. A typical spectrum shows wavelength peaks in the region 420–500 nm attributable to CuCl band spectra, a peak at 770 nm due to atomic potassium from the oxidizer, together with CuOH band spectra between 535 and 555 nm." (pp 84–85).

12. Hardt 2001[24]

"Many ionized species exist in the gaseous phase as bi- and tri-atomic molecules which give off molecular band spectra that arise from the ability of the molecule to absorb vibrational and rotational energy. Because molecules have fixed masses, sizes and interatomic spacing their rotational and vibrational energies are also quantized and so can take up and emit energies in discrete wavelengths. To the extent that these band spectra are in the visible range, they are of interest to pyrotechnics… The molecular species that give the best colours are the halides of the alkaline earths and copper" (p 40)

Table 6-2 (p 41) lists a number of metal monohalides, monoxides and monohydroxides and the wavelengths of some of their visible emission bands. All are neutral. The reference is to Herzberg.[25]

Summary of the Book Survey

The "neutral molecules" opinion is taught by Ellern[1,7], Shidlovskiy[4], Lancaster[13,14,15], Shimizu[17,19] and Conkling.[20] The "ions" opinion is taught by Cackett[6] and Akhavan.[22] McLain[16] teaches "ions", but also says that green flames are coloured by the emission band of neutral barium dichloride. Russell[23] teaches "neutral molecules", but gives an equation for the formation of BaCl that shows the formation of $BaCl^+$, as if there were no difference. Hardt[24] specifically refers to emitters as "ionized species (that) exist in the gaseous phase as bi- and tri-atomic molecules", but presents a table of emitters that consists entirely of neutral molecules.

Several authors mention the contribution of metal monohydroxides and monoxides to flame colours; this is clearly an important issue in any discussion of coloured flames. It will not be pursued here, however, because it is not relevant to the question of whether or not the metal chloride emitters are ions or neutrals.

References Cited by the Authors of the Books

1. Ellern 1961[1]

Ellern cited two references that are relevant to the present subject.[2,3]

The writer has not seen the 1953 encyclopedia article by Hart.[2] The 1949 paper by Barrow and Caldin[3] is very much more important than might be guessed from Ellern's remarks. Here is a part of what Barrow and Caldin wrote:

"Blue flames. These rely for their colour on emission of the spectrum of CuCl. Most of the light comes from the D and E systems in the range 4200–4600 Å.[26]; the blue-green systems B and C, and the green system A, are much weaker". (p 33)

"Green flames. BaCl, which gives rise to a well-known band system at 5050–5350 Å, is the obvious choice for a green emitter and it is in fact

generally used… The spectrograms of such flames…invariably show the extensive band system of BaO (4000–8000 Å). There is also strong emission from the near infra-red system of BaCl[27] which, however, lies beyond the visible region of the spectrum. Other discrete bands in the region 7000–7600 Å. have not yet been identified." (pp 33–34)

"Red flames. Strontium compounds are used to colour the red flames, but there are still some obscure features in the spectra. The simultaneous presence of strontium and chlorine compounds in the compositions leads to strong emission of the red system of SrCl (the violet system also appears weakly). However there are also present two closely-spaced sequences degraded to the violet which do not belong to the SrCl system. The long wavelength edges of these sequences are at 6884.5 and 6114.2 Å. In strontium flames containing no chlorine these heads are more strongly developed, and, in addition, the region between them can be seen to be filled with a very close pattern of what appear to be rotational structure lines. The most likely emitter would seem to be SrO, and it is some support for this suggestion that a heavy-current positive-column discharge through SrO contained in a silica tube leads to the production of the same bands." (p 34)

Barrow and Caldin, who were academic spectroscopists, clearly teach that the emitters are neutral molecules. The writer has not seen the 1941 edition of Pearse and Gaydon's book[26] that was cited by Barrow and Caldin, but the following quotes from the 1963 edition[28] are highly relevant:

"Without exception, flame bands have been found to belong to molecules which are electrically neutral, but very frequently the molecules are not stable in the chemical sense..." (p 322)

"BaCl Green System

"Occurrence. Barium chloride in carbon arc or flame". (p 77)

"(BaCl) Infra-red System

"Occurrence. In the flame of pyrotechnic compositions." (p 78)

"BaO

"Occurrence. When barium salts are introduced into carbon arc or flame". (p 82)

"BaOH

"The strong green coloration of flames containing barium salts has recently been shown to be due to the triatomic hydroxide, not the oxide." (p 82)

"CuCl

"Occurrence. Five systems have been observed in flames, in fluorescence and in absorption. They also appear when CuCl is introduced into active nitrogen, and in an arc. The bands frequently occur as impurities in flame spectra, especially of CO…The group of pairs of bands formed by systems D and E is quite characteristic. See Plate 10." (p 152)

"SrCl

"Occurrence. When strontium chloride is introduced into an arc or flame". (p 294)

"SrO

"Strontium salts give bright red banded radiation in flames and arcs, but the flame bands are mostly due to SrOH." (p 298)

"SrOH

"These bands are responsible for the strong red colour of flames and fireworks containing strontium." (p 299)

Pearse and Gaydon[28] often give details of the electronic transitions that are associated with the various bands in spectrum of each molecule, with references to the primary spectroscopic literature from the late 1920s to the late 1950s.

Barrow and Caldin's paper,[3] especially when supplemented by the information in Pearse and Gaydon's book[28], provides very strong support for the neutral molecule position and none whatsoever for the ion position.

2. Shidlovskiy 1964 (English translation 1974)[4]

Shidlovskiy did not cite specific reference for his statements on the nature of the flame emitters. The writer has not seen the report on German signal flare compositions[5] mentioned by Shidlovskiy.

3. Cackett 1965[6]

Cackett, who was the first to present the "ion" opinion, cited but one reference in his discussion of coloured flames: Barrow and Caldin.[3] Cackett did not mention that his identification of the emitters as positive metal monochloride ions was at odds with his cited reference, and he offered no justification for his new identification of the emitters.

4. Ellern 1968[7]

The two relevant references cited in Ellern's 1961[1] book are cited again in this book, but in a different context. Hart's encyclopaedia article[2] is mentioned as "an authoritative article on military pyrotechnics" in the section covering the literature of pyrotechnics (p 10) but there is no mention of his views on colour emitters. Barrow and Caldin[3] are cited in the chapter on colored lights in support of the statement that blue signal lights "seem to be somewhat maligned and deprecated, apparently not so much on optical grounds but because it is difficult and perhaps impossible to create a blue pyrotechnic flame of great depth of color." (p 123) The contribution of these authors in identifying the emitters is not mentioned.

Ellern also cited five works by Douda.[8–12] One of these[8] refers to another of Douda's works[10] for a discussion of the theory of coloured flames and one of the others[9] is a patent of no direct relevance to the present subject.

Of the remaining three works by Douda, the first[10] is a monograph covering all aspects of coloured flame production. It includes references to 18 sources, including five that discuss ionization in flames. Douda attributed the red colour of Sr flames to SrCl and SrOH, and the green of Ba flames to BaCl and BaOH. He explained that addition of halogen to the flame is expected to increase the concentration of the metal hydroxide, and he continued: "In both instances, because the pyrotechnic compositions are usually saturated with the metal and halogen, a very substantial amount of the metal halide will be present in the flame in addition to the hydroxide. The halide formation with barium and strontium is not objectionable because these molecules fortunately also emit energy as defined by their molecular band spectrum in the desired wavelength." (p 18).

Referring to flames containing copper, Douda wrote "As in the case of barium and strontium, the halogen combines with hydrogen to form the halide acid, thereby causing an OH excess which, in turn, contributes to the formation of more CuOH, Also, as in the case of barium and strontium, although more metal hydroxide is formed, the metal halide is formed in even greater amounts. Because the strontium and barium halides emit in desirable wavelengths, the net result is a quantitative increase of emission in desirable wavelengths. In the case of copper, however, the increase in CuOH is out weighed by the increase in copper halide formation, thus resulting in a shift from CuOH green emission to blue copper halide emission." (p 22).

The next work of Douda cited by Ellern[7] is a technical report[11] in which Douda wrote: "Strong BaCl emissions have been reported at 524 mμ and for BaOH at 527 mμ." (p 6)

"Strong SrCl and SrOH emissions occur in this region" [i.e., around 640 mμ]. (p 6)

"BaCl and BaOH dominate in green barium flames." (p 6)

"SrCl and SrOH dominate in red strontium flames". (p 6)

The last work of Douda cited by Ellern[7] is a paper[12] on green flares. Douda wrote:

"In the presence of chlorine, the suppression of MgO and BaO flame emission is a decreasing function of effective temperature, and the ratio BaO/BaCl is an increasing function of effective temperature accompanied by a shift of hue toward yellow and a reduction in excitation purity. By analogy with dissociation constants reported for BaF and BaOH, the dissociation energy of BaCl is estimated to be near 100 kcal/mole. Such an increased value more readily accounts for the sizable BaCl emission observed at a brightness temperature of 2200 K and an effective emitting temperature of 2700 K. Evidence concerning the contribution of BaOH is inconclusive. The 107 kcal/mole dissociation energy in comparison with the 100 kcal/mole estimated for BaCl suggests that BaOH should also be a substantial contributor." (p 793)

5. Lancaster 1972,[13] 1992,[14] and 1998[15]

Lancaster did not cite specific references for his statement about colour emitters. His first edition[13] has a list of 23 references including the first (Russian, 1943) edition of Shidlovskiy, both of Ellern's books[1,7] and a 1957 Japanese-language book by Shimizu.[29] The second edition has 40 references, including all of those in the first edition. Relevant additions include both of Shimizu's books discussed above,[17,19] the books by McLain[16] and Conkling,[20] and to *Pyrotechnica*.[30] The third edition of Lancaster's book[15] has 76 references, but none of those added since the second edition appear to be relevant to the present topic.

6. McLain 1980[16]

McLain did not cite specific reference for his statements quoted above. His chapter on "Light" has a list of 14 references including Ellern,[7] Shidlovskiy,[4] Cackett,[6] Lancaster[13] and a work by Douda[31] that deals with the characteristics of the spectra of magnesium-sodium nitrate-binder illuminating flares. McLain adopted the ion teaching of Cackett, despite the opposing views of Ellern, Shidlovskiy, Lancaster and Douda. It is noteworthy that Douda's writings on coloured flames[10,11,12] were not cited by McLain.

7. Shimizu1981[17]

Shimizu did not cite specific reference for his statements quoted above. His book has a list of 13 references including Ellern,[7] Shidlovskiy,[4] Lancaster,[13] and three of his own books.[29,18,32] He also lists *Pyrotechnica* Issues I– IV.[30]

8. Shimizu 1974[18] (English translation 1983)[19]

In this work Shimizu listed 11 references concerning flame spectra. These include Pearse and Gaydon's book,[28] along with 10 references to the primary spectroscopic literature. Many of these refer to oxide and monohydroxide emitters, but four deal specifically with the spectra of neutral metal monohalides.[33-36]

9. Conkling 1985[20]

As indicated above, Conkling cited specific references for his statements. As well as works of Douda[10] and Shimizu[17] that have already been discussed, Conkling cited a 1983 report by Webster.[21] The writer has not seen this report, but Webster published a paper[37] having the same title in 1986 and this presumably contains much the same information. It includes emission spectra of red, green and yellow flares. Webster wrote:

"The primary emitting species in the red flare are SrCl and SrOH. Emission bands from the SrCl $A^2\Pi \rightarrow X^2\Sigma^+$ system are observed at 661.4 nm, 662.0 nm 674.5 nm and 675.6 nm. Emission from the SrCl $B^2\Sigma \rightarrow X^2\Sigma^+$ system is observed at 623.9 nm, and 648.5nm. The band in both these systems show sharp band heads and are degraded to the violet. …Bands from the SrCl $C^2\Pi \rightarrow X^2\Sigma^+$ system were observed at 393.7 nm, 396.1 nm and 400.9 nm. Molecular emission from the SrOH band system (was) observed…at 605.0 nm, 646.0 nm, 659.0 nm, 667.5 nm and 682.0 nm. The bands at 646.0 nm, 659.0 nm and 667.5 nm overlap the SrCl bands at these wavelengths. This makes the SrCl bands appear stronger and more diffuse than would normally be expected." (p 2)

"The primary emitting species in the green flare are BaCl and BaO. Emission bands from the BaCl $C^2\Pi \rightarrow X^2\Sigma^+$ system are observed at 507 nm, 514 nm 524 nm and 532 nm. The molecular BaCl emission is superimposed on less intense, but equally important BaO, BaOH and Ba_2O_2 band emission extending from 460 nm to 678 nm. This emission, coupled with an underlying continuum from hot solid particles, is the contributing factor to the loss of color purity in the flare. The …flare composition also contains copper and the resulting CuCl emissions are observed from 412 nm–470 nm." (p 3) Webster cited the following references: Douda,[12,38] McLain,[16] Shimizu,[17] Barrow and Caldin.[3] and Ellern.[7] All of these have already been discussed, except Douda's 1972 paper[38] on the spectrum of a red highway flare. Douda wrote:

"The dominant emitting species are strontium oxide and the flame radicals SrCl and SrOH, the radicals being strong emitters[39,28] in the red region. The strong band systems with maxima

near 606, 646, 659, 669 and 682 nanometers are due mainly to emission from SrOH and SrCl." (pp 416–417) Reference [39] deals with magnesium-metal nitrate flares with no chlorine donors and is only marginally relevant to the present discussion.

10. Akhavan 1998[22]

Akhavan cited no specific references for her statements. Her bibliography includes Conkling[20] and Ellern[7].

11. Russell 2000[23]

Russell cited no specific references for his statements. His bibliography includes Ellern[7], McLain[16] and Lancaster[15].

12. Hardt 2001[24]

Hardt did not cite specific references for his statements, but he cited Hertzberg[25] for the information presented in his Table 6-2. Hardt's bibliography contains over 270 references, up to the year 1999. These include 14 works by Douda but of these only one[10] is clearly relevant to the present topic. Another of the cited works of Douda[40] deals with the emission spectra of flares but is concerned only with magnesium-sodium nitrate-binder illuminating flares.

Evidence That the Metal Monochloride Emitters Are Neutral Molecules, Not Ions

1) The spectra of the neutral metal monochlorides are very well known to spectroscopists. For example, in 1979 Huber and Hertzberg[41] published a volume of spectroscopic constants for all known diatomic molecules and ions, covering the literature up to 1975. They cited 14 references for data on BaCl, 14 for CaCl, 15 for CuCl and 11 for SrCl. More recently an on-line data base of references associated with the spectra of diatomic molecules[42] contained, in January 2004, 36 papers associated with the spectrum of BaCl, 61 for the CaCl spectrum, 50 for the CuCl spectrum, and 19 for the SrCl spectrum. All of these papers have been published since 1974.

2) The Ca, Sr and Ba monochlorides are members of a rather large family of univalent alkaline earth compounds that exist at high temperatures and that have been characterized spectroscopically in recent years.[43] The alkaline earth monohydroxide emitters are members of this same group of compounds.[43]

3) The electronic states of the metal monochlorides have been calculated from quantum mechanics. The predicted spectra are in good agreement with those measured experimentally. See, for example, the comparison of calculated results for the CuCl molecule with experimental results by Parekunnel et al.[44]

4) The number of electrons in an emitter can be determined from the characteristics of the spectrum.[45] Each electron carries half a unit of angular momentum ("spin") that can have one of two directions, corresponding to a spin of plus or minus ½ a unit in some reference direction. If two electrons of opposite spin "pair up", the spins cancel; if an atom or molecule has one or more unpaired electrons, the resulting electron spin interacts with the angular momentum associated with the movement of electrons around the atom or molecule and changes the energy of the electrons. If there is no unpaired electron, the electronic energy state is unaffected by electron spin. Such a state is called a "singlet". If there is a single unpaired electron, its spin can either add to, or subtract from, the component of the angular momentum of the electronic energy states in the reference direction, with the proviso that the resulting angular momentum must always be positive. Consequently, a state having an angular momentum component in the reference direction of 1 unit is split into two, one of the new states having angular momentum of ½ unit and the other 1½ units. Such a state is called a "doublet". Two unpaired electrons result in an electronic energy state splitting into three, called a "triplet". In general, the *multiplicity* of a state is one more than the number of unpaired electrons. If an atom or molecule has an even number of electrons, the multiplicity of all its electronic energy levels must be odd, and conversely. An obvious example of the effect of multiplicity on an electronic

spectrum is provided by the sodium atom, which has a single unpaired electron. The "doublet" nature of the electronic energy states of atomic sodium is revealed by the familiar yellow line in the spectrum of atomic sodium actually consisting of two lines.

The characteristics of molecular spectra that indicate the multiplicity of the emitter are more subtle. The analysis involves careful study of the rotational structure of the various bands and is possible only with spectra recorded at very high resolution. Details are given by Gaydon[46] and by Herzberg.[25,45] Analysis of the spectra of the alkaline earth monochlorides reveals that the electronic energy states are doublets.[28,34,47] This means that there is an odd number of electrons in the emitter, which is the case for the neutral monochloride molecules but not for the ions. Similarly, the spectrum of copper monochloride[44] reveals singlet and triplet states, showing that the emitter has an even number of electrons. This is consistent with the emitter being neutral copper monochloride but not with it being the ion.

5) Thermodynamic modeling of the combustion of coloured flame compositions[48,49] has shown the presence of neutral metal monochlorides in the predicted equilibrium mixture of combustion products, consistent with the observed emission spectra.

6) The ions $CaCl^+$, $SrCl^+$ and $BaCl^+$ would presumably have exactly the same electronic structure as the molecules KCl, RbCl and CsCl respectively. The alkali chlorides do not exhibit visible spectra[25, 41] and it is expected that the same would be true of the alakaline earth monochloride ions.[50] Huber and Herzberg[41] and the DiRef[42] database list no spectroscopic data for $CaCl^+$, $SrCl^+$, $BaCl^+$ or $CuCl^+$, Hildenbrand[51] measured the ionization energies of CaCl, SrCl, BaCl and CuCl by mass spectrometry, using electron impact ionization. Results, expressed as the appearance potential for each MCl^+ ion from the corresponding MCl precursor molecule, are shown in Table 1.

Table 1. Ionization Energies of CaCl, SrCl, BaCl and CuCl.[51]

Ion	Appearance potential (eV)
$CaCl^+$	5.6 ± 0.5
$SrCl^+$	5.3 ± 0.5
$BaCl^+$	5.0 ± 0.5
$CuCl^+$	10.7 ± 0.5

The ionization energy of CuCl is so high that only a very small fraction of any population of CuCl molecules present in a flame could possibly be ionized at flame temperatures. Furthermore, only a tiny fraction of those ions would be excited at flame temperatures. The number of emitting ions at flame temperatures would therefore be exceedingly small. This consideration alone is sufficient to rule out the possibility that $CuCl^+$ could be a significant emitter of light in a pyrotechnic flame.

Conclusion

The metal monochloride spectra that contribute to the colours of pyrotechnic flames are emitted by neutral metal monochloride molecules, MCl where M is Ba, Ca, Cu or Sr. This was clearly stated by Barrow and Caldin[3] as long ago as 1949 and has been confirmed since by Douda,[8–12,39–41] Shimizu,[17–19] and Webster.[21,37,47] The idea that the emitters are singly-charged metal monochloride ions (MCl^+) is erroneous, and can be traced to the 1965 book by Cackett.[6] At the time that Cackett wrote his book, no spectra of the monohalide ions of Ba, Ca, or Sr had been reported in the scientific literature,[41] none have been reported since[42] and there are good reasons for expecting that these ions would not emit visible spectra.[50] Similarly, there are no reports of spectra of $CuCl^+$;[41,42] the high ionization energy of this ion[51] make it most unlikely that it could exist in a flame in sufficient numbers to contribute in any significant way to the emission of light by the flame.

A Note on Nomenclature

The neutral MCl, etc. molecules are referred to herein as "neutrals". Douda[38] used the term "radicals" for SrCl and SrOH. This terminology was not adopted here, because Herzberg[46] used "radicals" to include all short-lived species, including molecules and ions.

Acknowledgements

I appreciate the interest of the "Ions or Neutrals?" group. This group is a collection of 14 authors and researchers, all having an interest in pyrotechnic flame colour, to whom the paper was submitted for critical comments.

I am grateful to Kenneth L. Kosanke for initiating this project and for supplying copies of many of the papers consulted for this review. Bernard E. Douda very kindly provided copies of some of his papers. I thank Peter F. Bernath for helpful comments and for drawing my attention to the "DiRef" database.[42]

References

1) H. Ellern, *Modern Pyrotechnics*, Chemical Publishing Co., Inc., NY (1961) pp 81, 98.

2) D. Hart, "Pyrotechnics (Military)", *Encyclopedia of Chemical Technology*, Vol. 11, Interscience Publishers, Inc., NY (1953) (cited by Ellern[1]).

3) R. F. Barrow and E. F. Caldin, "Some Spectroscopic Observations on Pyrotechnic Flames", *Proceedings of the Physical Society (London)*, 62B, pp 32–39 (1949).

4) A. A. Shidlovskiy, *Principles of Pyrotechnics*, 3rd Ed., Mashinostoyeniye Press, Moscow, 1964, translated by Foreign Technology Division, Wright-Patterson Air Force Base, OH (1974) pp 182–186.

5) H. Eppig, *The Chemical Composition of German Pyrotechnic Colored Signal Lights*, London, 1945 (cited by Shidlovskiy[4]).

6) J. C. Cackett, *Monograph on Pyrotechnic Compositions*, Ministry of Defence (Army), Royal Armament Research and Development Establishment, Fort Halstead, Sevenoaks, Kent, UK, 1965, pp 30, 32, 53, 56. (NOTE: This book is marked "RESTRICTED". The writer was fortunate enough to find a copy in a secondhand bookshop in Melbourne, Australia in 2003).

7) H. Ellern, *Military and Civilian Pyrotechnics*, Chemical Publishing Co., Inc., NY, 1968, p 97.

8) B. Douda, *Colored Flare Ingredient Synthesis Program*, RDTR No. 43, Naval Ammunition Depot, Crane, IN, 10 Jul 1964.

9) B. Douda, *Pyrotechnic Compound Tris(glycine) Strontium(II) Perchlorate and Method for Making Same,* US Patent 3,296,045, 1967.

10) B. Douda, *Theory of Colored Flame Production*, RDTN No. 71, Naval Ammunition Depot, Crane, IN, 20 Mar 1964.

11) B. Douda, *Relationships Observed in Colored Flames*, RDTR No. 45, Naval Ammunition Depot, Crane, IN, 25 Sep 1964.

12) B. E. Douda, "Emission Studies of Selected Pyrotechnic Flames", *Journal of the Optical Society of America*, Vol. 55, No. 7 (1965) pp 787–793.

13) R. Lancaster, T. Shimizu, R.E.A. Butler and R.G. Hall, *Fireworks Principles and Practice*, Chemical Publishing Co., NY, 1972, p 60.

14) R. Lancaster, with contributions from T. Shimizu, R.E.A. Butler and R.G. Hall, *Fireworks Principles and Practice*, 2nd ed., Chemical Publishing Co., NY, 1992, p 77.

15) R. Lancaster, with contributions from R.E.A. Butler, J. M. Lancaster, T. Shimizu and T. A. K. Smith, *Fireworks Principles and Practice*, 3rd ed., Chemical Publishing Co., NY, 1998, p 142.

16) J. H. McLain, *Pyrotechnics from the Viewpoint of Solid State Chemistry*, The Franklin Institute Press, Philadelphia, 1980, p 89.

17) T. Shimizu, *Fireworks – The Art, Science and Technique*, published by T. Shimizu, distributed by Maruzen Co., Tokyo, 1981, pp 57–63.

18) T. Shimizu, *Feuerwerk von physikalischem Standpunkt aus,* Hower Verlag, Hamburg, 1976. (Cited by Shimizu[17] – see reference 19 for English translation).

19) T. Shimizu, *Fireworks from a Physical Standpoint*, translated from the German *Feuerwerk von physikalischem Standpunkt aus*, 1976, by Alex Schuman, Pyrotechnica Publications, Austin, TX, 1983. Part II, p 74–83, Part IV, p 246.

20) J. A. Conkling, *Chemistry of Pyrotechnics*, Marcel Dekker, NY, 1985, pp 87, 157, 158, 160.

21) H. A. Webster III, "Visible Spectra of Standard Navy Colored Flares", *Proceedings, Explosives and Pyrotechnics Applications Section, American Defense Preparedness Association*, Fort Worth, TX, Sep 1983.

22) J. Akhavan, *The Chemistry of Explosives*, Royal Society of Chemistry, Cambridge, 1998, p 156.

23) M. S. Russell, *The Chemistry of Fireworks*, Royal Society of Chemistry, Cambridge, 2000, pp 70–74, 84–85.

24) A. P. Hardt, with contributions by B. L. Bush and B. T. Neyer, *Pyrotechnics*, Pyrotechnica Publications, Post Falls, ID, 2001, pp 40–41.

25) G. Herzberg, with the cooperation, in the first edition, of J. W. T. Spinks, *Molecular Spectra and Molecular Structure. Vol. I. Spectra of Diatomic Molecules*, 2nd ed., D. Van Nostrand, Inc., Princeton, NJ, 1950, pp 240–280.

26) R. W. B. Pearse and A. G. Gaydon, *The Identification of Molecular Spectra* , Chapman and Hall, London, 1941. (Cited by Barrow and Caldin.[3])

27) R. F. Barrow and D. V. Crawford, "Electronic Band System of BaCl", *Nature*, Vol. 157 (1946) p 339.

28) R. W. B. Pearse and A. G. Gaydon, *The Identification of Molecular Spectra*, Chapman and Hall, London, 1963.

29) T. Shimizu, *Hanabi*, Hitotsubashi Shobo, Tokyo, 1957. (Cited by Lancaster[14,15] and Shimizu.[17])

30) R. G. Cardwell, Ed., *Pyrotechnica*, Vol. I – Vol. XVII, Pyrotechnica Publications, Austin, TX (1977–1997).

31) B. E. Douda, "Spectral Observations in Illuminating Flames", RDTR No. 131, in *Proceedings of the First Pyrotechnic Seminar*, U.S. Naval Ammunition Depot, Crane, IN, October 1968, pp 113–125.

32) T. Shimizu, *Hanabi no Hanashi*, Kawada Shobo Shisha, Tokyo, 1976. (Cited by Shimizu.[17])

33) R. Ritschl, "Uber den Bau einer Klasse von Absorptionsspektren", *Zeitschrift fur Physik*, Vol. 42 (1927) pp172–210.

34) A. E. Parker, "Band Systems of BaCl", *Physical Review*, Vol. 46 (1934) pp 301–307.

35) R. R. Rao and J. K. Brody, "Structure of the Band Spectra of CuCl Molecule, I. Additional Knowledge in the Coarse Structure", *Journal of Chemical Physics*, Vol. 35 (1961) pp 776–787.

36) R. R. Rao, R. K. Asundi and J. K. Brody, "Structure of the Band Spectra of CuCl Molecule, II. Rotational Structure of the F-X Band System of CuCl, *Canadian Journal of Physics*, Vol. 40 (1962) pp 412–422.

37) H. A. Webster, III, "Visible Spectra of Standard Navy Colored Flares", *Propellants, Explosives, Pyrotechnics*, Vol. 10 (1985) pp 1–4.

38) B. E. Douda "Red Highway Flare Spectrum", *American Journal of Optometry and Archives of American Academy of Optometry*,Vol. 49, No. 5 (1972) pp 415–417.

39) B. E. Douda, R. M. Blunt, and E. J. Bair, "Visible Radiation from Illuminating-Flare Flames: Strong Emission Features", *Journal of the Optical Society of America*, Vol. 60, No. 8 (1970) pp 1116–1119.

40) B. E. Douda, *Atlas of Radiant Power Spectra of Four Flare Formulations at 8 Levels of Atmospheric Pressure*, RDTR No. 205,

Naval Ammunition Depot, Crane, Inn June 1972.

41) K. P. Huber and G. Herzberg, *Molecular Spectra and Molecular Structure, Vol. IV. Constants of Diatomic Molecules*, Van Nostrand Reinhold, NY, 1979.

42) P.F. Bernath and S. McLeod, "DiRef, A Database of References Associated with the Spectra of Diatomic Molecules", *Journal of Molecular Spectroscopy*, Vol. 207, (2001) p 287.

43) P. F. Bernath, "Gas-phase Inorganic Chemistry: Monovalent Derivatives of Calcium and Strontium", *Science*, New Series, 254 (issue 5032) (1991) pp 665–670.

44) T. Parekunnel, L. C. O'Brien, T. L. Kellerman, T. Hirao, M. Elahine and P. F. Bernath, "Fourier Transform Emission Spectroscopy of CuCl", *Journal of Molecular Spectroscopy*, Vol. 206 (2001) pp 27–32.

45) G. Herzberg, *The Spectra and Structure of Simple Free Radicals: An Introduction to Molecular Spectroscopy*, Dover Publications, NY, 1971, pp 74–88.

46) A. G. Gaydon, *Dissociation Energies and Spectra of Diatomic Molecules*, Chapman and Hall, London (1947) pp 25–26.

47) A. E. Parker, "Band Systems of MgCl, CaCl and SrCl", *Physical Review*, Vol. 47 (1935) pp 349–358.

48) R. E. Farren, R. G. Shortridge and H. A. Webster, III, 'Use of Chemical Equilibrium Calculations to Simulate the Combustion of Various Pyrotechnic Compositions", *Proceedings of the 11th International Pyrotechnics Seminar*, 1986, pp 13–40.

49) R. Webb and M. van Rooijen, "Optimizing Pyrotechnic Color Compositions using Thermodynamic Modeling", *Proceedings of the 29th International Pyrotechnics Seminar*, 2002, pp 823–828.

50) P. F. Bernath, personal communication, January 2004.

51) D. L. Hildenbrand, "Dissociation Energies and Chemical Bonding in the Alkaline-Earth Chlorides from Mass Spectrometric Studies", *Journal of Chemical Physics*, Vol. 52 (1970) pp 5751–5759.

Experimenting with High Explosive Fuel Explosions for Movies and Television

Stephen Miller
Live Action FX Ltd, 152 Ayelands, New Ash Green, Longfield, Kent DA3 8JU UK
e-mail: Steve@LiveActionFX.com

ABSTRACT

A number of 'brute force' techniques used within the special effects industry utilise high explosives to create the classic 'Hollywood' style fuel explosion seen in many a movie and television programme. Limited experiments have shown that application of techniques similar to those used in shaped charge anti-tank weapons (the Munroe effect) can produce higher and larger fuel explosion effects, while using less fuel and explosive material, thereby creating a more controlled effect.

Keywords: high explosive, fuel explosion, special effects, directional shaped charge, Munroe effect, compression tube

Introduction

As readers of this Journal probably know, the fiery explosions seen in movies and on television are unrealistic. The special effects (SFX) industry achieves these effects by using large amounts of fuel—petrol (gasoline), diesel, kerosene, alcohol or a mixture of these—that are thrown and spread by a suitable bursting or lift charge to create the classic 'Hollywood' explosion.

In the UK, high explosives (HE), generally in the form of detonating cords, are the preferred bursting or lifting charge, however large maroons (salutes) are also used. Whichever bursting or lift charge is used, a secondary ignition charge (usually Black Powder or a similar pyrotechnic heat or flame source) is required to ensure that the vaporised fuel is safely and reliably ignited.

These techniques produce a very satisfying 'Hollywood' type fireball explosion. They simply use the 'brute force' effect of the explosive material to burst a fuel container and/or throw the fuel into the air, forming a cloud of fuel vapour ready for ignition by the secondary ignition charge.

As with any other action, when an explosive charge is fired to burst or lift the fuel, there is an equal and opposite reaction, which can do considerable damage to the local surroundings. The SFX industry tends to use kicker plates (Figure 1), mortar pots—for more directional bursts (Figure 2) or similar items to "give the explosive something to push against" thus protecting the immediate surrounding area.

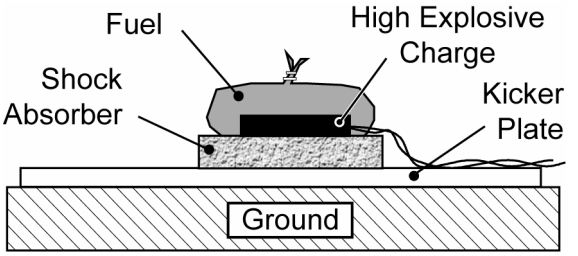

Figure 1. Example setup for a non-directional fuel explosion.

A sacrificial shock absorber (such as firm foam) is needed between the HE charge and the kicker plate or mortar pot to prevent the direct transfer of shock waves into the metal of the kicker plate or mortar pot. Direct contact between the metal and HE during detonation can cause metal fragments or scabs to break off and fly considerable distances.

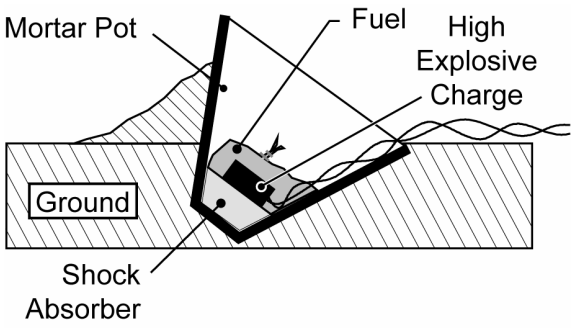

Figure 2. Example of setup for a directional fuel explosion.

However, HE has properties other than shear 'brute force' that may be harnessed and used with finesse to produce higher, larger and more controlled fuel effects while using lower amounts of fuel, thereby reducing the risk of secondary fires in the surrounding area.

Requirement

The requirement, and hence these experiments, originally came about through an enquiry from a conceptual artist who wanted to film a 100 foot (33 m) high column of fire and project the footage onto the wall of a gallery as part of a piece of 'installation art'.

After an initial meeting it was established that the column of fire needed to be 50 feet high rather than the stated 100 feet, as 50 feet (16 m) would be the approximate height of the frame seen by the camera. A number of pyrotechnic-based techniques were tried, but they did not produce the volume of instantaneous rich fire required in the column effect. Eventually it was decided to apply shaped charge techniques in an attempt to solve the problem.

Experiments

An ideal experimental assembly was designed (Figure 3) that consisted of a hollow cylinder of explosive that could be detonated at one end, simultaneously around its entire circumference, with the centre of the cylinder being filled with fuel. The theory was that the contents of the cylinder would be compressed toward the central axis. Since the charge initiates from one end, the compressed fuel is forced out through the open (yet to be detonated) end of the cylinder, thereby propelling the fuel high into the air. However, due to the complexity of achieving simultaneous initiation with the limited resources available, a more practical experimental assembly had to be designed (Figure 4).

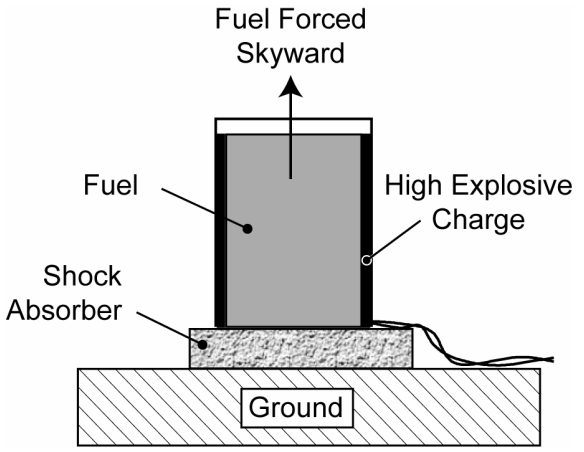

Figure 3. Ideal experimental assembly.

The assembly was based on a large diameter, thin walled cardboard tube, which was of a wound laminated construction, having a diameter of 500 mm, a wall thickness of 4 mm and a height of 600 mm.

The top three quarters of the cardboard tube would be wound with PETN-filled detonating cord (nominally 10 grams [150 grains] per metre), in a helix pattern around the tube with a pitch of approximately 30 mm; this would consume 18 metres of detonating cord.

Four equal lengths of detonating cord were to be attached (using duct tape) at equal spacing around the circumference and vertically down the outside of the tube. These lengths would be bound together where the detonator was to be attached, so that the length of detonating cord between the detonator and the cardboard tube was exactly the same for all four pieces. This was designed to produce four simultaneous and equally spaced points of initiation around the diameter of the cardboard tube.

The bottom quarter of the tube would be filled with approximately 12 litres of water in-

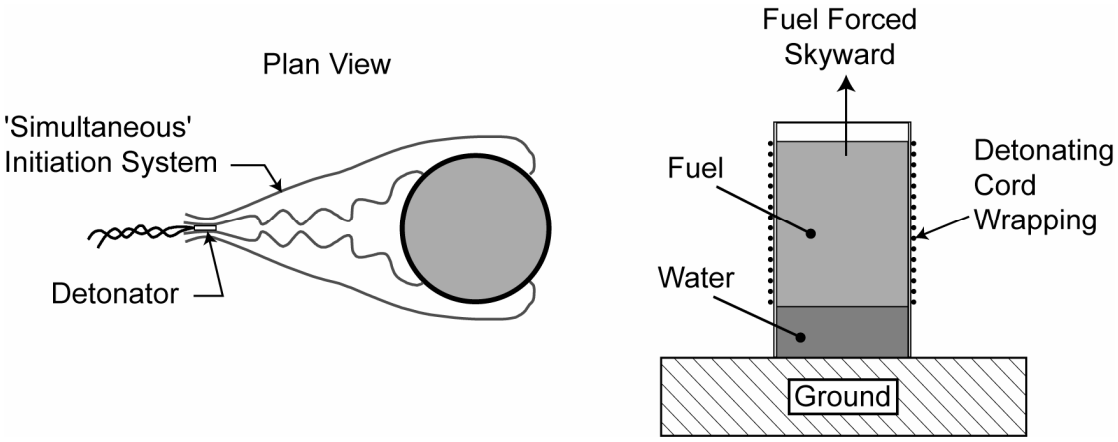

Figure 4. Practical experimental assembly.

side a polythene bag. The water was intended to elevate the fuel and explosives, thereby reducing the blast damage to the ground and surrounding area. In addition, the water would be rapidly dispersed over the local area to reduce the risk of secondary fires.

The top three-quarters of the tube was to be filled with fuel: a mixture of 12 litres of petrol (gasoline) and 24 litres of diesel oil. This mixture was chosen to give the required rich orange-yellow flame colour and good dark smoke to complete the effect, once the fire had died away.

To test the system cheaply a number of scaled-down versions were manufactured. The scaled-down versions were fired and compared with equivalently sized versions of the 'brute force' techniques detailed earlier (Figures 1 and 2). These versions contained only 1 litre of fuel; however the scaling of the explosive content left only a single turn of detonating cord wrapped around the small scale cardboard tubes. However, this was felt to be sufficient to act as a guide as to whether the full-scale version would achieve the required effect.

Scaled-Down Results

The scaled-down 'compression tube' firings produced higher, tighter and more impressive looking fuel explosions than the same sized 'brute force' firings. The 'compression tube' firings also produced less damage and lower incidents of secondary fires. The fireballs from 1 litre tests are documented in the series of three photos in Figure 5. These results encouraged us and indicated that the full-scale version should produce the required high, dense and rich column of fire that had been requested.

Full-Scale Experimental Firing

Following the small scale firings a single full-scale assembly was built and tested: the cardboard tube was positioned and filled as shown in Figure 6. The four equal lengths of detonating cord making up the 'simultaneous' initiation system were carefully laid out, so that they were well separated and not kinked. The secondary ignition charge was attached to a steel post approximately 1 metre away from the full sized 'compression tube' and the detonator was attached to the junction between the four lengths of detonating cord.

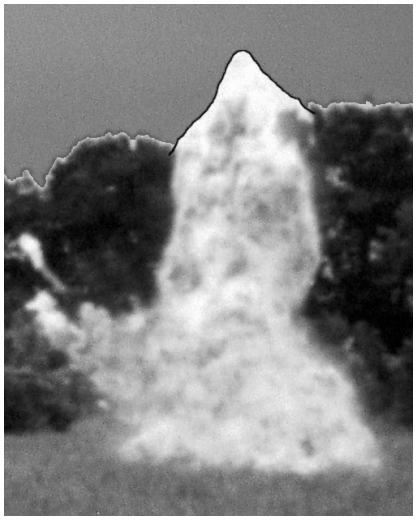

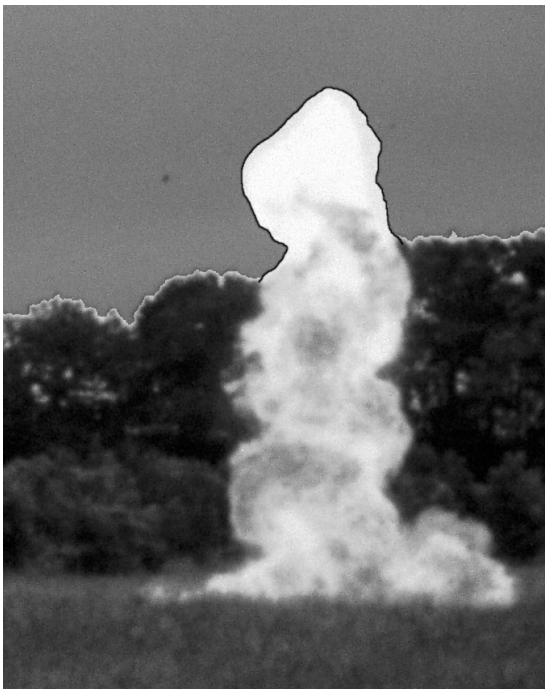

Figure 5. The fireballs from 1 litre tests. The upper left photo is from the non-directional fuel explosion (as per Figure 1). The lower left photo is from the directional fuel explosion (as per Figure 2) but aimed directly upward. The photo above is from the 'compression tube' firing. The figures were resized so that the trees are about the same scale.

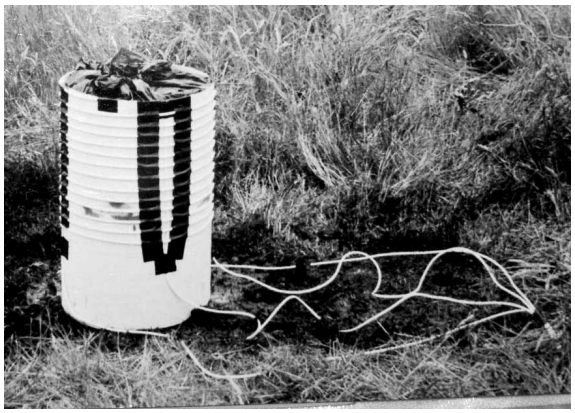

Figure 6. The first full scale experimental assembly.

The full-scale firing produced a dense and rich column of fire that was approximately 50% higher than the stated requirement of 50 feet and can be seen in Figure 7. Two, very successful, full scale firings were carried out in front of a child's 'A' frame swing and were filmed by the conceptual artist. One of these is now titled "Automation" and has been shown at an art exhibition in Barcelona. A shortened clip of "Automation" can be seen on the web at:

http://www.liveactionfx.freeserve.co.uk/SFX%20swing.htm

[NOTE: This leads you to a low resolution version of the photos in this picture and a link to where you can download a 2 MB movie clip.]

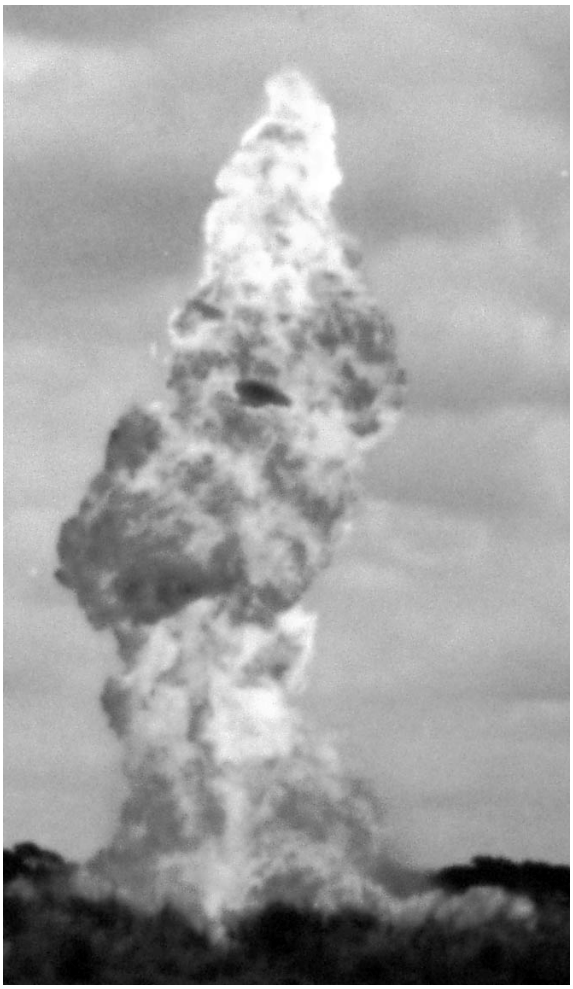

Figure 7. The full-scale firing.

Industrial Scale Nano-Aluminum Powder Manufacturing

David Pesiri, Christopher E. Aumann, Luke Bilger, David Booth, R. Doug Carpenter, Rob Dye, Edward O'Neill, Debbie Shelton, and Kevin C. Walter

Technanogy Materials Development, 2221 Cape Cod Way, Santa Ana, CA 92703 USA
www.technanogy.net

ABSTRACT

Producing nano-aluminum powder (n-Al) on a commercial scale places a great deal of emphasis on practical manufacturing issues. Scientists and engineers in the laboratory commonly evaluate nano-aluminum powder in the technical terms of its particle size, particle size distribution (PSD), morphology, and oxide shell thickness. The quality of nano-aluminum at the commercial scale, however, rests upon several additional parameters that emphasize manufacturing effectiveness (production rate, process reproducibility, raw material utilization, lot size and scalability) as well as product quality (powder purity, surface properties and extent of agglomeration). Balancing the practical demands of a commercially viable process with the technical needs of specialized end users has been the challenge throughout the life of Technanogy Materials Development (TMD). Today TMD stands as a company focused on the manufacture and commercialization of nano-aluminum powder and able to assist others in developing nano-aluminum applications. The issues and insights related to the scale-up of this technology during the past three years are described. The properties of nano-aluminum powder that have motivated this scale-up are also discussed.

Keywords: nano-aluminum, nanoparticle, particle size distribution, passivation, oxide layer thickness, nanomaterial

Introduction

The widely reported interest in nanotechnology and nanomaterials has brought many exciting new technologies into focus. This increased level of awareness has also brought an inevitable degree of optimism from technologists, investors and consumers alike. In contrast to the level of exuberance that nanotechnology has elicited, the commercial success of the nanotechnology industry has been modest at best. The challenges that face companies that commercialize products based on nanomaterials are nontrivial and range from practical barriers in production and processing, to end users who remain unsure of how to fully unlock the highly-touted benefits of these materials. Nanomaterials are often, in reality, very different from their more massive micron- and larger-sized equivalents. It is the combination of an ability to synthesize materials at the nanometer level and subsequently manipulate these materials to form commercially viable products that will be the real test for companies in this industry.

Technanogy Materials Development (TMD) is a small company located in Santa Ana, California that has chosen to focus on the commercialization of nano-aluminum (n-Al) powder. For the past three years TMD has had one objective, to produce the highest quality n-Al powder at affordable prices to meet the needs of a developing customer base. There are numerous methods for laboratory-scale nanoparticle production that have been well described in the literature.[1,2] Nano-aluminum has several properties that restrict its method of production. Aluminum's reactivity with oxygen, the unattractive properties of molten aluminum (corrosivity, high surface tension and solvent strength), and the thermodynamic driving force of aluminum metal to recombine into a bulk crystalline form are all challenges to the production of nanometer-sized particles of aluminum.

Inert gas condensation (IGC) is the technology favored by TMD for the production of nano-aluminum. IGC has been recognized as a route to ultrafine particles for over two decades.[3–5]

The origins of TMD's vapor phase synthesis of n-Al can be traced to the early 1990s when researchers at Los Alamos National Laboratory investigated the use of inductively heated surfaces to produce n-Al by a gas phase process. Researchers at several other laboratories within the U.S. Department of Defense were concurrently exploring similar methods for the production of n-Al. Initially, the n-Al production rate was roughly one gram per run and was limited to two grams per day. Scaling this batch process into a semi-continuous mode increased throughput to one gram per hour by early 2001. Within the next year, n-Al production rate was increased to over 40 grams per hour (one kilogram per day). By early 2003, production rate had increased to more than 300 grams per hour (over seven kilograms per day). Production capacity with current continuous operation is expandable to several times this value.

The key to scaling the vapor phase production of nano-aluminum has been the ability to base design engineering and powder handling decisions on an understanding of the n-Al product. Much of the development period focused on improving the characterization and testing procedures. This effort provided an extensive background of the physical and chemical properties of n-Al. Understanding the influence of the powder production route on the physical properties of the powder identified the important process variables for n-Al manufacturing. Tight control over the IGC production process allows production of aluminum powder with fixed and controllable diameter as well as having a fixed and controllable oxide film at the surface. Figure 1 shows the relationship between particle diameter and the percentage weight of aluminum for each particle for several fixed oxide shell thickness values. Current capabilities allow production of any practical combination of particle size and aluminum metal content.

Interest in nano-aluminum powder without any oxide coating is well founded, especially within the energetic and propellant communities. Rocket propellants, for example, are very sensitive to weight and energy density and carrying unwanted levels of unreactive oxide is undesirable. Unfortunately, it is well understood that aluminum metal is not stable in the absence of a passivating oxide layer. Since aluminum oxide is known to form at extremely low oxygen partial pressures, the formation of an oxide shell is not preventable without a robust, impermeable barrier that completely envelops the aluminum particle. In the absence of an oxide layer, aluminum nanoparticles also have a very strong tendency to agglomerate to form bulk aluminum metal. Several approaches to non-aluminum oxide coatings on aluminum nano particles have been reported including the use of inorganic and organic self-assemblies, polymeric barriers, inorganic salts and metallic coatings. Without describing the details of each process it is the belief of TMD that no other coating adequately replaces the native oxide as a reliable and robust protective layer suitable for mass production. In fact, many alternative coating technologies appear incapable of preventing oxygen from accessing the aluminum particle core resulting in oxidation and therefore both an oxide and an added coating layer.

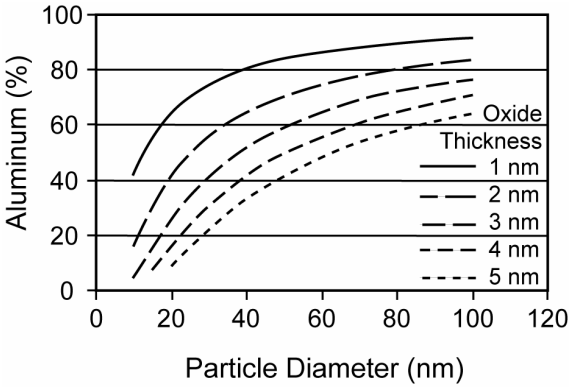

Figure 1. As the n-Al particle size increases, the weight percent of aluminum metal increases for a given oxide shell thickness (labeled in the graph). Technanogy Materials Development has independent control over both particle size and oxide shell thickness. Nano-aluminum powder can therefore be produced with any combination of size and aluminum metal content.

Control over both nano-aluminum powder size and aluminum content has been crucial to product development. Slight changes in particle size can have a dramatic effect on surface area and therefore surface area-dependent properties such as rheology, powder mixing, dispersion, surface adsorption of condensed species and bulk density. Aluminum metal content also has a large effect on nanopowder properties. The per-

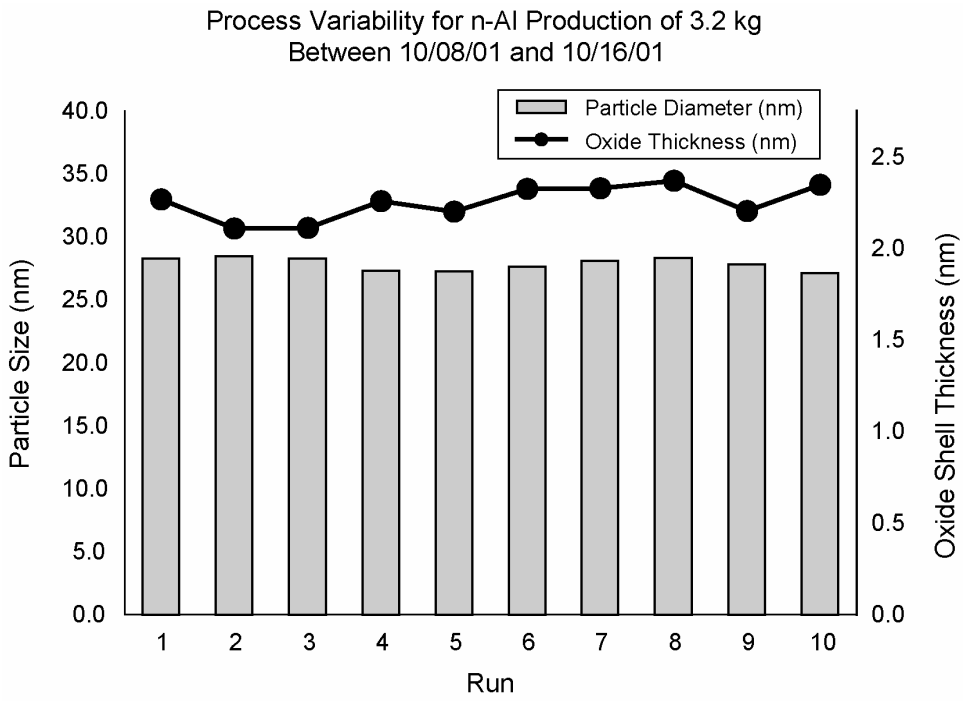

Figure 2. The reproducibility of the n-Al produced by TMD over several runs in 2001 is shown. The standard deviations of the particle size and the oxide shell thickness are 0.5 and 0.09 nm, respectively. Plotted values are calculated from surface area measurements and thermogravametric analysis as described in the text.

centage of aluminum metal is typically most critical to customers focusing on the energy release of the product. The aluminum weight percent influences particle properties such as density, reactivity, energy release rate, specific impulse and energy density as well as having implications for long-term storage and stability. Tight control over the particle size and oxide shell thickness is exhibited in the analysis of data from several runs from 2001 (Figure 2), and demonstrates the key capability necessary for any company producing nano-aluminum powder.

The Product

The nano-aluminum manufactured routinely is in the size range of 20 to 200 nm with a passivating oxide shell controllable to between 1.5 and several nanometers in thickness. The particles are discrete spheres of n-Al covered completely with an amorphous layer of aluminum oxide. As produced in the vacuum phase, the particles are free from necking, aggregation (defined in this context as the assembly of many particles held together by bonds or forces strong enough to resist breaking apart with energy input) or other permanent fusion. A scanning electron microscopy (SEM) image of n-Al produced by the IGC process is shown in Figure 3.

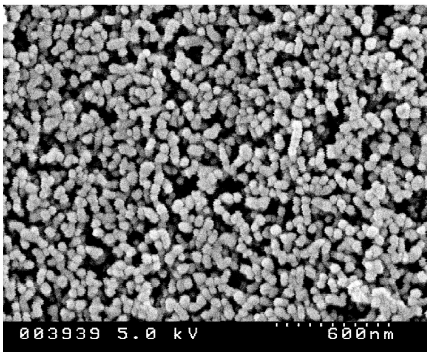

Figure 3. An SEM image of 40-nm aluminum powder produced by inert gas condensation (IGC).

The formation of soft agglomerates is unavoidable during routine powder processing and handling. The particles are agglomerated and exist as large collections of loosely associated particles upon collection in the manufacturing process, but they can be deagglomerated to yield discrete nanoparticles. As an undispersed powder in suspension, a sample of 40-nm n-Al is easily filtered using a 20-micron grade filter because the agglomerates behave more like particles of several microns. In circumstances where these agglomerates collect on the surface of a filter with much larger pores, the agglomerates create a filter with much finer pore size. Thus, the resulting network of soft agglomerates creates a "self-filter" at the nanometer scale.

Figure 4 clearly shows the inner metallic core and the amorphous oxide shell. The electron diffraction pattern from the core of a n-Al particle indicates its crystalline nature. Further, the oxide shell is consistently amorphous regardless of shell thickness or particle size, with no crystallinity apparent on any of the oxide coating locations. Elemental mapping of the nano-aluminum powder was used to confirm the presence of oxygen exclusively at the particle surface (Figure 5).

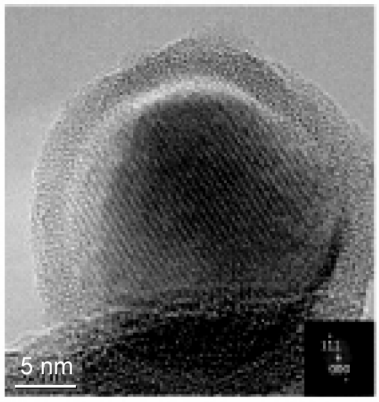

Figure 4. A transmission electron photomicrograph showing a 30-nm aluminum particle with a 3-nm oxide shell. The inset shows a selected-area diffraction pattern indicating a single-crystal and metallic aluminum core.

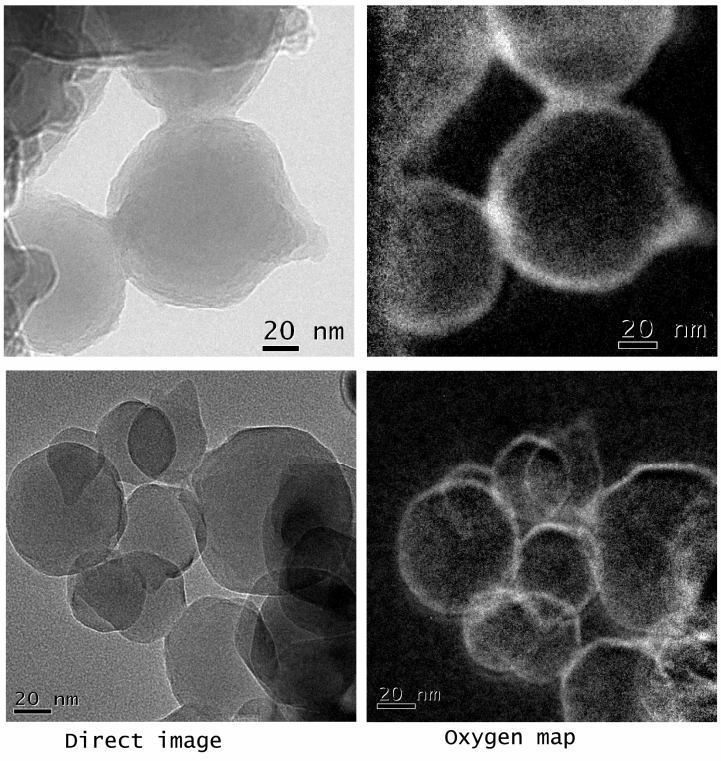

Figure 5. Elemental mapping, performed in a TEM, confirming the presence of oxygen solely in the alumina coatings of the n-Al powder.

Powder Analysis

Routine characterization is performed on every kilogram of powder produced. Analysis includes thermogravametric analysis (TGA) and particle size measurement by the gas adsorption technique and the Brunauer, Emmett and Teller (BET) calculation. The TGA and BET analyses are quantitative and well suited to quality control in a production facility where cost, maintenance and sample turn-around time of analysis results are crucial. The results from the TGA and BET analyses also provide good comparisons with the less standard electron microscopy tools. In combination these analysis tools provide a great deal of information about the physical properties of the nano-aluminum. To date an accurate methodology for measuring the particle size distribution (PSD) of n-Al produced by IGC has not been found, however, and more work is required. The specifics of particle size distribution will be discussed in more detail below. A summary of the calculation of the physical properties of n-Al from the analytical measurements follows.

Determination of Particle Size from BET

The BET surface area technique is used to calculate a mean particle size, d. The BET instrument introduces nitrogen gas into a test tube containing a known mass of powder and measures the volume of gas adsorbed on the surface. This value—divided by the mass of the sample—gives the specific surface area, σ, of the powder in m^2/g. Since the particles contained in the sample are spherical, combining the equations for the volume and surface area of a sphere allows the calculation of a mean particle diameter, d, as:

$$d = \frac{6}{\rho\sigma} \qquad (1)$$

where ρ is the density of the powder. Although the theoretical density of aluminum oxide (Al_2O_3) is 3.97 g/cm^3, pycnometry results have shown that the actual density of aluminum oxide is closer to 3.2 g/cm^3, which is the value used in all particle size calculations.

Determination of Oxide Thickness and Weight-Percent Metal from TGA

The second analysis performed on the powder is a thermogravimetric analysis or TGA. The TGA instrument measures the weight gained when the n-Al powder is heated in an atmosphere of 25% oxygen and 75% argon. The measured weight gain is then divided by the initial weight of the sample to determine the weight gain, Δm. A representative TGA curve indicating how Δm is determined is shown in Figure 6. Once Δm is known, it is used to calculate the oxide thickness and metal content of the powder as described below.

For the particle illustrated in Figure 7 the number of Al atoms in the core is:

$$\text{No. of Al atoms} = \frac{m_{Al} N_A}{A_{Al}} \qquad (2)$$

where m_{Al} is the mass of the Al core, N_A is Avogadro's number and A_{Al} is the atomic weight of aluminum. Furthermore, since the mass of the particle can be expressed in terms of its volume and density, Eq. 2 can be rewritten as:

$$\text{No. of Al atoms} = \frac{V_{Al} \rho_{Al} N_A}{A_{Al}} \qquad (3)$$

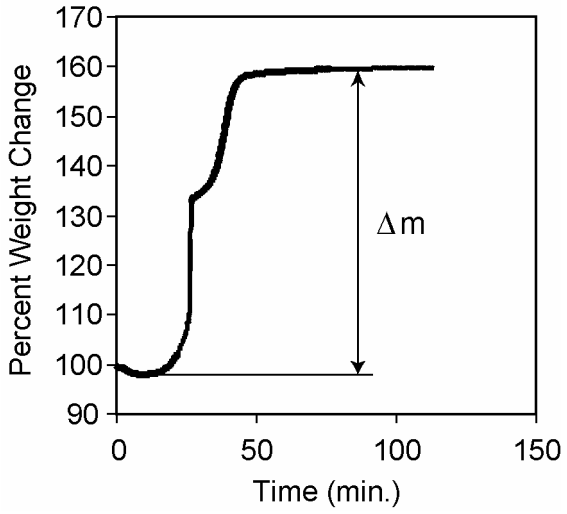

Figure 6. A representative TGA curve for a n-Al sample with the total weight gain, Δm, is shown.

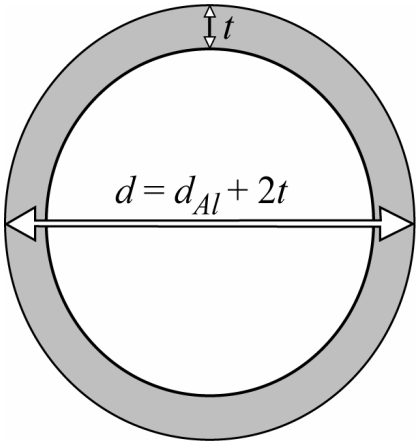

Figure 7. A spherical n-Al powder particle consists of an aluminum core with diameter equal to d_{Al}, surrounded by a thin oxide layer with a thickness of "t".

where V_{Al} is the volume of the core and ρ_{Al} is the density of Al.

The following analysis assumes that the oxide coating is stoichiometric Al_2O_3. The number of oxygen atoms, O, required to oxidize the aluminum core is 3/2 times the number of Al atoms based on the balanced equation for the oxidation of aluminum with molecular oxygen:

$$2\ Al_{(s)} + 3/2\ O_2 \rightarrow Al_2O_{3(s)}$$

$$\text{No. O atoms} = \frac{3}{2}\left(\frac{V_{Al}\rho_{Al}N_A}{A_{Al}}\right) \tag{4}$$

The added weight of these oxygen atoms is:

$$m_{ox} = \frac{3}{2}\left(\frac{V_{Al}\rho_{Al}N_A}{A_{Al}}\right)\frac{A_O}{N_A} = \frac{3A_O}{2A_{Al}}V_{Al}\rho_{Al} \tag{5}$$

Since the initial weight, w_{init}, of the particle is:

$$w_{init} = m_{Al} + m_{core} = V_{Al}\rho_{Al} + V_{ox}\rho_{ox} \tag{6}$$

the percent weight gain upon oxidation is:

$$\%\ \text{wt gain} = \frac{m_{ox}}{w_{init}} \times 100 = \frac{\frac{3A_O}{2A_{Al}}V_{Al}\rho_{Al}}{V_{Al}\rho_{Al} + V_{ox}\rho_{ox}} \times 100 = \Delta m \tag{7}$$

and Δm is the value reported by the TGA instrument. Equation 7 can be rearranged to solve for the ratio of the volume of the oxide to the volume of aluminum (β) so that:

$$\frac{V_{ox}}{V_{Al}} = \frac{\rho_{Al}}{\rho_{ox}}\left(\frac{3A_O}{2A_{Al}}\frac{100}{\Delta m} - 1\right) = \beta \tag{8}$$

The utility of Eq. 8 is that it allows the calculation of β directly from the percent weight gain as measured by the TGA, and this ratio is instrumental in calculating the particle's oxide thickness and the volume percent aluminum oxide, and other values, as described below.

For a spherical particle, Eq. 1 can be rearranged to give an expression for the specific surface area, σ, so that:

$$\sigma = \frac{6}{\rho d} \tag{9}$$

where d is the diameter of the particle as shown in Figure 7, and ρ is the density of the particle. For nano-Al particles this density is:

$$\rho = \frac{m}{V} = \frac{m_{ox} + m_{Al}}{V_{ox} + V_{Al}} = \frac{\rho_{ox}V_{ox} + \rho_{Al}V_{Al}}{V_{ox} + V_{Al}} \tag{10}$$

where V, which represents the total volume of the spherical particle, is calculated as:

$$V = \frac{\pi d^3}{6} \tag{11}$$

The total volume of a nano-Al particle is also equal to the sum of the volumes of the oxide shell, V_{ox}, and the aluminum core, V_{Al}, or:

$$V = V_{ox} + V_{Al} \tag{12}$$

Rearranging Eq. 11 to solve for the diameter of the particle and substituting in Eq. 12 gives:

$$d = \left(\frac{6(V_{ox} + V_{Al})}{\pi}\right)^{\frac{1}{3}} \quad \text{OR}$$

$$d^3 = \frac{6(\beta + 1)V_{Al}}{\pi} = \frac{36\pi(1+\beta)^2}{\sigma^3(\rho_{Al} + \beta\rho_{ox})} \tag{13}$$

Now, inserting Eqs. 10 and 13 into Eq. 9 allows the calculation of the specific surface area of the particle as:

$$\sigma = \frac{6(V_{ox}+V_{Al})}{(\rho_{ox}V_{ox}+\rho_{Al}V_{Al})\left[\frac{6(V_{ox}+V_{Al})}{\pi}\right]^{\frac{1}{3}}} = \frac{(36\pi)^{\frac{1}{3}}(V_{ox}+V_{Al})^{\frac{2}{3}}}{(\rho_{ox}V_{ox}+\rho_{Al}V_{Al})} \quad (14)$$

Substituting Eq. 8 into Eq. 14 and rearranging gives an expression for V_{Al} in terms of β:

$$V_{Al} = \frac{36\pi(1+\beta)^2}{\sigma^3(\rho_{Al}+\beta\rho_{ox})} \quad (15)$$

Having an expression for V_{Al} and utilizing that expression in Eq. 11 allows the calculation of the diameter of the aluminum core, labeled d_{Al} in Figure 7 as:

$$d_{Al} = \left(\frac{6V_{Al}}{\pi}\right)^{\frac{1}{3}} = \frac{6(1+\beta)^{\frac{2}{3}}}{\sigma(\rho_{Al}+\beta\rho_{ox})^{\frac{1}{3}}} \quad (16)$$

To determine the thickness of the oxide, the diameter of the aluminum core given in Eq. 16 must be subtracted from the total diameter given in Eq. 13. This task is simplified if both expressions are written in terms of β. Rewriting Eq. 13 in terms of β gives:

$$d = \frac{6(1+\beta)}{\sigma(\rho_{Al}+\beta\rho_{ox})} \quad (17)$$

Now, solving for the oxide shell thickness represented by t in Figure 7:

$$t = \frac{d-d_{Al}}{2} = \frac{3(1+\beta)^{\frac{2}{3}}}{\sigma(\rho_{Al}+\beta\rho_{ox})^{\frac{1}{3}}}\left[(1+\beta)^{\frac{1}{3}}-1\right] \quad (18)$$

The next parameter calculates the weight percent aluminum, which is related to the energy content of the particle.

$$\text{wt\% Al} = \frac{\rho_{Al}V_{Al}}{\rho_{ox}V_{ox}+\rho_{Al}V_{Al}}\times 100\% = \frac{2A_{Al}\Delta m}{3A_O} \quad (19)$$

Similarly, other values of interest can be simultaneously calculated by:

$$\text{vol\% Al} = \frac{V_{Al}}{V_{ox}+V_{Al}}\times 100\% = \frac{1}{\beta+1}\times 100\% \quad (20)$$

$$\text{vol\% aluminum oxide} = \frac{V_{ox}}{V_{ox}+V_{Al}}\times 100\% = \frac{\beta}{\beta+1}\times 100\% \quad (21)$$

$$\text{wt\% oxide} = \frac{\rho_{ox}V_{ox}}{\rho_{ox}V_{ox}+\rho_{Al}V_{Al}}\times 100\% = \left(1-\frac{2A_{Al}\Delta m}{300A_O}\right)\times 100\% \quad (22)$$

Process and Equipment

The manufacture of nano-aluminum is a vacuum process operating in the 1 to 10 torr range. High purity aluminum (grade 1199, 99.99% pure) is automatically fed into the reactor and introduced to a heated ceramic surface. The ceramic boats are resistively heated titanium diboride/ boron nitride at temperatures of roughly 2000 ºC and have inert gas flowing past them. The high temperatures at and near the boat surface mandate active cooling for many of the reactor fittings and surfaces. Upon contact with the heated boat, the aluminum wire is melted and spread over a controlled portion of the boat. The boat surface temperature is kept above the melting its boiling point (2467 ºC) to yield a steady evaporation rate from the heated surface. As vapor phase aluminum molecules travel away from the heated surface, they nucleate to form multi-atom clusters that are the genesis of individual nanoparticles. Subsequent growth in the aluminum vapor leads to the formation of discrete particles in the nanometer size range. As the particles travel from the heated growth zone, they cool and crystallize. The particles are shaped during this portion of the process. Nano-aluminum particles are typically spherical due to the high surface tension acting upon the particles in the molten formation phase. The growth zone is limited to a small fraction of the distance between the heated boats and the collection apparatus. The various reactors that have been used to scale

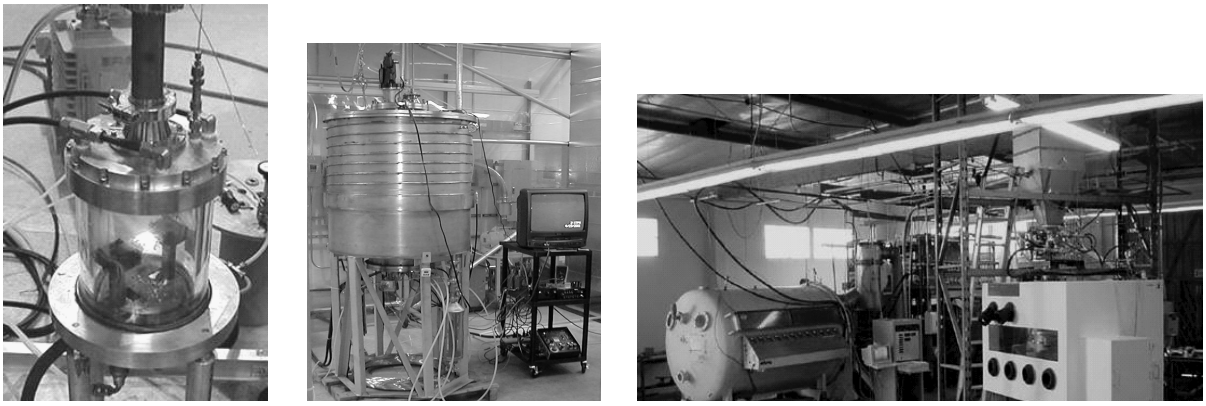

a. **b.** **c.**

*Figure 8. Technanogy Materials Development has scaled its n-Al production from **(a)** a 1 gram per hour to **(b)** a semi-continuous 40 gram per hour level (~ 1 kg/day). TMD's latest production level **(c)** is at 300 grams per hour (> 7 kg/day) in a continuously operating reactor (c) that also integrated a conveyance and packaging system.*

n-Al production to current levels are shown in Figure 8.

An important part of the nano-aluminum production process is the method in which oxygen is introduced to the powder stream. The passivating oxide shell must be formed only after particles of the correct size have been formed but before they congeal and cluster into larger particles or aggregate clusters that will not break apart. Precise control of the level of oxygen used to passivate the powder and the location at which the powder stream is exposed to the passivating gas are keys to this process. When properly introduced, the passivating oxygen forms a thin oxide layer around each n-Al particle that prevents them from forming aggregates. The particles are cooled as they are carried in the gas stream to the collection zone. Collecting the aluminum powder on a dry filter at near-ambient temperature and low pressure tends to form soft agglomerates, but it maintains the distinct character of individual particles. When the powder is removed from the collection filters, it is sent as an agglomerated cake to a collection zone via a series of vacuum valves. A schematic of TMD's manufacturing equipment is shown in Figure 9.

Handling and transferring the n-Al powder is accomplished by one of several processes that

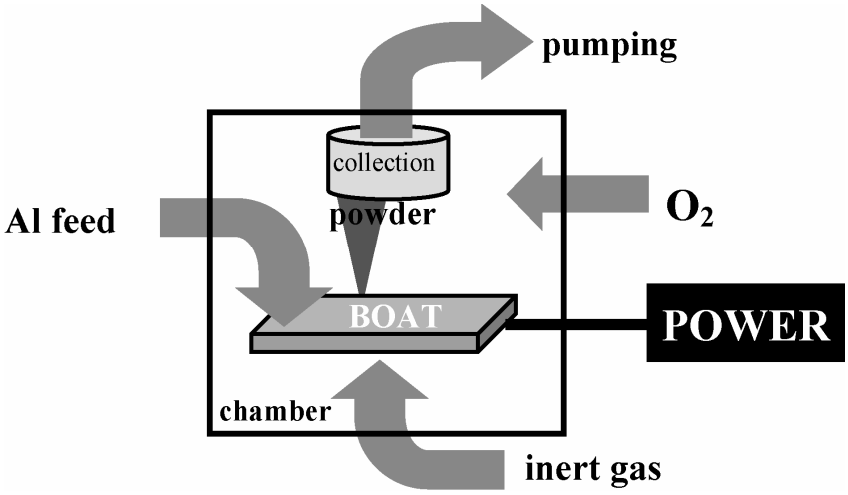

Figure 9. A schematic of TMD's nano-aluminum production process.

rely on an inert atmosphere of dry, oxygen-free purge gas. For example, the powder can be pneumatically transferred to an inert atmosphere glove box where it can be processed and packaged for shipment. In many instances the powder is still partially active due to imperfections in the passivation layer. Incomplete passivation may result from particles with incomplete oxide shells colliding and forming a zone of aluminum metal underexposed to oxygen. These clusters may resist passivation due to the inaccessibility of the active aluminum surface to oxygen. This sticking behavior is common for very small powder (< 40 nm) with a minimal oxide shell thickness (~2 nm). In such cases the level of passivation gas is low enough to lead to inhomogeneities in the powder. Under-passivation can be addressed by exposing all powder to a post-passivation process in which a batch of powder (approximately one kilogram) is mechanically agitated while being exposed to a low level of oxygen-containing gas. As the mechanical action breaks apart the particle agglomerates and exposes any under-passivated aluminum surfaces, the oxidation is carried out at a slow, controllable level. This post-passivation process is microprocessor controlled to prevent a runaway oxidation reaction. After the post-passivation treatment, the powder is fully coated with native oxide and is safe to handle. The n-Al is then sieved to clean and de-clump the material into a smooth, free flowing powder. The powder is then packaged under inert gas in metal cans with airtight lids, sampled for quality control and stored in a flammable materials cabinet.

Nano-Aluminum Powder Properties and Reactivity

Nano-aluminum powder is a broad term for aluminum with particle size in the sub-micron range. Typically, nanopowder is reserved for powders below 0.1 μm in diameter.[4] TMD focuses exclusively on n-Al powder in the size range between 20 and 200 nm. In spite of this reasonably small size range, the properties of this class of materials are amazingly dependent on both size and oxide shell thickness. The most obvious distinction between various-sized nanoscale aluminum powders is their color. Micron-sized aluminum powder is typically a light, metallic gray color. Nano-aluminum powder below 200 nm is dark gray. The color darkens as the particle size decreases. Typically, powder below roughly 40 nm is black. Figure 10 shows the color difference between >200-nm powder (gray) and 40-nm powder (black).

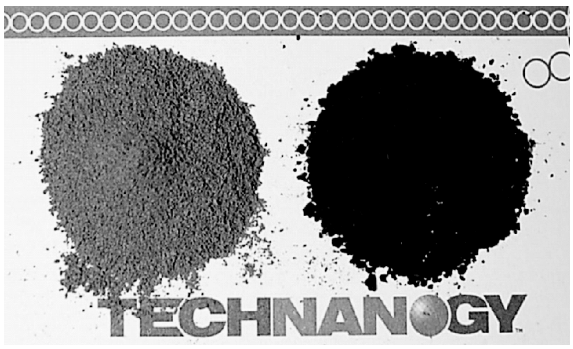

Figure 10. The color of aluminum is strongly related to particle size. Typically 200-nm powder is gray (left) and 40-nm powder is black (right).

The bulk density of aluminum powder is also strongly dependent on particle size. In general the smallest sizes of n-Al are very light and fluffy and exhibit bulk densities as low as 0.1 g/cm^3. Larger particle sizes exhibit bulk densities above 1.5 g/cm^3. The difference between micron- and nanometer-sized aluminum powders is also evident in the powder's surface area (and therefore all surface-area dependent properties such as reactivity). Figure 1 shows that the aluminum content decreases as particle size decreases for a fixed oxide shell thickness. The aluminum content of n-Al is one indicator of the large role that surface to volume ratio plays in nanopowders. A one-micron aluminum powder with a 3.0-nm oxide shell has a specific surface area of roughly 2.2 m^2/g and an aluminum metal content of 98%. A 40-nm n-Al powder with a 3.0-nm oxide shell would be only 57% aluminum metal by weight and would have a surface area of over 51 m^2/g. The high surface area of nanopowders is illustrated by considering a 100 g mass of aluminum metal, a mass roughly equivalent to the size of a golf ball. The surface area of this 100 g piece of aluminum would be 5.4×10^{-3} m^2, approximately the size of a typical 3-inch Post-It® note. When this 100 g mass of

aluminum is converted into 40-nm powder the surface area is increased to 5,500 m^2, or roughly the size of a soccer field. The single golf ball mass of aluminum would be converted into 10^{18} 40-nm n-Al particles, or roughly one particle for ever square centimeter of land on the planet Earth.

High surface areas translate to materials with very high reactivities. For example, a one-micron aluminum powder will burn only with a significant energy input (several hundred degrees of heat). In contrast, a 40-nm n-Al powder sample will burn very rapidly upon immediate exposure to an open flame. Many of the energetic applications of nano-aluminum rely on its increased reactivity directly attributed to its high surface area. Superthermites, initiators, igniters, rapid burning propellants and munition primers all capitalize on decreased diffusion distances for reactive species in contact with nano-aluminum. Another level of control over n-Al powder reactivity can be achieved by adjusting the thickness of the oxide shell on the particles. With independent control over both powder size and oxide thickness, the inert gas condensation method can deliver powders with specific energy density and energy release rate. Decreasing the oxide shell of a 40-nm n-Al powder from 3.0 to 1.5 nm increases the Al metal content in the powder from 57% to over 77%. A thin oxide layer increases the sensitivity of the powder and augments its stored energy, but this reactivity performance increase is achieved by decreasing the overall stability of the powder.

Powders with an oxide shell thickness less than 2.0 nm are generally considered unstable in the open atmosphere. Oxide shells thinner than 1.5 nm appear to be inadequate to protect nano-aluminum from pyrophoric behavior in air, or the formation of hard agglomerates during powder production. The reactivity of aluminum metal is well known, and exposed metal will reduce virtually any chemical species exposed to an unpassivated surface. The thermodynamic driving force (heat of reaction) for the oxidation of aluminum metal by molecular oxygen to form amorphous Al_2O_3 (alumina), ΔH^o, is –1676 kJ/mol.[7] Similarly, large thermodynamic driving forces also exist for the reduction of water, nitrogen, carbon dioxide and most metal oxides. A concern with aluminum powder stability is the initiation of a redox reaction that results from the exposure to either unpassivated metal or metal with a flaw in the passivating layer. Another route to chemical instability is the adsorption of moisture on the oxide surface. The hydration of the aluminum oxide surface can liberate heat (ΔH^o = 860 kJ/mol[7]) and destabilize the n-Al powder in one of several suspected routes.

One potential mechanism is that Al_2O_3 reacts with water vapor to form aluminum hydrates producing enough heat that thermal expansion of the aluminum core cracks the oxide shell. Aluminum metal thus exposed to the atmosphere would then react further with oxygen or moisture to liberate more heat as metal is converted to oxide. A single reacting particle is not a threat to destabilize an entire lot of n-Al as long as it remains an isolated event. If the exothermic oxidation energy propagates to nearby particles and is sufficient to initiate a similar oxidation event, then it is possible that a runaway reaction may proceed to completion. It is the initiation of oxidation of individual nano-aluminum particles under ambient condition, and the propagation of the heat to other particles that determines the pyrophoric behavior of n-Al. When an aluminum powder fire has initiated and the reaction is sustainable, it is nearly impossible to extinguish. The burning temperature of bulk nano-aluminum has been estimated at greater than 2500 ºC. At this temperature the aluminum metal will react with most anything including oxygen, water, nitrogen, carbon dioxide and carbonates in common class C fire extinguishers. The heat of this reaction will obviously melt most structural materials. Preventing undesired reactions is of paramount importance. Providing a n-Al product that can be safely handled in air is an important capability. Maintaining a minimum oxide shell thickness for all routine orders, post passivating the powder to quench any unpredictable reactivity, handling the powder in a controlled inert atmosphere, and packaging the powder in dry nitrogen are all important aspects of a commitment to safe handling.

The presence of adsorbed water on n-Al powder can have adverse effects even when safety is not a primary factor. Nano-aluminum powder will generally adsorb roughly five-weight percent water from the atmosphere within minutes of exposure. Moisture is liable to have adverse

effects on the end uses of the powder. Incorporating a powder containing five-weight percent water into a rocket propellant, or other pyrotechnic, may be problematic. The performance of propellants that contain reactive organics, moisture sensitive inorganic oxidizers, or water sensitive curing components may deteriorate in the presence of unintended levels of water. The formulation of n-Al into many other products may also be adversely affected by carrying unwanted water into the mixture. A high surface area power such as n-Al is well known to alter the rheology of most mixtures and can lead to increases of slurry viscosities by thousands of centipoise. Water may likely act to further affect the rheology or induce phase separation during or subsequent to the formulation process. A final detriment that surface adsorbed water may present is in the n-Al powder stability. In the presence of water the aluminum particles are liable to react, especially during processing or storage conditions that exceed room temperature or pressure. These disadvantages of surface moisture are the basis for a policy of not exposing n-Al to the open atmosphere.

To quantify the degree of powder aging, via the growth of the oxide coating over time, thermogravimetric analysis was performed repeatedly on specific lots of powder. The weight gain was translated into oxide shell thickness as discussed above and graphed versus time in Figure 11 for a specific powder lot. The trend indicates that the oxide layer will stabilize after about 2000 hours (about 3 months) of exposure to air. Several factors influence the aging behavior of n-Al powder including the atmosphere under which the powder is stored, the beginning oxide shell thickness and the particle size.

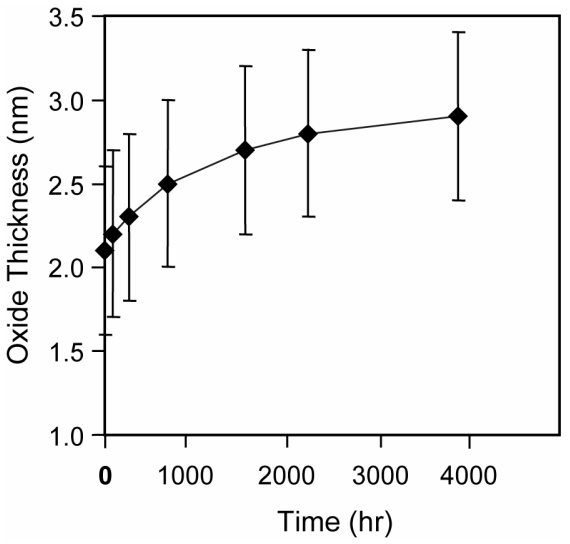

Figure 11. Plot of oxide coating thickness versus time for n-Al powder B080901B for storage in a non-air-tight clear glass vial. Note the error bar is ± 0.5 nm.

Particle Size Distribution

The particle size distribution (PSD) of powders can be measured in a variety of ways. One of the most common techniques for the analysis of ultrafine powders is the use of laser light scattering. Sophisticated instruments detect the reflected, refracted and scattered light from a laser's interaction with a suspended powder and then use complex models to compute the particle size distribution of the powder. This technology has been widely and successfully used for powders in the micron size range. Laser scattering has also been employed for various powder materials below 100 nm in size. The analysis of n-Al by laser light scattering has not been successfully accomplished to date. The most significant challenge to the use of laser light scattering for n-Al PSD appears to be the formation of stable, nonagglomerated dispersions of the material. Work continues to explore this technique for aluminum analysis. Other optical and particle counting technologies commercialized for the analysis of powders (particle counters, sieves, classifiers, etc.) are ineffective for n-Al, which is too small to be analyzed by methods that rely on mechanical techniques.

In the absence of a quantitative tool for PSD analysis the use of qualitative methods for determining size distribution information is possible. Powder color is the most obvious and the least quantitative. The use of electronic microscopy is a widely accepted tool for estimating PSD. Imaging over many fields of view with care—to accurately sample the powder—can provide an indication of PSD, but there are limitations to this approach.

Considering that one large particle in a sample of many million may skew a weighted distribution, it is important to look at many different

microscopic images of a given powder, to gain confidence in the true PSD. Imaging nanometer-sized powders intermixed with large micron-sized particles is complicated by the tendency for small particles to coat the large particles, obscuring the larger ones from the field of view. It is likely that SEM and TEM particle sizing will underestimate the mean size and the maximum particle size. BET analysis does not provide information about PSD, as it can only give the mean particle size calculated from a measurement of the specific surface area. TGA analyses also can be used to give information about PSD by studying the shape of the curve. The onset temperature of aluminum particle oxidation is dependent on particle size. Smaller particles are oxidized much more readily than larger ones and exhibit a weight gain on the TGA in an early, sharp curve. Larger particles tend to oxidize more slowly and persist at elevated temperatures in the TGA (>850 ºC) for many hours. The presence of unreacted aluminum in the later stages of a given TGA run may be used to suggest a broad PSD with large particles present. Extracting information about the size distribution of an aluminum powder sample by combining the information provided in electron microscopy, BET and TGA is possible, but it is time consuming and subject to many sources of error.

The particle size of nano-aluminum powder has been extensively evaluated using a combination of all of the techniques described above. The PSD of the n-Al is believed to be tightest at lower mean particle sizes. For example, powder with a mean particle size of 40 nm has been shown to have a very tight distribution with the vast majority of the particles below 60 nm in diameter. As the mean size of the powder increases, the PSD is believed to broaden. Powder with a mean particle size of 100 nm has a high fraction of particles that exceed 500 nm in diameter. TMD's 200-nm powder has an even higher fraction of large particles. SEM images of TMD's 200-nm powder reveal the presence of particles well above one micron in size. The physical basis for the broadening of the powder PSD as size increases is likely due to the contrasting process conditions between the production of the smallest (< 40 nm) and the largest (~200 nm) powders.

Applications

End uses for nano-aluminum were initially largely energetic and dominated by defense-related applications. Small caliber primers for defense munitions, additives for solid and hybrid rocket propellants, enhanced lethality explosives and thermite-based weapons had been widely researched and continue to be developed by government research laboratories. The interest in these applications prior to the year 2000 made them the most natural source for early commercial development, and defense and energetic applications continue to be important. Application development and collaborative research to accelerate the use of n-Al powder is ongoing with a number of public and private organizations in this area. During the last two years the non-defense energetic market for n-Al has also been explored. Private companies have probed the use of n-Al for products in pyrotechnics and fireworks, automotive inflators and airbag initiators as well as drilling and oil exploration. This sector of the market appears to rival the size of the government energetic market and is looked to as an area of expansion.

The largest growth area for nano-aluminum commercialization during the past three years has been in non-government, non-energetic applications. Recent interest in n-Al as an additive for plastics, a base material for sintering and consolidation, the formation of fully dense materials with nanoscale grain structures and the production of devices that capitalize on n-Al's special electrical properties are most notable. Unique properties and attributes of this nanomaterial continue to lead to innovative end uses for the product. The development of new products using n-Al has occurred in many different ways. In most cases customers require very little information about the material and work to produce products with little to no communication with the manufacturer. Other products are developed in close collaboration and in certain cases joint programs have been initiated that formalize relationships that draw from the strengths of one or more external collaborators.

Summary

TMD has demonstrated that it is possible to produce commercial quantities of n-Al by an inert gas condensation method. The n-Al powder is characterized by using a number of conventional analytical techniques such as TGA, BET and electron microscopy. More work is required on the important analytical challenge of n-Al particle size distribution. Energetic and non-energetic applications are being actively developed and the list of customers and applications continues to grow. Nano-aluminum powder price and quality are endless areas of development for TMD as it evolves to meet the needs of this emerging market.

References

1) H. S. Nalwa, *Handbook of Nanostructured Materials and Nanotechnology*, Vol. 1, Academic Press, San Diego, 1999.

2) V. Haas, R. Birdinger and H. Gleiter, "Preparation and Characterization of Compacts from Nanostructured Powder Produced in an Aerosol Flow Condenser", *Mater. Sci. and Eng.*, A246 (1998) p 86.

3) S. J. Savage and O. Grinder, "Ultra-Fine Powder Production Methods: An Overview," in *Novel Powder Processing – Advances in Powder Metallurgy and Particulate Materials*, J.M. Campus and R.M. German Eds., American Powder Metallurgy Institute, 1992, pp 1–17.

4) C. G. Granquist and R. A. Buhrman, "Ultrafine metal particles", *J. App. Physics*, Vol. 47 (1976) pp 2200.

5) M. K. Datta, S. K. Pabi, and B. S. Murty, "Thermal Stability of Nanocrystalline Ni Silicides Synthesized by Mechanical Alloying", *Mater. Sci. and Eng.*, A284 (2000) p 219.

6) C. Hiyashi, R. Uyeda and A. Tasaki, Eds., *Ultra-Fine Particles: Exploratory Science and Technology*, Noyes Publications, 1997.

7) *CRC Handbook of Chemistry and Physics*, 37th ed., CRC Press, Boca Raton, FL.

Essential Molecular Orbital Theory for the Study of Pyrotechnics

R. B. Lowry
School of Earth, Ocean and Environmental Sciences, Univ. of Plymouth, Drake Circus, Plymouth PL4 8AA UK

ABSTRACT

The Linear Combination of Atomic Orbitals (LCAO) model is presented as it applies to small heterogeneous molecules. A non-mathematical approach is used to enable the discussion of the terminology used. The production of light and the rules that govern it are examined.

Keywords: linear combination of atomic orbitals, LCAO, energy level, electronic transitions, color, molecular orbital theory

Introduction

The purity of colors produced by pyrotechnic compositions, together with the intensity of the light, is of utmost importance if a display is to capture the audience. The chemistry behind the production of these effects is not understood fully, but to make further improvements it will be necessary to consider the basic physical processes that lead to luminescence. This article considers the changes in energy of the electrons within the molecules of interest. To do so, the fundamental model of bonding within molecules will be considered so that the energy of the electrons can be evaluated. Only the essential parts of the model, as is necessary to the study of flame colors, will be discussed. The transitions between these energy levels are what leads to the production of light and, hopefully, a high-impact display.

Molecular Orbitals

When atoms come together to form molecules, and bonds form between them, the bonding electrons are "shared" between the atoms. In other words, these electrons are no longer held by one atom only, but orbit two (or more) atoms. There are a variety of different methods of considering this, but the most useful one when considering the energies of these orbitals is the so-called *Linear Combination of Atomic Orbitals* (LCAO) method. This assumes that *molecular orbitals* (MOs) can be "built" by combining two or more atomic orbitals. The mathematical method involves adding the wave functions that describe the individual atomic orbitals. For the purposes of this paper, it will be sufficient to consider the shapes of the atomic orbitals and their resultant MOs.

When two atomic orbitals interact to form molecular orbitals, two MOs are formed. One of these is lower in energy and hence stabilises the molecule. This is the *bonding orbital* and one way of looking at this is that the two atomic orbitals interfere constructively to form one MO. The other MO is higher in energy, hence destabilises the molecule and is called the *anti-bonding orbital*. This can be viewed as the two atomic orbitals interfering destructively to form two half-orbitals that repel each other. Figure 1 illustrates these two processes. Atomic orbitals that do not interact to participate in bonding are called *non-bonding orbitals* and the bonding process does not affect their energies.

Energy and Symmetry

For the majority of molecules, the number of possible interactions between atomic orbitals to form MOs is huge. However, several considerations reduce the number of possibilities:

- Only atomic orbitals of similar energies can combine to form MOs.

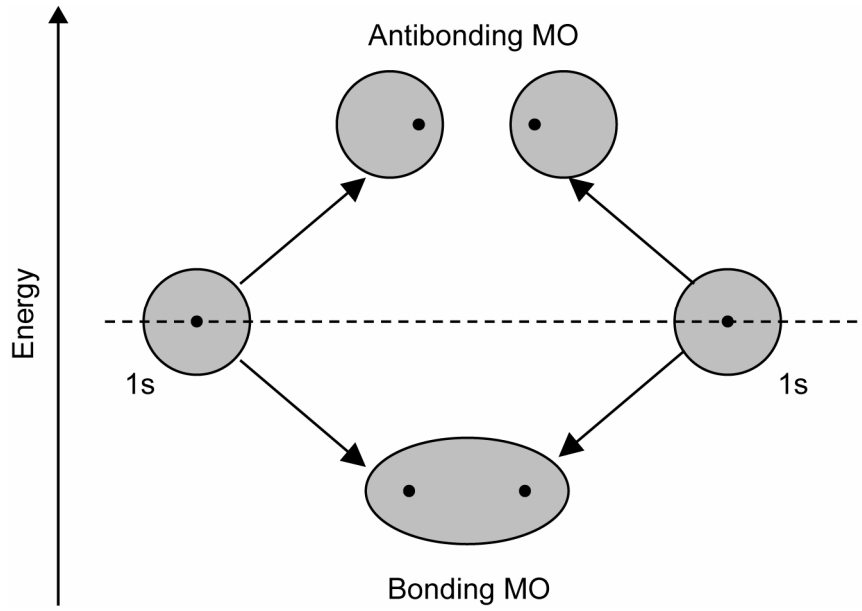

Figure 1. Combination of two atomic orbitals to form two molecular orbitals.

- Atomic orbitals from filled shells from two very different elements do not interact due to the difference in energies.
- Atomic orbitals from filled shells from similar elements can combine to form MOs, but there is no net effect upon bonding (see below).
- Only atomic orbitals of similar symmetry can combine to form MOs.

The notion of symmetry arises because there must be a significant overlap of the two atomic orbitals if a MO is to form. In addition, in heavier atoms, as the nuclear charge rises, the energy of each of the shells changes due to the increase in attraction between the nucleus and the electrons. Thus, it is possible to get sufficient overlap between orbitals from different shells providing there is a significant difference in the atomic masses. Figure 2 shows how the $3p_z$ orbital of Cl can interact with the 4s orbital of Ca. The $3p_y$ or $3p_x$ orbitals would not overlap significantly and hence cannot form MOs under these circumstances.

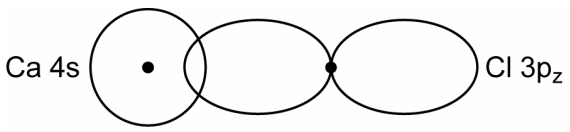

Figure 2. Illustration of how the $3p_z$ orbital of chlorine can interact with the 4s orbital of calcium.

MO Labels

To identify particular MOs, we ascribe labels to them. These labels have three parts:

1) σ ,π or n. This denotes whether the MO is a single envelope along the internuclear axis (σ) or one with two lobes—one above and one below the axis (π). Each MO can contain only two electrons, even if it has two lobes, much like a p orbital can only accept 2 electrons. A π bond is the second bond in a double bond, the first being a σ bond. n denotes a non-bonding orbital.
2) If a MO is marked with a superscript asterisk, it denotes that the MO is an anti-bonding one. Bonding MOs are unmarked
3) MOs are numbered consecutively from 1, with 1 being the orbital with the lowest energy. σ and π type MOs each have their own numeric series.

Unfortunately, there is more than one labelling scheme in place for MOs. The differences

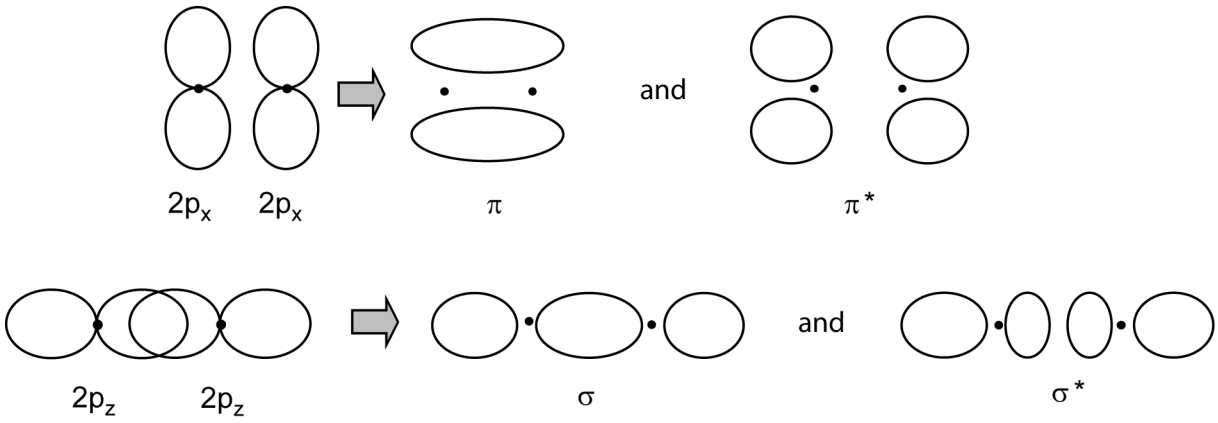

Figure 3. Example of the molecular orbitals and labels that arise when 2p orbitals from two atoms overlap.

are small, but significant care must be taken when comparing data from different sources.

Figure 3 shows the MOs and labels that arise when the 2p orbitals from two atoms overlap. These MOs would be involved in the bonding of the O_2 molecule, together with the σ and σ^* MOs formed from the combination of the 2s orbitals. Diagrams such as that in Figure 3 are useful to visualise a MO, but give no indication of the energy and therefore whether the MO contains any electrons. To demonstrate this, an energy level diagram similar to that in Figure 4 is used. In this figure, the diagram for the O_2 molecule is shown. The order of the MOs is not fixed, but varies as their energies change due to different elements. Another contributing factor is that the 2s and $2p_z$ atomic orbitals can interact, providing their energies are sufficiently similar. This is not the case in the O_2 molecule.

Figure 4 shows that there are 12 electrons involved in the MOs shown in the diagram. However, some are in bonding orbitals and some are in anti-bonding orbitals. The net effect of a filled bonding orbital and a filled anti-bonding orbital is no bond. Thus, the 1σ and $2\sigma^*$ orbitals cancel one another. Similarly, there are four 1π electrons and two $2\pi^*$ electrons which results in one bond. The 3σ MO is filled, whilst the $4\sigma^*$ is not. Hence this is another bond. Therefore, the O_2 molecule is held together by a double bond. The electronic configuration of the molecule can be quoted in a similar way to that used for atoms, O_2 having the configuration $1\sigma^2 2\sigma^{*2} 3\sigma^2 1\pi^4 2\pi^{*2}$.

The oxygen molecule also illustrates another property that exists in molecular orbitals. The two highest energy electrons exist in two MOs that are degenerate (have the same energy). Under these conditions, Hund's rule operates, just as it does in single atoms. Thus, the lowest energy state possible (the ground state) has the two electrons in separate MOs. Since these two electrons are not paired, they are free to take up (and change) any spin direction. This means that there are three possible situations: both spin "up", both spin "down" and one spin "up" and one "down". Note that "up"/"down" is the same as "down"/"up" as it is impossible to tell the difference between the two electrons. Therefore this electronic state can exist in three different ways and is called a triplet state. If the electrons were forced to pair up, then there is only one possible way that this can happen and so this is called a singlet state. The number of ways that a state can exist is called the *multiplicity*.

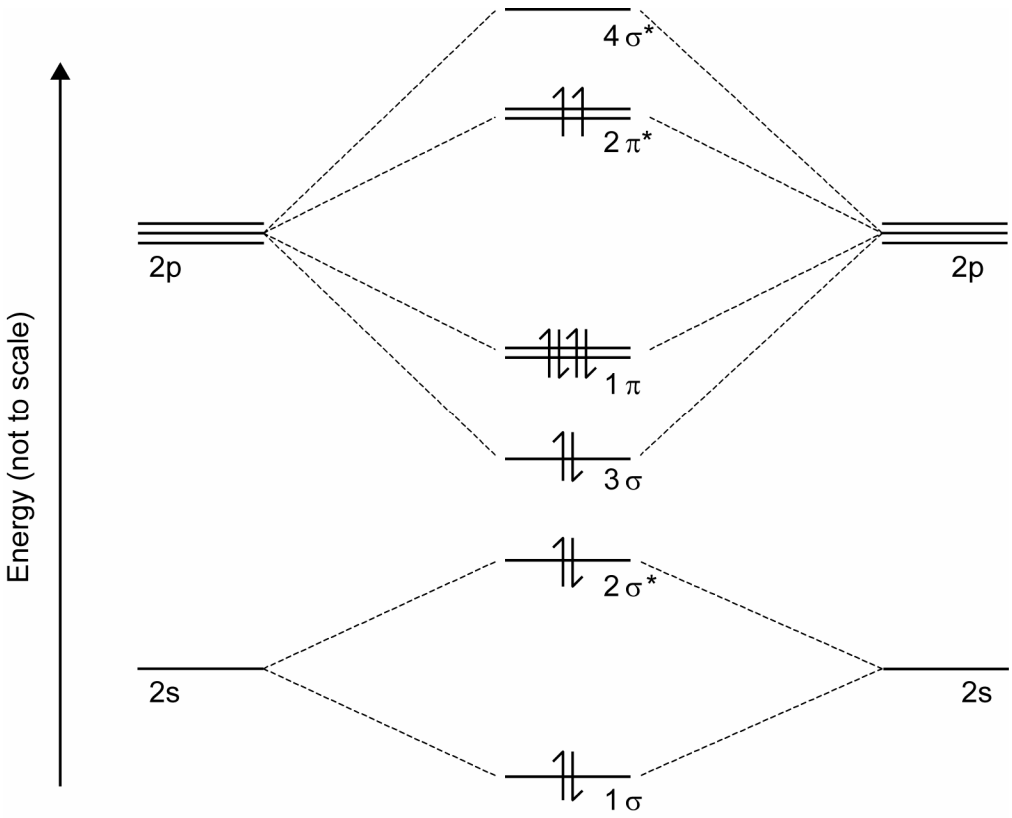

Figure 4. The MO diagram for O_2.

Excited States

If a molecule absorbs energy, or is created in such a way that it is not in a state of minimal energy, it is described as being in an excited state. This excess energy is manifested within the bonding of the molecule as the electrons are being distributed amongst the MOs in a way that is different to the ground state. This will involve more electrons existing in higher energy MOs. Thus, for O_2 the configuration $1\sigma^2 2\sigma^{*2} 3\sigma^2 1\pi^3 2\pi^{*3}$ is an excited state.

Term Symbols

Electronic configurations can be abbreviated and further information incorporated using *term symbols*. Filled orbitals do not contribute to the information in term symbols. The main part of the symbol is a capital Greek letter; Σ, Π or Δ. This part of the symbol contains information about which MOs are occupied. Each σ electron contributes 0 and each π electron +1. If there are two degenerate π orbitals, one contributes +1 and the other –1. These values are summed and written according to the code $\Sigma = 0$, $\Pi = 1$ and $\Delta = 2$. The other part of the symbol is the multiplicity and is written as a superscript before the Greek letter. The ground state of O_2 is therefore described as $^3\Sigma$. Other information can be attached to the term symbol, but is concerned with the mathematical representation of the MOs and will not concern us here.

Transitions

The emission of light from small molecules is caused by the relaxation of the molecule from an excited state to a lower (frequently ground) state. However, not all transitions are allowed, but are constrained by a series of selection rules. These rules specify which transitions are allowed based upon the term symbols of the excited and ground state. The selection rules for transitions between MOs are:

1) The Greek letter is allowed to remain the same, or change by one.

2) The multiplicity must not change.

In effect, the first rule forbids transitions from Σ to Δ or vice versa. In fact, these transitions can be observed, but occur rarely. This results in very weak output of light and is therefore not of interest in this context. The second rule can also be broken when one or more heavy atoms are present. The pyrotechnic emitters SrCl, BaOH, etc. are in this class.

The color of the light emitted as the molecule relaxes from excited state to ground state depends upon the difference in energy between the two states. Thus, the light emitted by SrOH at 606 nm can be used to calculate the difference in energy between the ground state and the excited state. In this case, it is 3.28×10^{-19} J. The ground state of SrOH is $^2\Sigma$ and applying the selection rules above leads to the deduction that the excited state is probably a $^2\Sigma$ state as well.

Studying Electronic Transitions

Electronic transitions can be studied by the use of a spectrometer, which measures the intensity of the incident light as a function of wavelength. Given the transitory nature of the species responsible for producing light in pyrotechnics, the study of these species has not been easy. Some studies have been performed that generate the species continuously under very specific conditions.[1,2] However, the growth of video technology has allowed real pyrotechnic events to be captured and then the data studied later.[3] Studies such as these can allow the correct identification of the species involved in the production of light and the conditions necessary for the efficient manufacture of the correct excited state. This can only lead to purer, brighter pyrotechnics.

References

1) M. A. Anderson, M. D. Allen, W. L. Barclay, Jr. and L. M. Ziurys, "The Millimeter and Sub-Millimeter Spectrum of the BaOH Radical", *Chemical Physics Letters,* Vol. 205 (1993) p 415.

2) M. A. Anderson, W. L. Barclay, Jr., and L. M. Ziurys, "The Millimeter-Wave Spectrum of the SrOH and SrOD Radicals", *Chemical Physics Letters,* Vol. 196 (1992) p 166.

3) K. L. and B. J. Kosanke, "Development of a Video Spectrometer", *Journal of Pyrotechnics*, No. 7 (1998) p 37.

Bibliography

W. G. Richards, and P. R. Scott, *Energy Levels in Atoms and Molecules.,* Oxford Science Publications, 1994.

J. M. Hollas, *Basic Atomic and Molecular Spectroscopy,* Royal Society of Chemistry, 2002.

R. W. B. Pearse and A. G. Gaydon, *The Identification of Molecular Spectra*, John Wiley, 1976.

P. Atkins and J. de Paula, *Physical Chemistry,* Oxford University Press, 2002.

Guanidinium Azo-Tetrazolate (GAT) as a High Performance Hybrid Rocket Fuel Additive

M. Keith Hudson,* Ann M. Wright,‡ Chris Luchini,* Paul C. Wynne,* and Sterling Rooke*

* Department of Applied Science and Graduate Institute of Technology
University of Arkansas at Little Rock, Little Rock, AR 72204, USA

‡ Department of Physics, Hendrix College, Conway, AR 72032, USA

ABSTRACT

The purpose of this investigation was to find a high regression rate fuel suitable for use as a mixture with hydroxyl-terminated polybutadiene (HTPB). Guanidinium azo-tetrazolate (GAT) is the compound that was the focus of our research. GAT is a salt containing a high percentage of nitrogen. It has two conjugated nitrogen rings, which are negatively charged, and a positively charged component consisting of nitrogen, carbon, and hydrogen. In addition to the high-energy content of this compound, as a salt, it has a lower heat of degradation due to the ease of breaking its ionic bonds.

GAT was found to react with N100, a common curative for HTPB. An alternative isocyanate curative was found, polyisocyanate (PAPI), with which it did not react. This polymer matrix was found to be suitable for GAT. The resulting fuel grains were difficult to cast due to the rapid polymerization of the HTPB/PAPI. Once grains were cast, they required no special care in storage or firing.

The fuel grains with the GAT additive were fired for 3-second runs with oxygen flows of 0.04, 0.06, 0.08, 0.10 and 0.12 lbm/s. The regression rate of each GAT concentration was computed and plotted vs. the oxidizer mass flux on a log/log scale. The resultant curve is fit to the equation, $r = aG_o^b$*, and the quantities a and b were recorded for each curve.*

GAT was found to increase the regression rate of HTPB when it was used as an additive. The resultant pressure and thrust from firing even the highest GAT concentrations at high oxygen flows still remained within safe operating parameters of the UALR hybrid rocket motor facility.

Keywords: GAT, guanidinium azo-tetrazolate, GZT, HTPB, hybrid rocket fuel, ground testing, regression rate

Conversion from English to Metric Units.

1 lbm = 1 pound mass = 454 grams
1 lb = 1 pound = 454 grams
1" = 1 in. = 1 inch = 25.4 mm
1 psia = 1 pound per square inch = 0.145 kPa

Introduction

The hybrid rocket facility at the University of Arkansas at Little Rock (UALR) consists of a labscale hybrid rocket motor, several transducers to measure various physical properties such as pressure and thrust, a control computer, and a data acquisition computer. The facility was originally built to investigate combustion instabilities and plume diagnostics.[1,2,3] Several hybrid rocket fuels and fuel additives have also been studied.

One quantization of hybrid rocket fuel performance is regression rate. The regression rate of a fuel is the rate of fuel depletion from the surface of the fuel grain during combustion, measured in inches per second. Generally speaking, regression provides a measure of how much of the solid fuel is burning for a given time. Hence an increase in regression implies an increase in thrust and output and therefore performance. Regression is relatively easy to study and quantify and is often used for basic comparisons of fuels. Since this was the first study of guanidinium azo-tetrazolate (GAT), we decided to utilize regression as a basis for com-

parison to plain HTPB and HTPB with other additives. Regression rate is calculated as:

$$r = \frac{\left[\left(\sqrt{\frac{m_i - m_f}{\rho \pi l} + r_i^2}\right) - r_i\right]}{t} \qquad (1)$$

where r is the regression rate (in./s); m_i is the initial fuel mass; m_f is the final fuel mass (g); r_i is the initial fuel port radius; r_f is the final fuel port radius (in.), ρ is the fuel mass density (g/in^3); l is the fuel grain length (in.); and t is the burn time (s). While the formula provides average regression rates, it also provides a good description of the motor for short burn times.

The standard fuel used in hybrid rockets is hydroxyl-terminated polybutadiene (HTPB). This fuel is characterized by a low rate of regression. Several fuel additives have been proposed and/or studied to determine if those additives increase the regression rate and improve the performance of the hybrid rocket fuel. One such additive is guanidinium azo-tetrazolate (GAT).

GAT is an organic salt with high nitrogen content. It is a highly energetic compound due to the energy stored in the π-bond system. The regression rate of this additive is large because it is a salt.[4] The large size of the ions in GAT, along with relatively low ion charge, leads to a relatively low heat of degradation. The bond structure of GAT is shown in Figure 1.[5] The authors know of no published thermodynamic data for GAT, with the exception of calculated values for computational studies.[6]

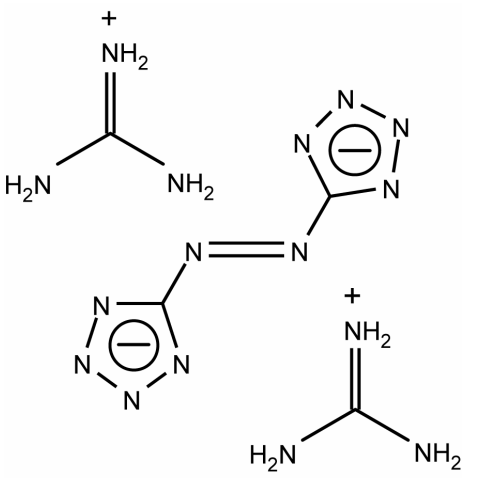

Figure 1. The bond structure of guanidinium azo-tetrazolate (GAT).

The work in this paper was done in two steps. Initially, the feasibility of using GAT as a fuel additive with HTPB was studied. The results of that study detailed solutions to problems in the casting of the fuel grains and the possibility of increased regression rate. However, more data was needed to fully describe the properties of the GAT/HTPB fuel mixtures and to determine reliable regression rates. At that point, a much larger amount of GAT was synthesized at the UALR Rocket and Combustion Laboratory. Fuel grains were cast with various percentages of GAT and a complete regression rate study was performed.

Experimental

Initial investigation of the suitability of GAT included testing using a Mettler Model DSC 20 Differential Scanning Calorimeter. Test results confirmed that GAT releases a large amount of energy and generates high quantities of gas when it reaches its thermal degradation point at about 220 °C. Additional lab studies were performed to ascertain the reactivity, if any, of GAT with HTPB resin and, N100 curative or polyisocyanate (PAPI) curative. The guanidinium component of the GAT salt was found to react with the N100 curative, releasing hydrogen gas. A test grain made with N100, HTPB, and GAT formed a foam, about one and a half times its original volume. All further polymerization and fuel grain studies were performed using PAPI as the curative, which does not react with GAT. The use of PAPI also had the effect of speeding up the curing process, so the amount of dibutyltin dilaurate was adjusted to help slow the curing process to allow proper grain casting. If the mixture sets up too quickly, voids are too easily formed.

GAT, as used in firings, was synthesized in the laboratory starting with the precursors 5-animotetrazole (Olin Chemicals) and guanidinium hydrochloride (Aldrich Chemicals). This synthesis was necessary due to the fact that there are no commercial producers. Small batches were made using standard lab glassware and following the procedure of Hiskey et al.[5] These amounts were thoroughly dried and combined

with the HTPB/PAPI polymer. This mixture was then mixed for 60 seconds, and 10 microliters of dibutyltin dilaurate was added to catalyze the polymerization process. The grains had to be cast as quickly as possible because the mixture became unpourable within ten minutes. Initially, each grain contained 15% GAT, 1% graphite (added as an opacifier), with the balance made up of a polymer base containing 85% HTPB and 15% PAPI.

Rocket fuel grain casting for the labscale system is accomplished using a 10-inch paper phenolic casing, sized to fit the inside of the combustion chamber (2 in). A mandrel is used to form the cylindrical grain that results in a 0.75-inch diameter bore. Firings of the GAT/ HTPB mixtures were made using our labscale hybrid rocket system, which has a 2 × 10-inch thruster, capable of operating at pressures to 500 psi and supporting oxygen flows to 0.16 lbm/s. This system is computer controlled and is instrumented for pressure. Additional details on the Hybrid Rocket Facility may be found in a previous papers.[1,2]

GAT was mixed in several percentages by mass with HTPB, and PAPI was used as the curative agent. Fuel grains were prepared in 15, 20, 25 and 30% by mass concentrations of GAT. Graphite was added to the fuel grain mixture at 1% by mass concentration as an opacifier. The remaining fuel composition was again a mixture of 85% HTPB and 15% PAPI.

The fuel grains were fired in the UALR hybrid rocket. To ascertain the magnitude of the difference that the addition of GAT would have, an initial set of six firings at 0.06 lbm/s oxygen flow were performed. These firings were used to set the conditions for a test matrix for data reporting. The gaseous oxygen flow was then varied between 0.04 and 0.12 lbm/s in 0.02 lbm/s increments. Each percentage of GAT fuel was fired at each of the oxygen flow rates, for a total of 20 firings. The mass and the initial and final port radii of the fuel grain were measured for each run. The rocket was fired for three seconds per run. Regression rate was calculated for each run using equation 1. Results are presented in Table 1.

For each percentage GAT fuel, regression rate r vs. oxidizer mass flux G_o was plotted on a log/log scale. The five data points for each percentage GAT were plotted and fit to the equation

Table 1. Regression Rate Results.

Fuel Run	O_2 Mass Flux, G_o (lb/in.^{2}s)	Regression (in./s)
0% GAT		
1	0.0565	0.034
2	0.102	0.039
3	0.113	0.038
4	0.115	0.030
5	0.123	0.027
15% GAT		
1	0.057	0.032
2	0.068	0.028
3	0.090	0.031
4	0.101	0.040
5	0.197	0.049
20% GAT		
1	0.072	0.037
2	0.099	0.044
3	0.138	0.054
4	0.156	0.051
5	0.178	0.055
25% GAT		
1	0.073	0.038
2	0.089	0.034
3	0.100	0.045
4	0.138	0.043
5	0.156	0.053
30% GAT		
1	0.049	0.029
2	0.083	0.036
3	0.097	0.047
4	0.110	0.039
5	0.150	0.055

$$r = aG_o^b \tag{2}$$

Fit results for the regression rate calculations are presented in Table 2, and the curves are shown in Figures 2 to 5.

Table 2. Fit Results for the Regression Rate Calculation $r = aG_o^b$.

Fuel	a	b
15% GAT	0.099	0.435
20% GAT	0.113	0.416
25% GAT	0.107	0.418
30% GAT	0.156	0.559

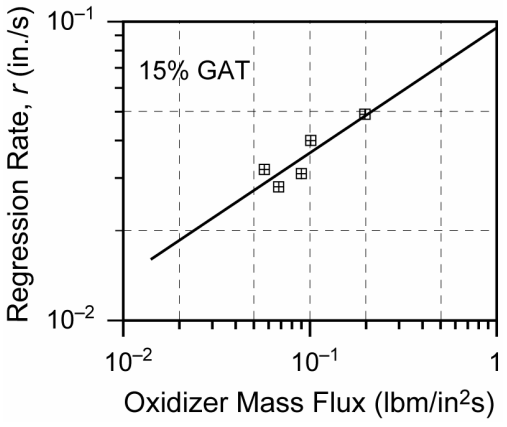

Figure 2. 15% GAT regression rate.

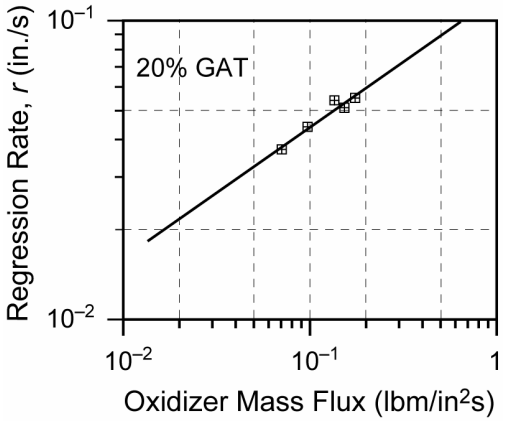

Figure 3. 20% GAT regression rate.

Results and Discussion

The addition of GAT to the standard hybrid rocket fuel, HTPB, increased the regression rate and therefore the performance of the fuel. Regression rates in general are increased not only by degradation but also by the release of energy by the azo-compounds during combustion. In addition, this compound breaks down into more reactive radicals with higher volume per unit mass. Casting of GAT grains was somewhat difficult. Due to the relatively fast polymerization of the HTPB/PAPI, thoroughly mixing the catalyst into the fuel creates small bubbles. These generally do not have time to escape before the polymer solidifies. This problem can be overcome by investigating alternative HTPB/PAPI base polymer mixes to slow the polymerization process. Otherwise the resulting GAT fuel grains were satisfactory for storage and labscale hybrid

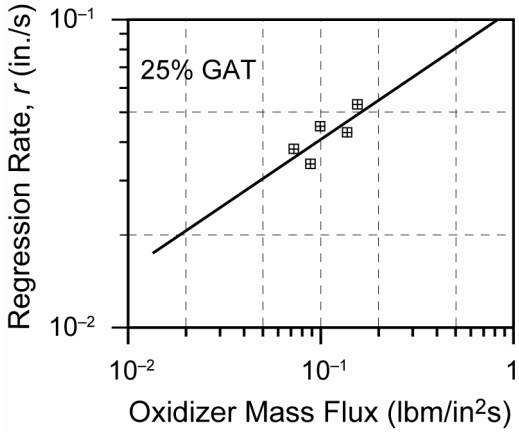

Figure 4. 25% GAT regression rate.

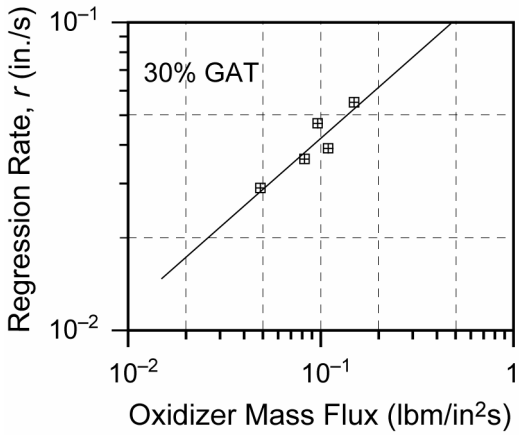

Figure 5. 30% GAT regression rate.

testing, with the GAT dissolving completely at the percent concentrations tested in this study.

Our first firing of GAT was performed at a 20% by mass concentration level, but high-pressure conditions (over 575 psi), felt to be due to a high regression rate, caused a system safety shutdown. Another five test firings were conducted on fuel grains using a lesser percentage GAT additive (15% by mass concentration), and suitable data was obtained for these to indicate safe firing parameters. We had expected this firing to generate perhaps 300 psi. Another five test firings were conducted on 15% by mass concentration of GAT fuel grains, and suitable data was obtained for these to indicate safe firing parameters. These tests indicated the conditions for the test matrix that resulted in Table 1. Tables 1 and 2 show that the addition of GAT increases the performance as measured by fuel port regression for a set oxygen mass flux. See

Figure 6 for a comparison of the various percentages of GAT. This increase can be as much as 150% when compared to the firing of plain HTPB grain. For example, a "plain HTPB" fuel grain (one containing no regression additives) in previous work showed a regression rate of 0.0363 in./s for an oxidizer mass flux of 0.1562 lbm/(in.^{2}·s).[2]

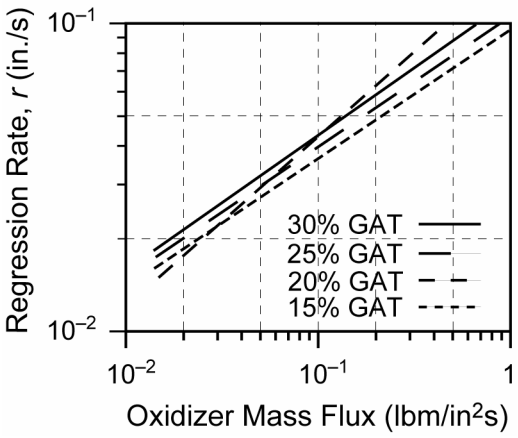

Figure 6. Comparison of all GAT firings reported. Note the increase in regression rate for each percentage increase (with the exception of the 20% line).

Utilization of GAT/HTPB fuel therefore shows significant promise when compared to plain HTPB.

It is felt that the addition of GAT gives an increase in regression due to several factors. One is that GAT has a lower degradation temperature and takes less energy to pyrolyze than HTPB. However, GAT releases significantly more energy during its degradation than HTPB and does so at the fuel surface. This results in even more fuel breakdown, including both GAT and HTPB. GAT should break down into highly reactive radicals with a high gas volume per unit mass. This high volume tends to sweep the fuels from the degradation zone into the combustion zone more quickly than the relatively lower volume gases produced by HTPB and related fuels. The properties of GAT may also result in the physical ejection of fuel particles into the burn zone of the chamber and the plume during firing, adding to a higher regression rate.

A possible concern with using GAT as a fuel additive is the increased risk of environmentally dangerous compounds, such as NO, released in the plume. Preliminary UV-Vis absorption data does not show significant amounts of NO in the plume of the fuel grains fired in this study.[7]

Conclusions

GAT has been shown to increase the regression rate of HTPB fuel in hybrid rockets as much as 150% when compared to plain HTPB. However, the synthesis of GAT is time consuming and difficult on the lab scale. Also, the components needed to synthesize GAT are moderately expensive. This expense will be diminished on a production scale due to buying the chemical components in bulk and streamlining the production process.

Acknowledgments

We would like to thank the National Aeronautics and Space Administration for NASA Grant NCCW-55 and the Arkansas Space Grant Consortium for student scholarships, which have supported this work and underwritten the operation of the rocket facility. Thanks to Armand Tomany for machine fabrication and to Mike Hiskey for supplying his synthesis procedure and a small amount of GAT. Special appreciation is extended to Ken Kalb, Warfield Teague, Kari Maxwell, and Daryl Breithaupt for their assistance on this project.

Portions of this work were presented at the 1996 and 1998 AIAA Joint Propulsion Conferences as papers 96-2592 and 98-3186.

References

1) R. B. Shanks and M. K. Hudson, "The Design and Control of a Labscale Hybrid Rocket Facility for Spectroscopic Studies", AIAA Paper No. 94-3016, June 1994.

2) R. Shanks and M. K. Hudson, "A Labscale Hybrid Rocket Motor for Instrumentation Studies", *Journal of Pyrotechnics*, No. 11 (2000) pp 1–10.

3) M. K. Hudson, R. Shanks, D. Snider, D. Lindquist, "UV, Visible, and Infrared Spectral Emissions in Hybrid Rocket Plumes", *International Journal of Turbo and Jet Engines*, Vol. 15 (1998) pp 71–87.

4) G. Lengelle, B. Fourest, J. C. Godon, and C. Guin, "Condensed Phase Behavior and Ablation Rate of Fuels for Hybrid Propulsion", AIAA Paper No. 93-2413, June, 1993.

5) M. Hiskey, N. Goldman, and J. R. Stine, "High-Nitrogen Energetic Materials Derived From Azo-Tetrazolate", unpublished manuscript, Los Alamos National Laboratory, January, 1996.

6) C. Chen, M.H. Liu, S.R. Cheng, and L.S. Wu, "Theoretical Study of the Inter-Ionic Hydrogen Bonding in the GZT Molecular System", *Journal of the Chinese Chemical Society*, 50 (2003) pp 765–775.

7) M. W. Teague, J. R. Welborn, T. M. Flelix, M. K. Hudson, and J. Willis, "UV-Vis Absorption as a Diagnostic for NO in Rocket Plumes", *International Journal of Turbo and Jet Engines*, Vol. 13 (1996) pp 211–21.

Editorial Policy

Articles accepted for publication in the *Journal of Pyrotechnics* can be on any technical subject in pyrotechnics. However, a strong preference will be given to articles reporting on research (conducted by professionals or serious individual experimenters) and to review articles (either at an advanced or tutorial level). Both long and short articles will be gladly accepted. Also, responsible letters commenting on past Journal articles will be published, along with responses by the authors.

A Report on the Fireworks Accident at Carmel, Western Australia

R. I. Grose[+] and K. L. Kosanke*

[+] Defence Science and Technology Laboratory, Porton Down, Salisbury, Wiltshire, SP4 0JQ, UK

* PyroLabs, Inc., 1775 Blair Road, Whitewater, CO 81527, USA

ABSTRACT

The investigation into an accident at Carmel, Western Australia in March 2002 found that the magnitude of explosions occurring in licensed and unlicensed storage areas was significantly greater than would have been expected from the UN hazard classification of items stored within them. Use of revised UN default classification tables for the items in storage, instead of the previous classification, goes towards accounting for the violence of the explosions. The official report into the accident makes a number of recommendations that are of direct international relevance, such as a minimum safety distance of 400 m (from residential housing or defined vulnerable facilities) for licensed UN Hazard Division 1.1 magazines regardless of mass of contents (above 50 kg minimum), removal of a concession that allows for the temporary storage of fireworks in unlicensed areas for up to 14 days prior to a display, the adoption of the UN default classification table throughout Western Australia and the importation of incorrectly classified fireworks to be made an offence.

Keywords : Carmel explosion, UN hazard classification, safety distance, unlicensed storage

Introduction

On 6th March 2002, a fireworks storage facility at Carmel, near Perth in Western Australia, was severely damaged by a number of explosions and fires. There were three major explosions, occurring over a period of 14 minutes, which resulted in the total destruction of some storage units and serious damage to a number of others. Significant damage was caused to several houses and structures in the vicinity of the site, and shrapnel pieces produced by the explosions were found several hundreds of metres away from the explosion sites. The incident did not result in death or injury, but this can only be regarded as being fortunate.

The incident was thoroughly examined by the statutory investigatory body (the Department of Mineral and Petroleum Resources (MPR), Western Australia), which published a detailed report[1] of the incident in a commendably thorough, well documented and timely manner (the report was published in July 2002). In addition to containing a description of the events at the facility and in its vicinity, the report makes a number of recommendations, the implementation of which may have significant consequences for the worldwide pyrotechnic community.

This paper briefly describes the events at Carmel and also briefly examines the recommendations made by the investigatory body. Some of the nine main recommendations made in the MPR report are intended for introduction within the state of Western Australia, some are directed towards federal implementation across Australia and a number are of potential worldwide applicability. This report of the incident and presentation of the recommendations arising from an incident at Carmel is consistent with this Journal's commitment to the advancement of pyrotechnics through the sharing of information.

Brief Summary of the Carmel Incident

A comprehensive report and examination of the incident is contained in an official MPR report.[1] The description in this paper is a brief summary of those events. However, it should be acknowledged that much of the information in this summary and in the MPR report relies heavily on statements provided by the operators of the facility. In some instances, record keeping was not sufficiently detailed to confirm the statements from the operators. In other instances, the physical evidence is contrary to the statements of the operators. The net result is that the conclusions presented in this article and MPR report cannot be considered absolutely reliable. Also, while one of the authors of this paper has had discussions with one of the on site investigators of this incident, it must be acknowledged that the authors have neither inspected the site nor participated in the investigation of the incident.

The facility at Carmel was operated by a fireworks importer and display company. As such, the main business activity of this company was the storage and preparation of fireworks intended for public displays. Pyrotechnic items for those displays were imported into Australia for storage at Carmel; from there, they would be taken to display sites throughout the country. The first firework storage license for the Carmel site was issued in 1985, and this was subsequently altered and added to several times prior to the incident.

There were four licensed storage magazines (termed M1 to M4) present on the site. The details of these magazines are given in Table 1, and their distribution around the site is presented in Figure 1.

The normal practice in the days prior to a display was to remove the required items from magazine storage to temporary preparation areas for sorting, assembly, preparation and dispatch to the display venue. The temporary preparation areas used consisted of freight containers, termed FC1 to FC4 in Figure 1. Use of such temporary areas for processing and storage was permitted at the time of the incident, although the incident report notes that the regulatory body was unaware of the placement on-site of container FC4.

The trigger for the chain of events that led to the explosions at Carmel reportedly started in Shed 2. Container FC3 was primarily used for the storage of mortars and the preparation of various display pieces. The shed in which FC3 was located was used for the storage of unfired ground pack tubes, full ground packs (also called cakes or cake items), rolls of quick match, lances and portfires. On the morning of 6th March 2002, it is estimated that Shed 2 contained a range of items, such as confetti bombs, quick match, fountains and a quantity of electric fuseheads (electric matches).

Reportedly, as a 25-shot ground pack was placed on a bench within Shed 2, a shot initiated. This initiated the rest of the shots within the pack. Within a few seconds, burning stars ejected from the ground pack initiated other

Table 1. Licensed Magazines at Carmel Site.

Magazine	Description[a]	Licensed Capacity[b]	Estimated Content (NEQ)[c] on 6 March 2002
M1	10 t steel container	5000 kg HD 1.4	700 kg ground-level items
M2	10 t steel container	5000 kg HD 1.4	725 kg ground packs
M3	Steel container	300 kg HD 1.3	941 kg aerial shells (up to 300 mm) and salutes (up to 75 mm)[d]
M4	Steel container	1500 kg HD 1.3	1626 kg (aerial shells, up to 400 mm)

a) t = metric ton.

b) HD = hazard division.

c) NEQ = Net Explosive Quantity (mass of explosive material in items, excluding packaging).

d) The initial contents estimate is given. The contents were later reported to be 300 kg.[1]

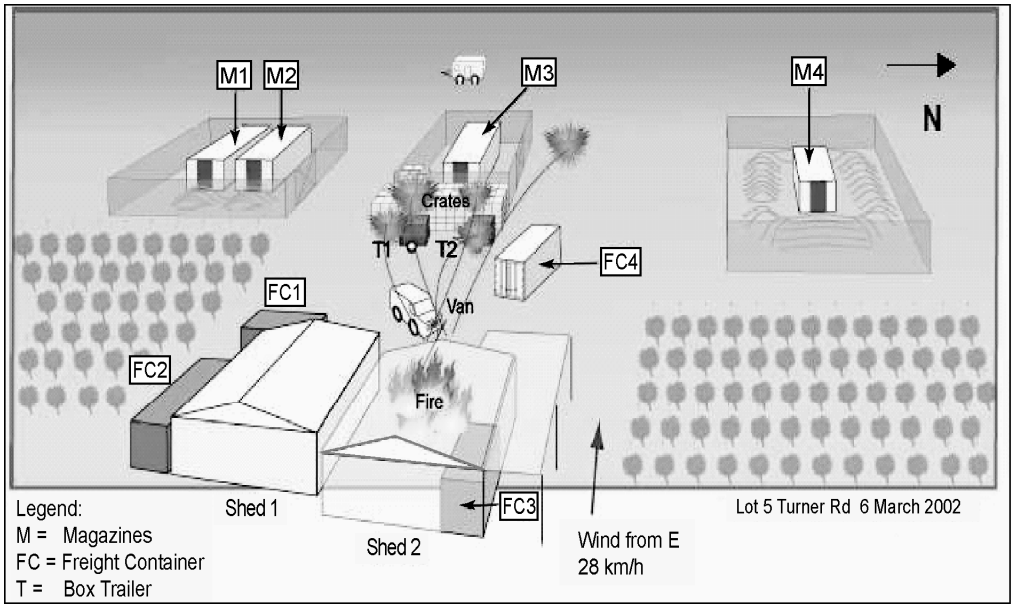

Figure 1. Outline plan of Carmel site (during initial phase of incident).

items stored within the container and the shed. The staff present within the shed quickly assessed the situation as being out of control and left the building. Many burning items were observed coming out of the shed through the open door in the direction of container FC4. Soon the adjacent shed was also ignited by the fire, which spread to containers FC1 and FC2, eventually completely destroying them.

Witnesses reported seeing effects from ground packs being fired through the roller door of the shed towards container FC4. This container, the placement of which was unknown to the licensing authority, was positioned 16 m from the door of Shed 2 with the doors of FC4 opening in the direction of Shed 2. There were plastic crates, empty cardboard boxes and a quantity of wooden stakes stored close to the container walls. It is likely that stars from the ground packs struck and ignited the combustible material. Based on witness statements that the doors of FC4 were closed at the time, the ignition of the contents of FC4 would seem to have been as a result of the ignition of its contents from the heat conducted through the steel walls of the container. This is known to be sufficient to ignite the contents of such containers, and the effects of external fires on fireworks stored in steel ISO containers have been recently described in this Journal.[2] However, there is physical evidence that suggests one of the doors of FC4 was at least partially open at the time. If that was the case, the fairly rapid ignition of the contents of FC4 is even more understandable.

Shortly after the ignition of materials inside FC4, it exploded violently, sending a large quantity of steel shrapnel pieces toward magazines M2 and M3. These magazines were penetrated by the shrapnel pieces, and their contents were initiated by impact, friction or heat from the impacting fragments or, more likely, from a combination of these mechanisms. Around 5 minutes after the explosion in FC4, the contents of M2 underwent a partial detonation or a rapid deflagration. There was insufficient evidence to determine which of these explosion mechanisms was responsible for the resultant pressurization of the steel container, which failed at its welded seams. Some parts of the structure, such as roof panels and doors, were projected a short distance, and the remaining burning contents were ejected from the container.

Eleven minutes after the partial destruction of M2, magazine M3 was completely destroyed by a large explosion of unexpected violence. The investigation attributed this explosion to the partial detonation or rapid deflagration of the contents. Witnesses reported a large fireball (approximately 100 m in diameter), and a large

cloud of smoke following this explosion. Small pieces of hot shrapnel were projected several hundred meters from the magazine site by the explosion in M3. Only the floor of M3 remained – the door (weighing 170 kg) was projected 370 m and the roof (380 kg) was found 295 m away. The rest of the magazine had fragmented.

Hot fragments from the explosion of M3 penetrated magazine M1, initiating its contents. No explosion occurred in this magazine, but its contents were consumed by fire. The air blast from the explosion of M3 toppled M1 over by 90 degrees.

Magazine M4, which was protected by a surrounding earth mound, was unaffected by fire or explosion. It is considered that this was due to

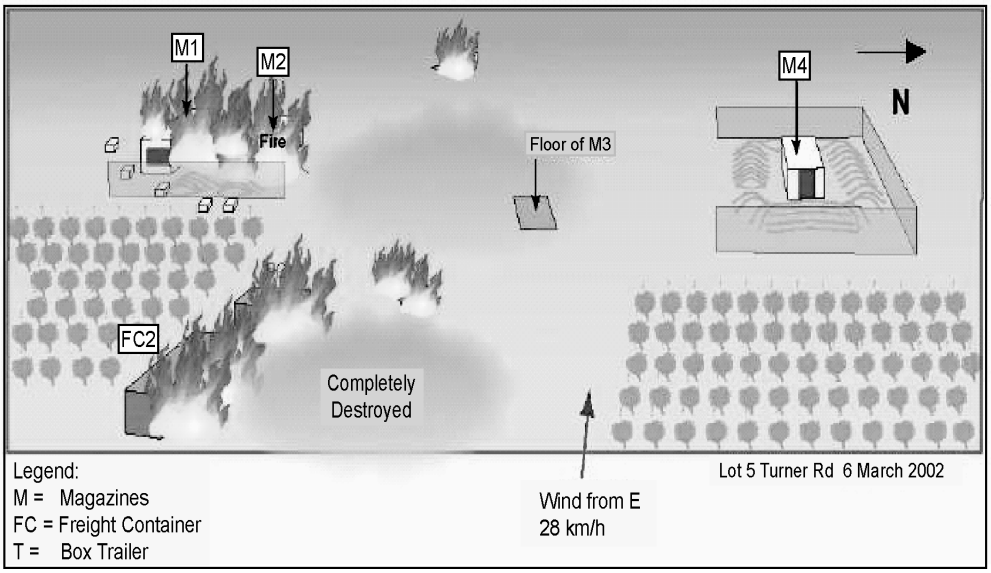

Figure 2. Location of structures following explosions.

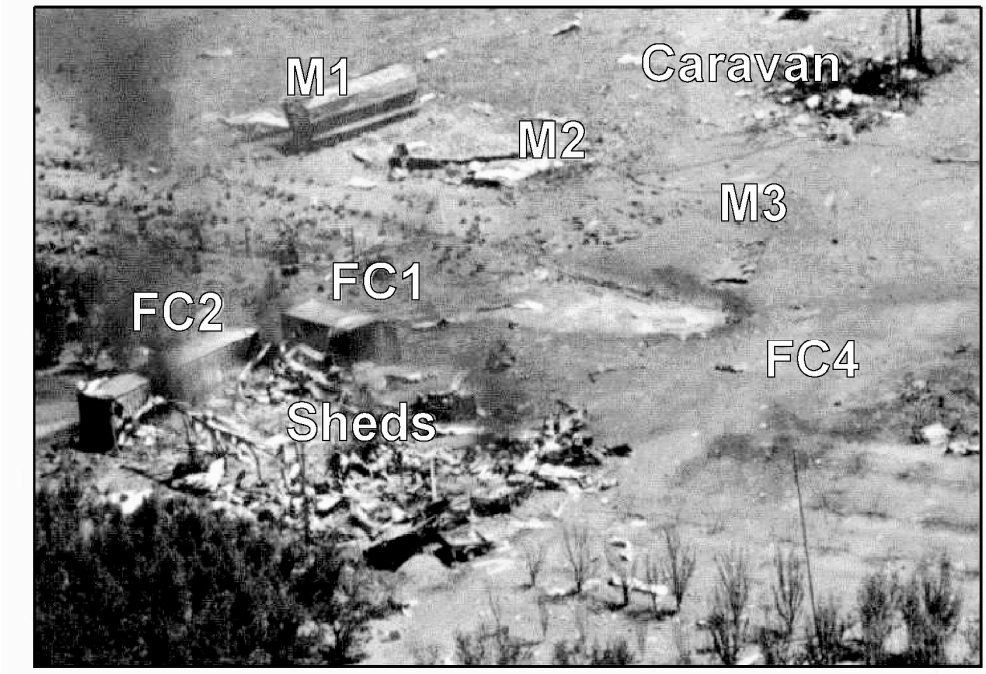

Figure 3. Aerial photograph of site following explosions.

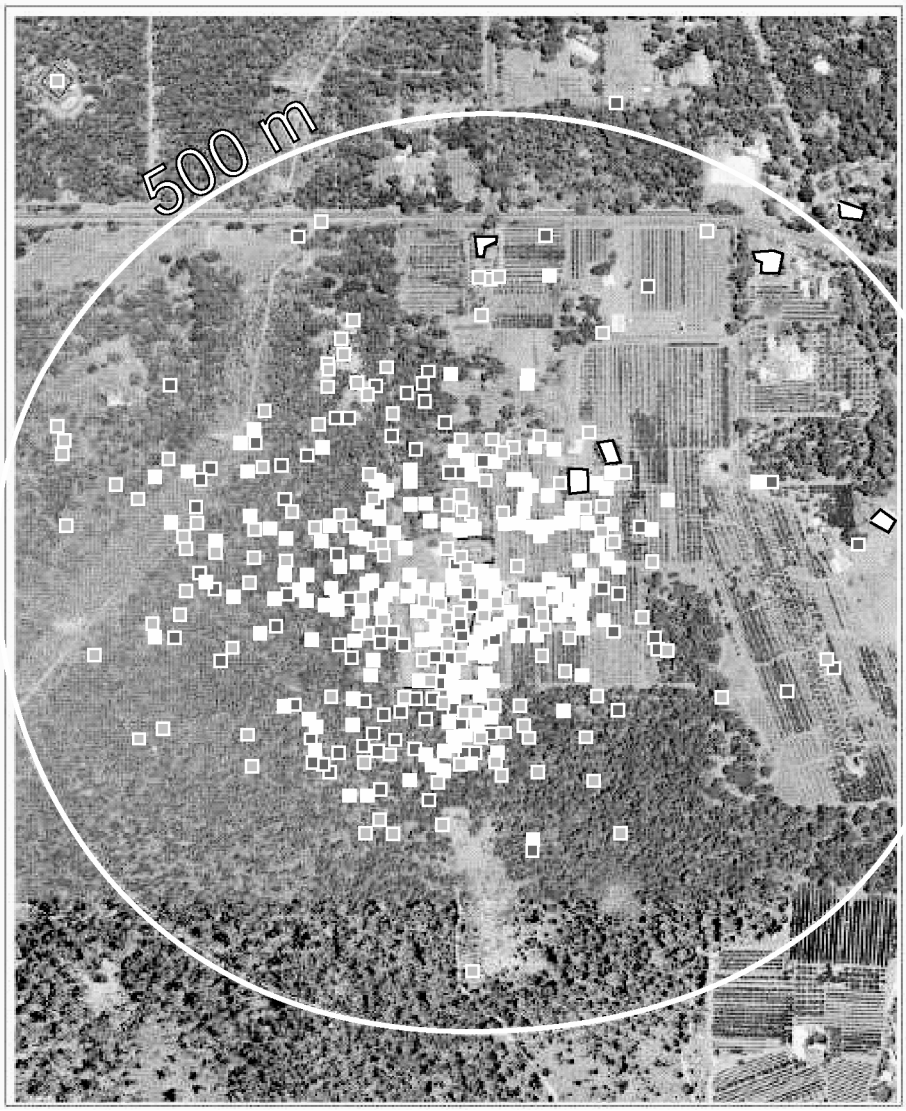

Figure 4. Combined distribution of shrapnel pieces.

the protection from flying shrapnel afforded by the earth mound.

Several bush fires started in the locality as a result of shrapnel and burning fireworks. The local fire service did not fully extinguish all fires started by the incident until the following day.

The remaining structures at the site are shown in Figure 2. A photograph of the damage is shown in Figure 3.

In addition to the damage at the site of the facility, damage to houses and other structures was reported up to a distance of 4.5 km from the facility. Most of the shrapnel was within 500 m of the facility. Figure 4 shows the distribution of fragments produced in the course of this incident.

Cause of Initiation of the First Ground Pack

The sequence of events culminating in the series of explosions at the site reportedly began with the ignition and firing of a single tube in a 25-shot 30-mm ground pack. The circumstances leading to this event merits a closer examination, since there was no obvious means of initiation.

The ground pack in question was one of a batch that had failed to fire at a previous display.

The packs were intended to be fired electrically, but they had failed to do so. The reason for failure at these displays is not known. Reportedly the packs were being adapted for hand-firing at a future display, and a key part of the modification process was the removal of the electric fusehead from the main fuse.

An operator would remove the metallic foil from the top of the ground pack tubes and then remove the electric fusehead from the ground pack. The pack would then be picked up by a second operator, who would transport the pack to another part of the working area, prior to refusing. Reportedly the pack in question ignited at the point when it was placed onto the ground by the second operator.

The investigation was not able to determine the reason why the shot initiated. Fuseheads are known to be quite sensitive to accidental ignition; however, most of the various possible modes of ignition involving the fusehead would be eliminated since reportedly no electric fusehead was present in the pack at the time of its initiation. Electrostatic discharge from the operator was considered to be unlikely in the belief that any such charge would likely have been dissipated during the handling of previous packs, and a discharge would have been expected at the point of picking up the pack, not when it was set down.

One possibility for the ignition of the ground pack is that there was displacement of some composition from within the ground pack, possibly caused by removal of the fusehead or disintegration of some of the several clay plugs present in the pack. This composition could then have become trapped between other materials (such as tissue paper and cardboard) within the pack. The impact from placing the pack onto the bench may then have been sufficient to ignite the composition.

The Subsequent Fires and Explosions

Following the ignition of the first shot in the first ground pack, the rest of the shots in the pack fired, projecting burning stars throughout Shed 2. This shed, which was not a licensed magazine, contained a considerable amount of pyrotechnic and other flammable material. There were at least 144 75-mm diameter aerial shells, some 15 to 20 ground packs, 25 cases of confetti bombs, 2000 electric fuseheads, some boxes of surplus quick match and assorted tubes from small ground pieces. There was also a substantial quantity of empty cardboard boxes and other combustibles in the shed at the time.

There are contradictory witness statements as to the contents of container FC4. Some state that there were no fireworks at all stored inside the container and that only packaging material was stored there. One witness statement suggests that a moderate quantity of pyrotechnic material (about 450 75-mm shells and 30 100-mm aerial shells) was stored in FC4, and that these shells were close packed instead of being in their original packaging. The violent explosion which destroyed the container within a few minutes of the incident starting in Shed 2 would suggest that the latter statement is a better reflection of the true situation.

The explosion that destroyed container FC4 was a mass explosion characteristic of high explosives of hazard division (HD) 1.1 rather than an event in the manner expected of fireworks of HD 1.3 (i.e., a minor blast and/or projection hazard but no mass explosion hazard). Previous tests described in this Journal[2] have illustrated the expected results from the initiation of a considerable quantity of HD 1.3 material inside a steel freight container, where mass explosion was not observed.

That a mass explosion did occur inside FC4 might be explained by (a) the 75-mm shells present in the container being close-packed (108 shells per box instead of 72), and (b) there may have been some salutes (which are now considered to exhibit HD 1.1 behavior) amongst the shells, as was normal company practice.[1] However, the absence of definitive information on the contents of the container makes it difficult to accurately establish the cause of the mass explosion, and the reported contents of FC4 seems inconsistent with the power of the explosion. This stresses the need for accurate record keeping if post-incident investigations are to produce reliable recommendations to prevent future incidents.

The explosion that resulted in the structural failure of magazine M2 was somewhere between the behaviors expected for HD 1.1 and HD 1.3. The magazine was known to contain mainly boxed ground packs (HD 1.4) and had an overall NEQ estimated at 725 kg. One of the firework types stored in M2 had a report as its main effect, and it is now accepted that such items can exhibit HD 1.1 behavior.[3] This may explain the unexpected violence of the event that partially destroyed the magazine.

Magazine M3 was destroyed by a very large explosion, characteristic of a detonation of a large quantity of HD 1.1 material. The magazine had an estimated 941 kg (NEQ) of up to 300-mm aerial shells and up to 75-mm salutes. According to the incident report, the blast took the authorities and the industry by surprise, since the items stored in M3 were all considered to be in HD 1.3 display fireworks.

The classification of some firework types was investigated following the Enschede disaster in the Netherlands in May 2000, and it was found that some high energy firework types tested as HD 1.1 under the UN testing regime[3,4,5] rather than HD 1.3. If these findings, which are summarized in Table 2, are applied to the contents of M3, then the hazard classification of the contents changes significantly.

Under the revised classification scheme given in Table 2, the contents of M3 would have been regarded as HD 1.1. The size of the explosion, which was thought to be from an estimated 941 kg of HD 1.3 material, is perhaps less surprising if it is thought to have come from 941 kg of HD 1.1 material. It should be stated that the firework company provided an NEQ estimate of 941 kg for magazine M3 early in the investigation, but this was revised downwards to 300 kg at a later date.[1]

Magazine M1, which reportedly contained material, mostly ground packs, with a NEQ of 700 kg classified as HD 1.4, was severely damaged by fire during the incident, but it was not destroyed by an explosion. The report considers it likely that a mild deflagration, consistent with HD 1.3 behavior, occurred within M1 as a result of its contents being initiated by hot fragments from M3. The magazine was licensed for the storage of HD 1.4 material, but reference to Table 2 shows a revised classification of HD 1.3 for ground packs, and the events within M1 are consistent with this revised classification.

Magazine M4, which contained much more material than M3, was left relatively unscathed by the events on the rest of the site. The earth mound around it reduced the likelihood of fragment impact. One wall of the magazine was struck by shrapnel, but the wall was not penetrated and the contents did not ignite.

In summary, the magnitude of the explosions came as something of a surprise to the regulatory authorities. The classifications of the items stored at the site were HD 1.3 and 1.4, for which no mass explosion would have been expected. However, if the revised classifications and the conditions of storage are taken into account, then the observed mass explosions may be explained. According to the classifications given in Table 2, magazines M1 and M2 would have had a classification of HD 1.3 (rather than HD 1.4) and magazines M3 and M4 would have had a classification of HD 1.1 (rather than HD 1.3).

The revised UN classification scheme alluded to in Table 2 is subject to revision, and it is not expected to be published until late 2004 at the earliest.

Table 2 Revised Firework Classifications Arising from Enschede Investigation Findings.[1,3,5]

Firework Type	"Old" UN Classification	Revised UN Classification
Report shells (all sizes)	1.3	1.1
Color shells (200 mm or greater diameter)	1.3	1.1
Color shells (below 200 mm diameter)	1.3	1.3
Roman candles (less than 50 mm diameter)	1.4	1.3
Boxed ground packs – report as primary effect	1.3	1.1
Boxed ground packs – color as primary effect	1.3	1.3

Report Recommendations

Nine specific recommendations were made in the incident report. Those recommendations and brief comments by this paper's authors follow:

Recommendation 1: Fireworks operators worldwide note the unforeseen explosions witnessed at the Carmel facility and conduct risk assessments of all their activities in preparing fireworks for displays and prepare Safe Operating Procedures for these activities.

Risk assessment is a key part of reducing the risk associated with any activity to a level which is as low as reasonably practicable (ALARP). This approach has been adopted in a number of countries.[6,7] The initiation of the ground pack, which triggered the whole sequence of events described in this paper, illustrates that the unexpected may occur at any time, so proper and thorough risk assessment should always incorporate such events. In addition, the consequences of unexpected initiation should be taken into consideration during the assessment of risk – in this case, the positioning of freight container FC4 may have been changed if the risk assessment had considered the possibility of an initiation of the type experienced.

Recommendation 2: That fireworks operators worldwide store all their fireworks in licensed magazines and not in preparation areas.

Short-term storage in unlicensed areas was permitted in Australia at the time of the incident. The incident report makes it clear that storage in unlicensed areas (Shed 2 and container FC4) was the major contributory factor in the escalation of the incident.

Recommendation 3: MPR considers what action, if any, is warranted in relation to compliance issues at the storage facility.

This recommendation is particular to the incident in question, and allows potential legal action (if any) to be taken. While the results of any legal action taken may be of interest to the pyrotechnic community in Australia and elsewhere, comment upon them is outside the scope of this paper.

Recommendation 4: That for the purpose of storage and transport, fireworks in Western Australia be classified in accordance with either UN testing, or by analogy of type using the UN default classification table.

This recommendation deals with the manufacturer self-classification of fireworks that are imported into Western Australia. Such classifications need to be carefully checked as a result of the incident. The notes to the recommendation make it clear that Western Australia should make use of the UN default classification table in its revised form, rather than relying on self-classification from manufacturers. The UN transport classifications for fireworks are not necessarily the same as their storage classifications. This has been addressed in the United Kingdom by the introduction of Hazard Types (HT's),[8] but this approach has not yet been applied in most other countries.

Recommendation 5: For the purpose of licensed storage of fireworks of HD 1.1, separation distances to off-site residential housing shall be in accordance with vulnerable facilities as per Table 3.2.3.2 of Australian Standard 2187.1 – 1998 "Explosives – Storage, Transport and Use Part 1: Storage", except that a minimum separation distance of 400 meters shall apply at all times.

The quantity-distance concept is consistent with common practices for establishing separation distances, and the table cited in this recommendation is similar to those cited elsewhere.[9] However, the minimum distance of 400 meters is the separation distance for 731 kg NEQ of HD 1.1 material. Failing to accept the lesser hazard posed by smaller quantities of HD 1.1 fireworks is tantamount to declaring fireworks to be significantly more hazardous than other HD 1.1 explosives. This is a position that must be hard to defend, especially in this case where the accuracy of statements of the operators regarding the quantities of fireworks present at the Carmel site is in serious question. As a matter of comparison, it might be of interest to compare this 400 meter distance with the amount of HD 1.1 material allowed for storage under the American Table of Distance for Storage of Explosives,[10] which is 4000 pounds (approx. 1820 kg) for unbarricaded magazines and 40,000 pounds (approx 18,200 kg) for barricaded magazines.

Recommendation 6: That MPR develops a Safety Bulletin to inform fireworks operators world-

wide of requirements based on revised classification of fireworks.

The changes to various regulations that are proposed by the recommendations made in the incident report need to be communicated to the industry. This recommendation proposes a mechanism for doing so.

Recommendation 7: That WA (Western Australia) takes a leadership role in discussions with other jurisdictions to adopt a nationally consistent approach to the revised classification of fireworks.

Each State within Australia has its own set of regulations. This recommendation proposes that these regulations are revised to ensure consistency. This approach is likely to be of benefit to the industry, since it can be expensive and time-consuming to deal with, for example, having different regulatory requirements at the place of importation and the place of storage.

Recommendation 8: That MPR amends the Firework Permit application form to enable the checking of safety controls for temporary storage at a display.

It is a requirement in Western Australia that display operators have to apply in advance for a permit for each separate display. This recommendation proposes that the application form is adjusted to incorporate the identification of revised requirements for the temporary storage of fireworks based on changes in classification.

It should be noted that in Western Australia, the use of fireworks by the general public has been prohibited since 1967.

Recommendation 9: That Government gives a high priority to the development of both the Dangerous Goods Safety Bill and associated explosives (incorporating fireworks) and dangerous goods regulations for a number of reasons, in part to put in place appropriate controls for the preparation and assembly of fireworks and to make it an offence to import incorrectly classified fireworks.

At the time of the incident, the main pieces of legislation governing the use and storage of explosives in Western Australia were the Explosives and Dangerous Goods (Explosives) Regulations 1963 and the earlier Explosives and Dangerous Goods Act of 1961. The report recommends a complete revision of these pieces of legislation, since it considers both to be out of date.

Conclusions

There is some uncertainty about the precise cause of the initiation of the first ground pack, the ignition of the contents of FC4, and the quantities of fireworks being stored. That not withstanding, the nature of the explosions in FC4, M2 and M3 surprised many. The magnitude of the explosions was unexpected from material of HD 1.3 and 1.4, but use of a revised UN classification table, in which many items previously considered as showing HD 1.3 behavior have been reclassified to HD 1.1, goes some way to explaining why the magazine contents behaved as they did.

Use of the revised classifications is likely to have significant consequences for the worldwide pyrotechnic community. Such reclassification will place additional restrictions on the storage and transport of a significant proportion of the items in use. This is very likely to adversely affect the business position of the commercial pyrotechnic community, since added expense is inevitable.

Some other aspects of the incident are familiar to the pyrotechnic community. The storage of flammable material near or beside a magazine or storage area is again shown to be incompatible with safe practice. The use of unlicensed and inappropriately located storage areas is shown to be a major contributory factor in the escalation of the incident from a fire in a small area to the final situation described. Finally, some unwise work practices are likely factors in the initiation and spread of the fire and explosions.

Acknowledgements

The permission of the Department of Industry and Resources (formerly the Department of Mineral and Petroleum Resources), Western Australia, to reproduce figures from, and otherwise draw upon, the official incident report is gratefully acknowledged. The authors are also

grateful to T. Smith and L. Lim for commenting on a draft of this article.

References

1) P. Drygala, H. Zuidersma, L. Lim, and M. Comber*, "The Carmel Explosions – Report of the Investigation into the fireworks accident at Carmel, Western Australia"*, Department of Mineral and Petroleum Resources, Western Australia, July 2002.

2) S. G. Myatt, "The Effects of External Fire on Fireworks Stored in Steel ISO Transport Containers", *Journal of Pyrotechnics*, No. 16 (2002) pp 59–70.

3) C. P. Weeth, "Enschede : Lessons to Re-Learn", *Proc. 6th Intl. Symp. on Fireworks* (2001) p 347.

4) *Recommendations on the Transport of Dangerous Goods, Manual of Tests and Criteria (3rd rev.)*, United Nations, doc ref. ST/SG/AC.10/11/Rev 3 (ISBN 92-1-139068-0).

5) *Report of the UN Working Group on the Classification of Fireworks*, 16–18 October 2001 (Den Haag, Netherlands), United Nations, doc ref. ST/SG.AC.10/C.3/2002/1 (29th January 2002).

6) M. J. Bagley, "Control Systems for the Storage of Explosives, Including Fireworks", *Journal of Pyrotechnics*, No. 18 (2003) pp 43–52.

7) T. Smith, "Assessing the Risks – Suggestions for a Consistent Semi-Quantitative Approach", *Journal of Pyrotechnics*, No. 18 (2003) pp 32–42.

8) R. Merrifield, "Hazards Associated with the Storage of Fireworks", *Journal of Pyrotechnics*, No. 14 (2001) pp 1–14.

9) *Explosives – Storage, Transport and Use, Part 1 – Storage*, Australian Standard 2187.1 – 1998, Standards Australia (see www.standards.com.au).

10) *Code for the Manufacture, Transportation, Storage and Retail Sales of Fireworks and Pyrotechnic Articles,* NFPA-1123, National Fire Protection Association, 2003. (As revised and approved by the Institute of Makers of Explosives in June 1991, and as incorporated in the Storage regulations of the US Bureau of Alcohol, Tobacco, Firearms and Explosives.)

Illuminants and Illuminant Research

David R. Dillehay
107 Ashwood Terrace, Marshall, Texas 75672 USA

ABSTRACT

The use of pyrotechnic compositions for the production of light has a long history. Most improvements were made mainly by trial and error with many misunderstandings about the cause and effect relationships from observations. Significant advancements in the mechanisms and theory of combustion have increased the understanding of many effects and led to improved illuminants both theoretically and practically. Radiative transfer theory explained most of the observed variations in illuminant functioning. Effects of spin, liner thickness and binders have been analyzed, and application of the results has been used to improve illuminant performance and solve production problems.

Keywords: illuminant, photoflash, efficiency, magnesium, sodium, nitrate, binder, radiative transfer

Introduction

Illuminants have been a major factor in pyrotechnic applications for many years. The earliest application was the use of torches prepared with pitch or tar, ignited and used to ward off darkness. This simple application was extended with the utilization of oxidizers, such as saltpeter or niter to enhance burning. When more light was needed, it was found that sodium added to a flame produced an astonishing increase in illumination efficiency.

An early application of illumination was photoflash devices for the military. Photoflash devices released pyrotechnic compositions that burned to produce millions of candela in visible light for a fraction of a second. This allowed aircraft to fly over a region with a camera lens open and release a huge "flashbulb" to illuminate a number of square miles. This was the only way to do night surveillance. The development of airborne radar and forward-looking infrared (FLIR) has made photoflash obsolete. Photoflash compositions were based on aluminum powder mixed with potassium perchlorate with confinement until ignition which was followed by an explosive dispersion of excess aluminum reacting with the air. It should be noted that aluminum will react with both oxygen and nitrogen in the air.

The efficiency of an illuminant is given in candela per unit weight. Candela is the unit of luminous intensity equal to 1/60 of the luminous intensity per square centimeter of a blackbody radiating at the temperature of solidification of platinum (2,046 K). In jargon, it is frequently referred to as the "candlepower" of a composition. The preferred term, however, is candela. There is an approximation in efficiency that relates burning rate and intensity over a range. This relationship is shown in equation 1.

$$\text{Light Integral}\left(\frac{\text{cd}\times\text{s}}{\text{g}}\right) = \left(\frac{\text{candela}\times\text{burn time}}{\text{mass of composition}}\right) \quad (1)$$

This equation shows that it is possible to trade burn time for candela by adjusting the burning rate of the composition without changing the formulations total energy. However, this is only true over a limited range of formulation and candle size. It can be shown that there is an ideal burning rate for a given composition to produce the most efficient output. If the burning rate is slower than the optimum rate, then radiant heat losses will reduce the efficiency. If the burning rate is faster than the optimum rate, then material will be expelled from the flare plume without complete combustion and energy will be lost.

Pressure Effect on Flame

Douda[1] published a definitive work on the effect of radiative transfer on alkali metal D-line radiation. This treatise identified several *a priori* factors that influence the resonance line broadening in pyrotechnic flames.

This author[2] extended Douda's work through flame modeling to determine the effects of these factors without *a priori* assumptions and verified the theory over a wide range of pressures, candle diameters, alkali metals, atmospheric interactions and fuels. This effort finally gave a clear understanding of the effects of combustion on illumination, including interactions with the surrounding atmosphere. This work also provided answers for many of the anomalies that had been observed, such as the increase in light output even though the theoretical flame temperature decreased with increasing magnesium content. It further showed that almost 90% of the visible light from conventional sodium nitrate-magnesium flares comes from the broadened D-line radiation.

Mixtures of magnesium and sodium nitrate, with a binder, have been well characterized. When magnesium and sodium nitrate are burned, the sodium nitrate first melts and then decomposes to release oxygen and form sodium nitrite. The oxygen released immediately reacts with the pyrolyzing binder that coats the sodium nitrate and magnesium and releases enough energy to raise the magnesium to a reactive state. This increase in energy promotes a more rapid decomposition of the sodium nitrite and the magnesium oxidizes on the surface to form a porous capsule of magnesium oxide. The magnesium oxide density is such that it cannot completely encapsulate the magnesium particle, so the internal magnesium starts to vaporize through the pores. This provides gaseous magnesium to mix and burn with the oxygen from the decomposing sodium nitrite and increases the efficiency of combustion. Thermochemical calculations readily show that the maximum temperature of the reaction of magnesium and sodium nitrate will occur at the stoichiometric composition around 46% magnesium. It is well established that the maximum candela occurs well above the stoichiometric composition with a considerable excess of magnesium present. The thermochemistry is represented by the following equations:

$$2\ NaNO_3(s) \xrightarrow{\Delta} 2\ NaNO_3(l) \qquad (2)$$

$$\xrightarrow{\Delta} 2\ NaNO_2 + O_2$$

$$3.5\ O_2 + C_5H_5O \rightarrow \qquad (3)$$

$$4\ CO + CO_2 + 2\ H_2O + 0.5\ H_2 + \text{Heat}$$

$$2\ NaNO_2 \xrightarrow{\Delta} Na_2(g) + N_2(g) + 4\ O_2 \qquad (4)$$

$$Mg(s) \xrightarrow{\Delta} Mg(g) \qquad (5)$$

$$O_2 + 2\ Mg \rightarrow 2\ MgO(s) + \text{Heat} \qquad (6)$$

$$Na_2 \xrightarrow{\Delta} 2\ Na^* \qquad (7)$$

$$Na^* \rightarrow Na^* + 589\ \text{nm photon} \qquad (8)$$

The sodium nitrate first melts and then decomposes to sodium nitrite with the release of some oxygen (eq. 2). The oxygen reacts with some of the binder to form carbon monoxide, carbon dioxide and water with the release of more heat (eq. 3). The heat causes the sodium nitrite to decompose into sodium vapor, nitrogen and oxygen (eq. 4). The magnesium is heated and vaporized to provide magnesium gas for easy oxidation (eq. 5). The additional oxygen from equation 4 reacts with the remaining binder and the magnesium fuel (eq. 6). The oxidation of the magnesium provides a very high temperature (3073 K) that is adequate to dissociate the sodium vapor into individual atoms and raise them to a higher state of excitation (eq. 7). The excited sodium atoms then radiate their excess energy as sodium D-lines (a doublet at 589 nm) (eq. 8). This D-line radiation is broadened by a number of mechanisms with pressure as the strongest contributor. This can be seen from sodium vapor street lamps that use high pressure sodium vapor, excited electrically, to produce a high level of visible light. The broadening of the radiation increases the amount of light over a wider range of the spectrum, which reduces the monochromatic nature of the atomic spectra. Examples of this broadening due to increasing pressure are shown in Figures 1 a to c.

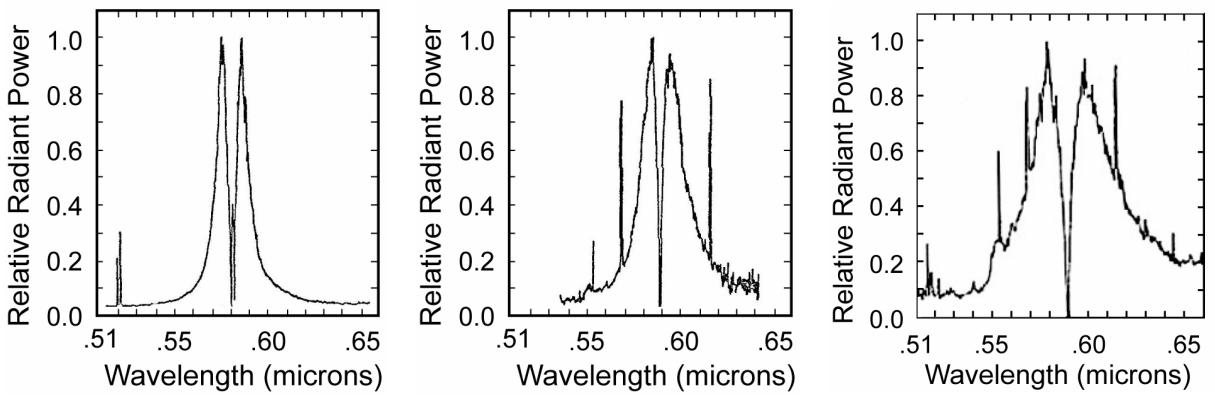

(a) Pressure is 76 torr. *(b) Pressure is 300 torr.* *(c) Pressure is 760 torr.*

Figure 1. Spectra showing that increased pressure results in a broadening of the D-line radiation.

Plume Effect

The plume of a burning flare entrains air as it exits the canister and the oxygen in the air reacts with the magnesium to increase the outer temperature of the plume and keep the sodium atoms at a highly excited state. A diagram of the plume of a burning flare is shown in Figure 2. When the temperature drops below about 1800 K, radiation of the sodium D-lines ceases. The more magnesium present in the flame, the longer the flare plume becomes as the magnesium continues to react with the air and bolster the surface area. The insulated central portion of the plume continues to cool by radiation and lose radiative efficiency but the overall increase in flare plume surface area compensates and provides the observed increase in candela.

Figures 3 a to c show the decrease in broadening for sodium D-lines at a fixed distance above the surface as the percent magnesium increases.

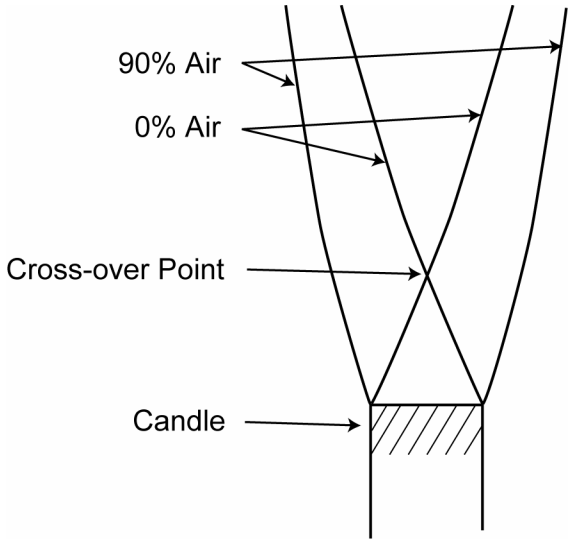

Figure 2. Plume diagram.

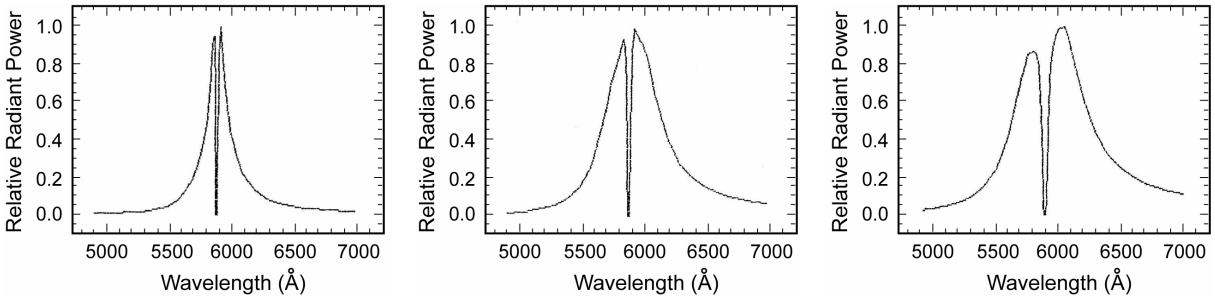

(a) 40% magnesium. *(b) 50% magnesium.* *(c) 60% magnesium.*

Figure 3. Graphs showing that the sodium D-lines broaden as the percent of magnesium increases.

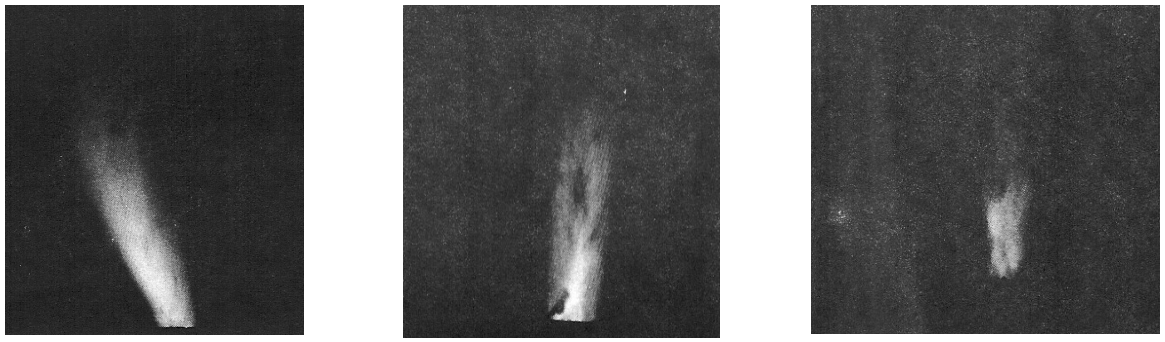

(a) in air *(b) in argon* *(c) in nitrogen*

Figure 4. Plume length effect on a stoichiometric formulation burned in (a) air, (b) argon, or (c) nitrogen.

The plume length was experimentally found to increase as a function of diameter and fuel richness so that flare surface area increases as the fuel increases. This analysis also explains the effect of candle diameter on efficiency.

As the diameter increases, the entrainment of air into the central portion of the plume is less efficient and the radiative transfer mechanisms lose efficiency.

An interesting set of tests were performed in a large chamber (6 m^3) with different atmospheres. The purpose of the tests was to determine how much the oxygen in the air was contributing to the efficiency of magnesium-sodium nitrate flares. Stoichiometric and fuel rich compositions were burned in atmospheres of air, nitrogen or argon. The results from the stoichiometric formulations clearly showed little difference in plume length and candela. See Figures 4 a to c.

With the fuel rich composition, however, the tests in air showed a much longer plume and higher candela. See Figures 5 a to c. In argon, the plume length was shorter and the candela much lower. In nitrogen, the plume was very short and the candela was very low. The argon does not react with the excess magnesium, so the lower flame temperature of the fuel rich composition results in greatly reduced D-line radiation.

The flare plumes in a nitrogen atmosphere are much shorter than the plumes in an argon atmosphere in keeping with the prediction that nitrogen is more effective in collisional de-excitation of excited sodium atoms. This is another of the radiative transfer mechanisms that is treated in the theory.

Hooymayers and Alkemade[3,4] reported measured values for quenching cross sections of various species with sodium and potassium. Their results indicated that the apparent quench-

(a) in air. *(b) in argon.* *(c) in nitrogen.*

Figure 5. Plume length effect of a fuel rich formulation burned in (a) air, (b) argon, or (c) nitrogen.

ing cross section of a species with an alkali metal would be inversely proportional to the atomic weight of the alkali metal. A higher value indicates a more efficient quenching cross section for the species. See Table 1 for a compilation of quenching cross sections for various species with sodium.

Table 1. Quenching Cross Section Values for Species with Sodium.

Species	Temperature (K)	Na Value
CO	2000	72
CO_2	1670	113
Ar	2070	2.3
H_2O	2070	1
N_2	1940	40
O_2	1885	66

Formulation Effect

Effective illumination is based on magnesium, sodium nitrate and a binder. The binders are important in the production processes of the illuminant composition, where they serve to maintain homogeneity of the composition while in process and then hold the composition together and bonded to the container during functioning. The binder also provides an initial reaction with the oxygen released from the sodium nitrate to provide a transition to burning of the magnesium. There can be some difference in performance as the binders change due to their stability under pyrolyzing environments (i.e., some binders are more stable and pyrolyze more slowly and reduce burn rates). Magnesium particle size and shape also play a role in the burning rate of the composition. Use of other metals has been shown to be less effective than magnesium in illuminants. This is mainly due to the low melting and boiling points of magnesium coupled with the very high heat of combustion. Other low melting and boiling metals do not have the high heat of combustion and are, therefore, not as effective in sodium excitation. Sodium nitrate particle size distribution affects the consolidation characteristics of formulations.

A typical illuminating composition consists of 50% (200 μ) magnesium powder, 43% (30–50 μ) sodium nitrate and 7% binder. Early binders included linseed oil and polyester resin. Army formulations currently use vinyl-alcohol acetate resin (VAAR) or polysulfide-epoxy resin binder systems. The VAAR binder is dissolved in a solvent and then mixed with the magnesium and sodium nitrate until the solvent is evaporated. This composition can then be stored and used whenever needed. No curing is required after consolidation. The polysulfide-epoxy combination is mixed with an amine cure agent and mixed with the magnesium and sodium nitrate. This mixture has a pot life and must be consolidated before the cure has progressed to the point that it will no longer flow under pressure. After consolidation, the candles are cured at an elevated temperature to complete the process. This binder gives a small amount of flexibility to the composition to prevent shrinkage and separation from the case.

Diameter Effect

It can also be shown that increasing the diameter of a candle does not produce a corresponding increase in output. This can be shown to be the effect of the entrainment of air into the plume along the plume axis. Diffusion of air into the plume can only occur at a certain rate. As the diameter increases, the central portion of the flare plume will begin to cool from radiative heat loss and there will be a corresponding loss of efficiency from the composition. The graph in Figure 6 shows a typical response of candela for a fixed composition as the diameter of the flare increases.

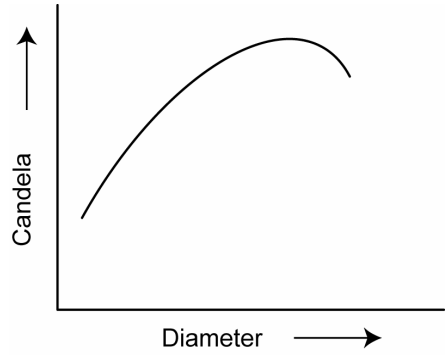

Figure 6. Typical response of candela for a fixed composition as flare diameter increases.

Spin Effect

A number of physical effects on flares were observed and their causes identified. For example, in military illuminants, many of the larger caliber illuminants are gun launched with high spin rates. Air brakes were frequently used to stop the spin on ejection of the payload. Field tests sometimes showed that the illuminants put out very low intensity light, followed by a large illuminant drop-out about half-way into the burn. Recovery of the rounds usually showed that the air brakes had failed and the illuminant in the canister had an unusual appearance. There were marked protrusions up from the center of the illuminant composition remaining in the canister. It appeared that the composition was burning faster around the periphery of the canister. It was assumed that the failure of the air brakes led to the flare spinning at a high rate, but the mechanism for reduced output was not obvious. The prevalent theory assumed that the sodium nitrate was melting and centrifugal force was carrying the reacting materials to the sidewall of the canister and choking the canister to cause a rise in pressure and shorten the burn time. The reduced opening for the plume explained the loss in light intensity. To test the theory, a spin test fixture was built to spin the illuminant canisters at controlled speeds while suspended upside down. A water jet was positioned to extinguish the burning composition at any point during the burn. The 105-mm candle was tested first. The graph in Figure 8 shows the results of the first set of spin tests.

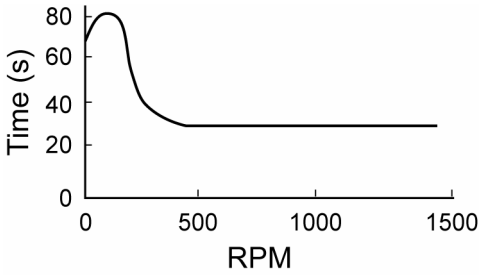

Figure 8. Results of the first set of spin tests.

The tests were repeated several times and the slight rise in burn time followed by a precipitous drop around 250 rpm was noted each time. This provided the proof that the effect was spin related. A series of tests were then run with extinguishment of the burning candle at various times into the burn. Examination of the surface provided an unexpected result. The illuminant was noted to regress faster at the edge producing a spiked appearance towards the end of the burn. This is shown in the Figure 9.

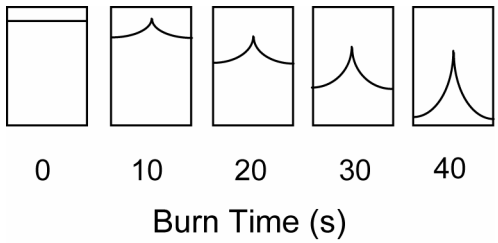

Figure 9. Diagrams showing the change in burn surface inside spinning candle over time.

The patterns observed did not agree with the original expectation of more rapid combustion down the center of the candle. A new theory was developed that involved the effect of decoupling of the gases from the illuminant surface. As the illuminant starts to spin, the gases evolved from the surface start to rotate with the surface. At a critical rpm, in this case 250 rpm, the gases start to lag behind the surface. The difference in rotation produces an increase in heat transfer. (This effect is well known and demonstrated by many physical phenomena, such as blowing on your hands to warm or cool them. The increased velocity of your breath either warms or cools the skin depending on which has the highest heat content.) As the spin velocity increases, the effect increases up to a maximum value determined by the thermal conductivity of the illuminant composition. Since the rotational velocity is greatest at the periphery, the heat transfer is greatest at that point. The slowest rotational velocity—in the middle—results in the slowest burn rate and leads to the formation of the spike. When the edge burning reaches the bottom of the canister, the center spike falls out, explaining the observed illuminant dropout. To test the theory, a set of candles was loaded with a "paddle-wheel" of metal plates inserted in the canister. A split ram was used to press illuminant into each quadrant to load the candles. See Figure 9.

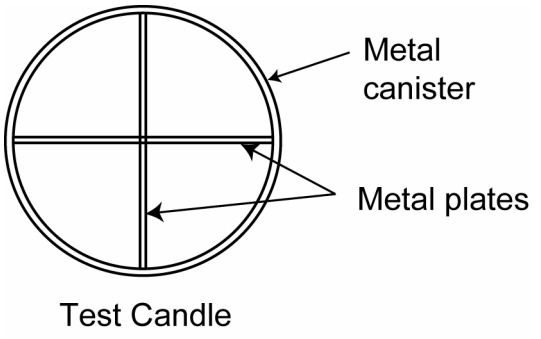

Figure 9. A cross-section of the "paddle wheel" of metal plates in a canister.

When these candles were burned in the spin fixture, there was no change in the burn time even at 1500 rpm. This is consistent with the paddles acting to keep the gases in sync with the burning surface thus preventing the differential spin rates and eliminating the increase in heat transfer. Once the principle was understood, other problems could be addressed.

The 60 mm illuminant was changed from a fin-stabilized round to a spin-stabilized round. The small size of the candle precluded the use of air brakes to stop the spin. The burn times were observed to change from 60 seconds in the static testing to 40 seconds in flight tests. The problem obviously resulted from the spinning of the illuminant, but there was no way to stop the spin, or even reduce it. The only control available seemed to be the thermal conductivity of the illuminant composition. The oxidizer was being ground from prilled sodium nitrate to a weight mean diameter (WMD) of about 50 μ; the magnesium was 30–50 mesh (about 200 μ WMD); and the binder content was about 6%. The formulation gave the needed candela and could not be readily changed. By grinding the sodium nitrate to a much finer particle size, it was possible to provide a more uniform distribution of the oxidizer to isolate the particles of magnesium, thereby reducing the thermal conductivity. This provided a reduced sensitivity to the heat transfer induced by the spin and the flight burn times were raised to about 55 seconds, which met the specification requirements. This is a prime example of the benefits of understanding both the chemistry and physics of the pyrotechnic reactions.

Liner Effect

Another example of applying analysis to the solution of problems involved the use of liners in illuminants. The 81-mm illuminants were changed from a cardboard tube to a metal canister. The canisters were lined with the binder solution and cured to provide a bonding surface for the illuminant composition. The liner thickness was not considered a serious problem and was allowed to vary during production. It soon became obvious that too little liner resulted in unbonded areas and high heat transfer down the canister wall resulting in short burn times. To avoid this, the liner amount was doubled. While this stopped the short burn times, it was noted that the candela of stationary flares had dropped to an unacceptable level. To determine the magnitude of the problem, a series of candles were loaded with carefully controlled liner thickness. It was found that a maximum thickness could be applied without loss of candela. Analysis revealed the cause. At low liner thickness, the heat transfer through the liner was absorbed by the metal canister, and this kept the liner from pyrolyzing from the heat of the flame. When a critical thickness was reached, the thick layer of liner could not transfer heat fast enough to keep the surface below the pyrolyzing temperature of the liner and the liner began to decompose and add carbonaceous residue to the flare plume. This acted just like an increase in inert binder, which reduced the thermochemical energy of the flare plume and lowered the candela. Again, the understanding of the chemistry and physics of the pyrotechnic reactions allowed a knowledgeable solution of the problem.

Shifting Spectral Output

The latest move in battlefield illumination is now directed towards "covert" illuminants. These illuminants are loaded with compositions that radiate most of their energy in the infrared part of the spectrum. The use of these illuminants with advanced night vision devices permits the observation of troops, equipment or areas without visibly showing illumination in the observed area. This covert illumination has definite advantages in operations that are close to the observers. They can light up an area with

infrared light without showing themselves to an enemy that does not utilize the same night vision devices. The formulations used in the covert illuminants vary but generally do not use metal powders to avoid a broad continuum from hot particles producing visible light. The alkali metals cesium and rubidium have their D-line radiation in the near infrared with little overlap in the visible. Achieving higher burning rates without the use of metal powders has been one of the main challenges to their use.

Pyrotechnic illuminants continue to be a major battlefield item to permit identification and targeting of enemy positions. The shift in spectral output provides new challenges to the formulation developers to keep up with advancing technology.

Acknowledgment

The author wishes to express thanks to Dr. Bernie E. Douda and David W. Turner for reviewing this paper and providing helpful comments.

References

1) B. E. Douda, *Radiative Transfer Model of a Pyrotechnic Flame*, RDTR No. 258, Naval Weapons Support Center, Crane, Indiana, Sept. 1973. AD-769 237.

2) D. R. Dillehay, *Resonance Line Broadening of Alkali Metals in Pyrotechnic Flames*, PhD Thesis, Clayton University, St. Louis, Missouri, April 1983.

3) H. P. Hooymayers, and C. Th. J Alkemade, "Quenching of Excited Alkali Atoms and Related Effects in Flames: Part I. Theoretical Analysis", *J. Quant. Spectrosc. Radiat. Transfer*, Vol. 6, pp 847–874 (1966).

4) H. P. Hooymayers, and C.Th.J. Alkemade, "Quenching of Excited Alkali Atoms and Related Effects in Flames: Part II. Measurements and Discussion", *J. Quant. Spectrosc. Radiat. Transfer*, Vol. 6, pp 501–526 (1966).

Bandwidth in Electro-Magnetic Compatibility (EMC) Testing

James Stuart
Franklin Applied Physics, 98 Highland Avenue, PO Box 313, Oaks, PA, 19456 USA

ABSTRACT

Electro explosive devices (EEDs) are often required to undergo a test in which they are placed near a high-power radio transmitter. The purpose is to see whether electromagnetic energy might fire the EED.

Consideration of the "Q" or quality factor of an EED system affords guidance in choosing a transmitter and test procedure. This can lead to shorter, simpler tests, and to improved efficiency in electromagnetic-exposure tests of all kinds.

Keywords: bandwidth, EED, electro explosive device, electro-magnetic compatibility test, EMC test, HERO test, irradiation test, quality factor

Any system that contains an electrically fired explosive device may be required to undergo electro-magnetic compatibility (EMC) testing. In practice, the system is placed near the antenna of a radio transmitter. The transmitter output is increased to a high level. Thus, the system is "bathed" in electromagnetic radiation, usually very intense. Any possible ill effects are noted. In particular, for an electroexplosive device (EED), the purpose of this test is to see whether such exposure to an intense electromagnetic field might cause the explosive to fire. This kind of EMC test, where the device under test is explosive, is called a HERO test. HERO is an acronym for "Hazard of Electromagnetic Radiation to Ordnance". Ordnance, of course, is anything explosive.

Figure 1 illustrates the type of EMC test to be discussed. A radio-transmitting antenna is at the upper left. At the lower right is a system containing an EED. The system might be a weapon, an automobile with airbags, or anything else. The whole system has not been drawn, only the EED part of it.

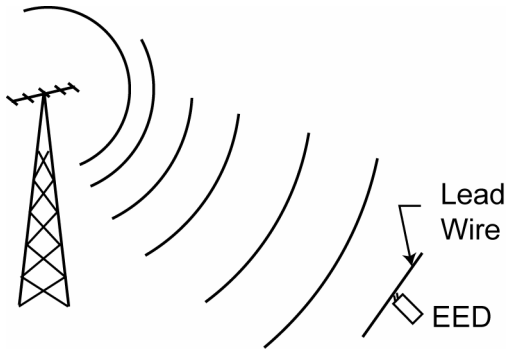

Figure 1. Setup for an EMC test that irradiates an EED.

An electroexplosive device, or EED, is a little can containing explosive material with a fine metal bridgewire inside. The bridgewire leads to longer wires that connect the EED to its firing circuit. When electric current passes through the bridgewire, it gets very hot and causes the charge to explode. In Figure 1, the leadwires are stretched out to form a radio-receiving antenna. The purpose of the EMC test is to determine whether the electromagnetic radiation might produce enough current in the bridgewire to fire the EED.

Test engineers generally conduct this kind of EMC test over a "band" or range of frequencies. The idea is to include all frequencies where, in real life, one might encounter a significant amount of electromagnetic energy. This should include the range of frequencies at which radio transmitters might be operating at the site or sites where the EED system will be located.

The antenna that is used for the test needs to be set to emit radiation that has the same strength at any frequency.

Initially, often nothing is known about the response of the EED system to radio frequency (RF) energy. Initially, the simplest case possible is considered where it is assumed that the same

amount of RF power dissipates in the EED at any frequency.

Figure 2 depicts such a case. The power dissipated in the EED is along the vertical axis. The irradiation frequency is along the horizontal axis. This picture shows the response of this imaginary EED system. It is a flat line. For this type of EED system, irradiation at any frequency is as effective as irradiation at any other frequency, so it is not necessary to test the system at more that one frequency to determine whether the field is a hazard to the EED. This is an idealized, extreme case. Usually, the amount of RF power dissipated in the EED will depend upon frequency. In other words, there will be some kind of resonance in the EED system.

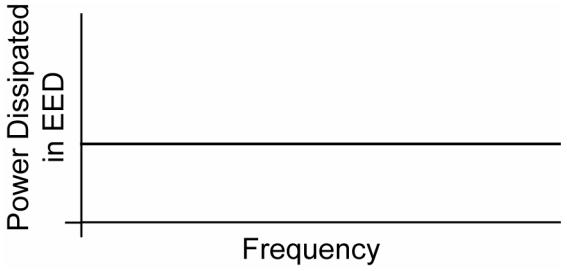

Figure 2. Frequency-independent EED system.

In Figure 3 the power dissipated in the EED is along the vertical axis, and it seems to peak at one particular frequency. This is called resonance. At one particular frequency f_0, the resonance frequency, more power dissipates in the EED than at other frequencies for the same incident field strength. Again, it is assumed that an electromagnetic field, whose strength does not change with frequency, irradiates the EED system. This resonance affects the EED itself, and the system of which it is a part, but it does not affect the transmitter. The peak of the resonance is at frequency f_0. That is where the power absorbed in the EED has its maximum value. The arrows to the left and right of the peak indicate the place on the curve where the power absorbed is half the maximum. The width between the arrows Δf is called the full-width at half-maximum (FWHM) power. This is the bandwidth of the EED system.

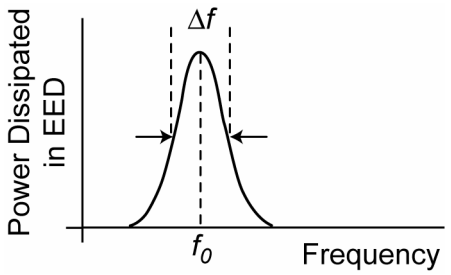

Figure 3. Resonance in EED system.

Clearly, when the transmitter is operated in an EMC test, the EED system needs to be irradiated at or near its characteristic resonance frequency, that is, near the peak of the curve. This is to try to determine the possible bad effects of electromagnetic radiation. In fact, this is trying to see whether the EED will fire. Thus, the system should be irradiated at the frequency where the system absorbs the most energy, to reveal any bad effects.

However, neither the resonance frequency of our EED system nor the width of the resonance is known in advance. Since only the frequency of the transmitter can be controlled, looking for the resonance in the EED system can be like looking for a needle in a haystack.

This is how test engineers perform an EMC test. A radio-transmitting antenna irradiates an EED system as in Figure 1. The radio transmitter can operate on only one frequency at a time. Therefore, the transmitter covers the whole range of frequencies, or bands, in a stepwise fashion. The technicians first set the transmitter to the lowest frequency, then to the next higher frequency, and so on. The difference between successive test frequencies is the frequency interval, or step size. One must specify the step size, in advance, as part of the test plan. At each frequency, the transmitter is turned on for a certain amount of time, perhaps several seconds, before moving to the next frequency. The time when the transmitter is on, at a single frequency, is the dwell time.

Both the frequency step size and the dwell time will affect the total duration of the EMC test. To make this clear, some values will be selected; for example, assume that the transmitter is on for 10 seconds at each test frequency; in

other words, the dwell time is 10 seconds. Assume that an EED system is being irradiated over the frequency band from 5 to 11 MHz. The step size is 0.1 MHz (100 kHz). One first turns on the transmitter at a frequency of 5.0 MHz for 10 seconds, then 5.1 MHz for 10 seconds, then 5.2 MHz for 10 seconds, and so on. The total number of steps will be 60. Since each step takes 10 seconds, the total duration of this test will be 600 seconds or 10 minutes. If engineers desire to cover a larger frequency band, then the total test duration will be longer. If technicians need to change or adjust the transmitting equipment to provide RF power at certain frequencies, then the time required for the test will increase. To cover a very large band of frequencies, sometimes engineers must irradiate an item for a whole day or even for several days. For practical reasons, such a long test time can be inconvenient, or even impossible.

In these circumstances, one should remember that the total time for the EMC test also depends upon the size of the frequency-step chosen. To shorten the test, a test engineer can pick a larger step size. How can the appropriate step size be determined?

In Figure 4 the frequency step size is very small. The test frequencies are shown as vertical bars. There are a great many of them. The spacing between these test frequencies is δf. During an irradiation test, the transmitter steps from one frequency to the next. It can take from a few minutes to many hours for the transmitter to step through the whole sequence of test frequencies.

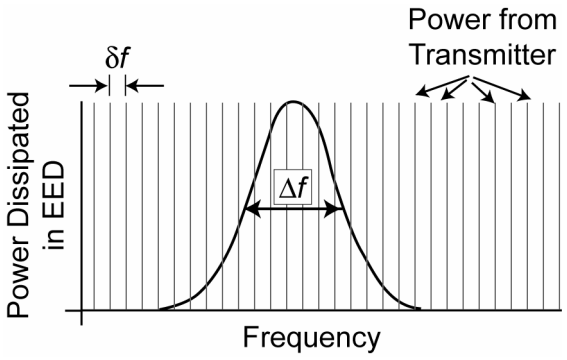

Figure 4. Too many frequencies.

If the EED system under test has a resonance, shown as the curved line in Figure 3, then the width of this resonance is Δf. The technicians performing the EMC test do not know where the EED system resonance is located, nor do they know the width of the resonance. In Figure 4, δf is much smaller than Δf. The reason for stepping the irradiating transmitter through such closely spaced frequencies is ensure that some of the test frequencies fall inside the resonance curve. However, with this particular choice of test-frequency spacing, there is needless duplication of data. The interval between test frequencies, δf, is too small in relation to the bandwidth of the EED system resonance, Δf. Stepping the transmitter through all these frequencies wastes time.

Figure 5 illustrates the opposite problem. The step size, between adjacent test frequencies, is too large. As the test engineer steps the transmitter from one frequency to the next, it completely misses the EED resonance. The entire extent of the EED resonance is between two test frequencies. Note that the spacing between test frequencies is quite large compared to the width of the EED system resonance. This is not good. The step size needs to be smaller than the inherent bandwidth of the EED system under test. In other words, as the transmitter is stepped through the sequence of test frequencies, it is important the peak of the EED system's response is not missed.

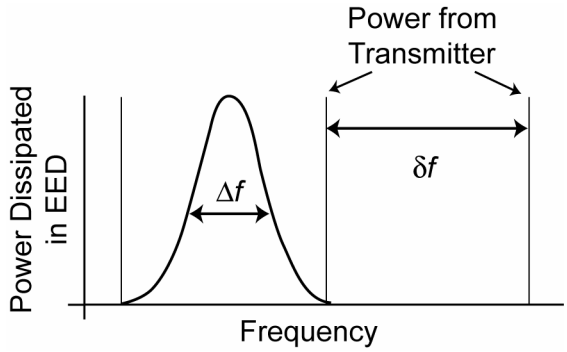

Figure 5. Too few frequencies.

Figure 6 shows the best choice of test-frequency interval. Note that several test frequencies fall within the envelope of the EED system sensitivity. There are enough test frequencies to determine the response of the EED system at the very peak of sensitivity. However, the test frequencies are far enough apart to avoid needless duplication of data.

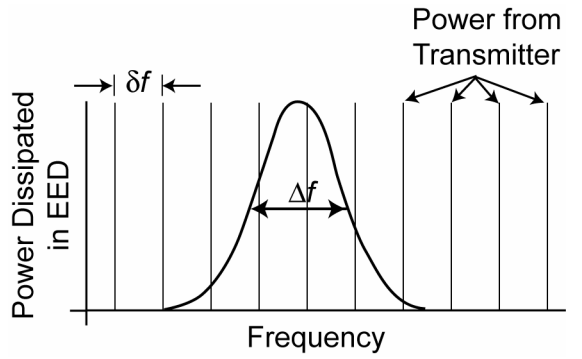

Figure 6. Ideally spaced frequencies.

The spacing between the test frequencies is δf. The width of the EED resonance is Δf. The optimum choice is to have δf smaller, but not too much smaller, than Δf. This relationship can be quantified by saying that the test-frequency interval δf should be approximately half of Δf. In general, the EED bandwidth Δf is not known. However, a reasonable estimate can be made that will choose the best step size for δf.

Remember that the electroexplosive device (EED) is part of a system. A radio transmitter beams RF energy toward this system. The strength of the transmitter's electromagnetic field needs to be at least as large as that which the EED system is likely to encounter while it is in use. Since the transmitter can be set to discrete frequencies in the chosen band, the frequency band is chosen to coincide with the frequencies in the environment where the EED system will be used. The purpose of the EMC test is to determine whether this radiation might adversely affect the EED and the system of which it is a part. It is certainly important to know if the electromagnetic field, to which the system will be exposed during use, could possibly cause the EED to fire unexpectedly. The safety of personnel and equipment depend on this knowledge.

The EED's response to the electromagnetic field has a resonance; that is, it absorbs more power in a certain range of frequencies than it does at other frequencies. It is assumed that the EED and the wires attached to it form a resonant circuit like the one shown in Figure 7. The curves in the line at the top represent a coil, that is, an inductive component. The zigzag line at the top represents a resistor. This is the resistance of the EED bridgewire. The parallel lines at the bottom represent the circuit capacitance. The EED circuit under test may not have components that look exactly like the ones illustrated in Figure 7. However, if there is a resonance in the EED system, then this is an adequate representation. The ensemble in Figure 7 has a resonance frequency, and it can store energy. The wires in Figure 7 that stretch to the left and right form an antenna. This antenna can pick up radio frequency energy from any nearby transmitter.

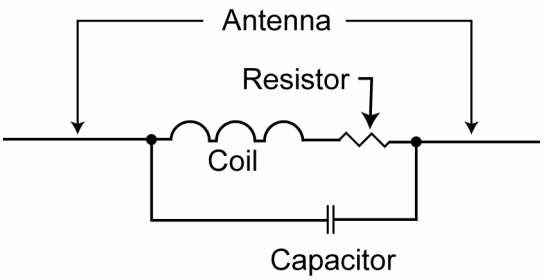

Figure 7. Model of resonant EED system.

Radio engineers have been building resonant circuits like that in Figure 7 for a long time. At low frequencies, the best ones are made with silver-plated wire. At high frequencies, silver-plated cavities are used. The characteristics and the attainable limits of this type of resonant circuit are well known.

When discussing the width of the resonance, it is useful to bring in the concept of Q, the quality factor. The quality factor Q is defined as the ratio of the resonance frequency f_0 to the resonance bandwidth Δf of the EED-system, as shown in equation 1. Both the frequency and the bandwidth must be in the same units (e.g., if f_0 is given in megahertz, then Δf must also be in

megahertz; if f_0 is given in kilohertz, then Δf must also be in kilohertz).

$$Q = \frac{f_0}{\Delta f} \quad (1)$$

The quality factor is not merely a mathematical abstraction. Radio engineers have found that for any circuit composed of wires, resistors, and capacitors, like that in Figure 7, Q will be less than 100. This practical limit is expressed in equation 2

$$Q < 100 \quad (2)$$

Therefore, if our EED system has a resonance, the Q of this resonance will be less than 100. This means that the bandwidth of the resonance in our EED system, if there is a resonance, will be greater than one percent of the resonant frequency, as expressed in equation 3.

$$\Delta f > \frac{f_0}{100} \quad (3)$$

Recall our discussion regarding the spacing between the test frequencies, δf. If this quantity is too small, the test procedure will waste time and resources. However, if δf is too large, the test may not reveal important details of the EED response such as a resonance. The optimum choice is to have δf smaller, but not too much smaller, than Δf, the width of the EED system power absorption curve. Ideally stated the test-frequency interval δf should be approximately half of Δf.

$$\delta f \approx \frac{1}{2}\Delta f \quad (4)$$

Because of the practical limit on Q, it is known that the EED system bandwidth is greater than one percent of the operating frequency as shown in equation 1. As a general rule, the best choice for the test-frequency interval is greater than, or equal to, one two-hundredth of the operating frequency as shown in equation 4.

$$\delta f \geq \frac{f_0}{200} \quad (5)$$

Remember that the limit on the quality factor is independent of the precise location of the resonance frequency or of its width. It applies to any resonance, wide or narrow. Therefore, the lower limit on the step size δf is also independent of the details of the resonance. It is not necessary to know anything in advance about the resonance. When an engineer is preparing a test plan for an EMC test on an EED system, the engineer needs to specify a test-frequency interval δf greater than, or equal to, one two-hundredth of the operating frequency f_0. This will guarantee the discovery of any resonances of the system in the frequency range being considered, yet it will avoid unnecessary duplication of data. Equation 6 shows how to calculate the best test-frequency interval for any operating frequency.

$$\delta f \geq \frac{f}{200} \quad (6)$$

Table 1 shows sample test frequencies, with recommended intervals (step size).

Table 1. Optimum Step Size for Various Operating Frequencies.

Operating Frequency	Step Size
200 kHz	1 kHz
1 MHz	0.005 MHz
10 MHz	0.0550 MHz
100 MHz	0.5 MHz
800 MHz	4 MHz
2000 MHz	10 MHz

A Brief Description of the Construction and Function of Common Electric Matches

Lawrence Weinman
Schneier/Weinman Consultants, LLC, Huntsville, AL USA

and

K. L. Kosanke
PyroLabs, Inc., Whitewater, CO USA

ABSTRACT

A simple description of the construction and the physical principles governing the function of common electric matches and some implications of these principles for testing and firing them are presented.

Keywords: electric match, heat resistance, current, volt, pyrogen

Introduction

This article offers a brief and not overly technical description of how typical electric matches function. It is hoped that this information will be of assistance to those who use them. As a general aid to readers with somewhat limited technical experience, a series of definitions have been included at the end of this article. Because the information presented in this article can be found in numerous texts, except for some direct quotes included in the definitions, specific references are not cited in this article.

In concept, the basic operation of an electric match is quite simple. An electric current is passed through the resistance of the bridgewire. Over time, as energy is dissipated in the bridgewire, it heats-up. A portion of that heat is transferred to the chemical composition (pyrogen) of the electric match. When the pyrogen reaches its ignition temperature, it reacts to produce the desired output of fire from the electric match.

An Idealized Electric Match

Figure 1 is an illustration of a cross sectioned idealized (i.e., imaginary) electric match. The adiabatic barrier is meant to imply that, for the purposes of this example, no thermal energy (heat) may flow through the barrier, not even into the electrical conductors by means of conduction through the ends of the bridgewire. In the center of the bridgewire is a *very small* amount of pyrogen in intimate contact with the bridgewire. It will be assumed that the contact is sufficiently good such that the temperature of the pyrogen is always equal to the temperature of the bridgewire. It will also be assumed that the amount of pyrogen is so small that its heat capacity is a negligible addition to that of the bridgewire.

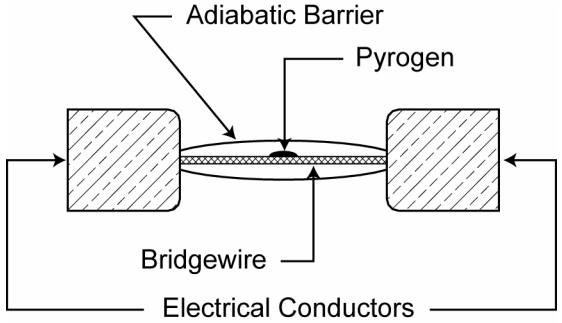

Figure 1. Illustration of an idealized (i.e., imaginary) electric match.

Given the conditions descried above, and after providing somewhat typical physical characteristics for the system, it is possible to calculate

the minimum energy needed to function (fire) this ideal device. Specifically, it will be postulated that:

- The bridgewire:
  - Diameter (d_{bw}) is 0.025 mm.
  - Length (l_{bw}) is 2.0 mm.
  - Density (ρ_{bw}) is 8.0 g/cm^3.
  - Specific heat capacity (C_{bw}) is 0.46 J/g°C (independent of temperature).

  The ambient temperature (T_a) is 27 °C (81 °F).
- The ignition temperature for the pyrogen (T_{ig}) is 327 °C.

Using this information some useful calculations can be performed. First, the mass of the bridgewire (m_{bw}) is simply the product of its density and its volume (V_{bw}),

$$m_{bw} = \rho_{bw} \cdot V_{bw} = \rho_{bw}\left(\pi \cdot \frac{d_{bw}^2}{4} \cdot l_{bw}\right)$$
$$= \left(\frac{8.0\ \text{g}}{\text{cm}^3}\right)\pi\frac{(0.0025\ \text{cm})^2}{4}(0.20\ \text{cm}) \quad (1)$$
$$= 0.0000079\ \text{g} \ \ (\text{i.e.,}\ 7.9\times10^{-6}\ \text{g})$$

The amount of energy (J_{bw}) required to raise the bridgewire temperature by one degree Celsius (1 °C) is just the product of its specific heat capacity (C_{bw}) and its mass (m_{bw}),

$$J_{bw} = C_{bw} \cdot m_{bw}$$
$$= (0.46\ \text{J/g°C})(7.9\times10^{-6}\ \text{g}) \quad (2)$$
$$= 3.6\times10^{-6}\ \text{J/°C}$$

Since the pyrogen needs to be raised from ambient temperature to its ignition temperature to cause its ignition, the electrical energy required for ignition is (J_{ig}),

$$J_{ig} = (T_{ig} - T_a)\ J_{bw}$$
$$= (327\ °\text{C} - 27\ °\text{C})(3.6\times10^{-6}\ \text{J/°C}) \quad (3)$$
$$= 1.1\times10^{-3}\ \text{J} \ \ (\text{i.e.,}\ 0.0011\ \text{J})$$

In calculating the *minimum* energy required to function this idealized electric match, note that no consideration needed to be given to bridgewire resistance, the voltage applied, the current flowing, or time to ignition. When performing this type of analysis only the mass, specific heat capacity, and ignition temperature are needed to determine the minimum firing energy. Any combination of the applied voltage, total circuit resistance, electric current and time that provides the minimum firing energy will cause the functioning of this idealized electric match.

A More Nearly Real World Electric Match

Figure 2 is an illustration of a cross section of a more nearly real world electric match, and for which there are both similarities and differences from the ideal case. The most important differences are that there is no adiabatic barrier to preclude the escape of thermal energy and by no means does the pyrogen present a negligible contribution to the heat capacity of the bridgewire. (Complicating the situation is that typically the thermal characteristics of the pyrogen are not well known.) There also exists a heat transfer path out the ends of the bridgewire into the electrical contacts. However, this path is generally considered to be negligible, provided that the length of the path is a minimum of approximately 6–12 wire diameters to each of the electrical contacts. Thus, allowing for an additional distance of 5–10 bridgewire diameters at the center of the electric match, if the total bridgewire length is approximately 25 times its diameter, then the loss of heat through its electrical contacts will be negligible.

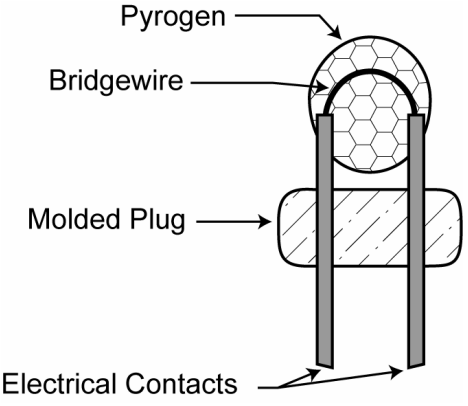

Figure 2. An illustration of a more realistic electric match.

For this more realistic electric match, the primary added consideration is the additional energy required to heat that portion of the pyrogen in immediate contact with the bridgewire while at the same time this thin layer of pyrogen is transferring heat further outward into the bulk of the pyrogen. Taking a somewhat simplified approach to the problem, at any given time the net amount of thermal energy having accumulated in the thin layer of pyrogen in immediate contact with the bridgewire (J_{net}) is simply the difference between the energy into (J_{in}) and the energy out of (J_{out}) that pyrogen layer.

$$J_{net} = J_{in} - J_{out} \tag{4}$$

The total energy into (or out of) the layer is the rate of energy (i.e., power) being supplied (or leaving) multiplied by time. However, because the rates of energy into and out of the pyrogen layer are not constant over time, this problem must be treated as an integral equation from calculus. While this approach could be taken, it would not be consistent with the "not overly technical" approach promised for this article.

Instead, consider the following analogy, pouring water into a bucket with a hole in its bottom. At any time the amount of water in the bucket will be the difference between the amount of water that has been put into the bucket, minus the amount that has leaked out. (In this analogy, the amount of water in the bucket represents the amount of thermal energy in the layer of pyrogen closest to the electric match bridgewire.) If one adds water only very slowly to the bucket, because the water is leaking out as fast as it is being added, only an insignificant amount of water will accumulate in the bucket no matter how long the process continues. If the rate of pouring into the bucket is increased, more water will begin to accumulate in the bucket (i.e., the pyrogen will get hotter). However, as the level of the water in the bucket increases, so does the rate at which it leaks out of the hole. Accordingly, even after adding water for a long time, it may not continue to accumulate to the point of the bucket becoming full (i.e., the pyrogen may not get so hot as to ignite). At some further increased rate of adding water to the bucket, continuing to add water will eventually cause to bucket to fill completely. However, the length of time required to fill the bucket depends on the size of the bucket and the size of the hole. In this analogy, the way to fill the bucket using the least amount of water, is to pour the water into the bucket very rapidly, before much water has a chance to leak out.

For an electric match, the rate of adding thermal energy *(W)* is equal to the current through the bridgewire (I_{bw}) times the voltage drop across the bridgewire (E_{bw}). However, from Ohm's law, the voltage drop across any resistance is equal to the current through the resistance times the value of the resistance ($E = I \cdot R$). Thus, in the case of the bridgewire, the rate of adding thermal energy equals the current through the bridgewire squared (I^2), times the resistance of the bridgewire (R_{bw}).

$$W = I_{bw} \cdot E_{bw} = I_{bw}^2 \cdot R_{bw} \tag{5}$$

Further, the amount of energy added (J) is the rate of addition (W) multiplied by time (t).

$$J = W \cdot t = I_{bw}^2 \cdot R_{bw} \cdot t \tag{6}$$

Following the thinking of the leaky bucket analogy, if the rate of adding energy to the bridgewire is too low (i.e., the rate of adding water to the bucket is too low), the pyrogen layer directly against the bridgewire will heat-up a little, but it will never become hot enough to ignite (i.e., the bucket will never get full) no matter how long the electrical energy is supplied. Although not strictly correct, for the purposes of this discussion the resistance of the bridgewire will be considered to remain constant during the heating process of this particular electric match. With this assumption, referring to equation 5, only the current determines the rate of energy being added to that electric match, and if that current is too low the electric match will fail to ignite no matter how long the current is applied. The maximum electric current that fails to be capable of igniting the pyrogen even after some specified (long) time, may be called the *no-fire current* for that electric match under a specific set of conditions.

As the amount electric current passing through the bridgewire is increased beyond the no-fire current level, there will come a time when the electric match will ignite providing one is willing to wait long enough. (In the leaky bucket analogy, this corresponds to the mini-

mum rate of adding water that will eventually cause the bucket to fill completely.) This minimum electric current, that will eventually cause the ignition of an electric match, may be called the *all-fire current* for that electric match under a specific set of conditions.

The least amount of energy needed to ignite the electric match occurs when that energy is supplied very quickly (i.e., when the water is poured very quickly into the leaky bucket so that almost none has a chance to leak out). Using equation 6 above, this *minimum firing energy* can be calculated for a specific electric match.

Some of the principles discussed above are illustrated in Figure 3, which is a graph of firing time as a function of applied current for a generic electric match. Note that the curve takes the approximate shape of a hyperbola. At low currents, the firing time is effectively infinite (i.e., the electric match never ignites). As higher currents are applied, some electric matches fire but on average it takes a relatively long time. As still higher currents are applied, the average time to fire becomes less. However, as the applied current continues to be increased, while the firing times still decrease, the amount of decrease becomes smaller and smaller. Finally, when the applied current becomes very large, there comes a point where the firing time has become essentially constant, because the time for thermal energy to 'leak' away before the device fires has become negligible.

No-Fire Current

In Figure 3, the left and lower edge of the shaded band is an estimate of the no-fire current for this particular electric match, under the test conditions used. However, just specifying the no-fire current of an electric match does not fully define its firing characteristics. To be fully definitive, one also needs to consider both the time during which the current is applied and the thermal environment of the electric match. For example, even applying a minimal test current will cause the match composition to begin to heat up. If that electric current is maintained long enough, and if the heat being produced is allowed to accumulate because the electric match is extremely well insulated, eventually the

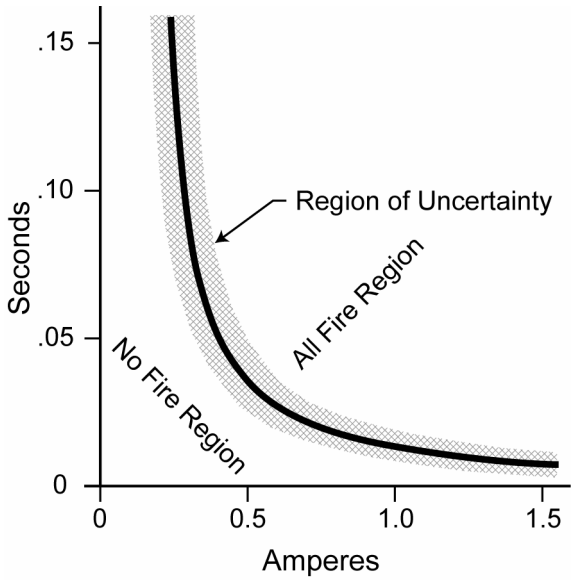

Figure 3. Firing time as a function of applied current for one type electric match.

pyrogen could reach its ignition temperature. (Note that when information about time and thermal environment is not specifically provided, a time of application of 5 to 10 seconds and a thermal environment of free air at 20 °C are typically meant to be implied.)

Because it cannot be absolutely assured that no electric match of a given type would ever ignite if a current equal to its no-fire current were applied, the maximum continuity test current is generally required not to exceed 20% of the no-fire current stated by the electric match manufacturer. (Note that some manufacturers may not specify the no-fire current for their electric matches. However, in all cases strict adherence to a manufacturer's maximum test current is required.)

All-Fire Current

In Figure 3, the right and upper edge of the shaded area is an estimate of the all-fire current for this particular electric match, under the test conditions used. As with the no-fire current, the same cautions apply to interpreting the meaning of this all-fire current. Changes in test conditions and variations in the performance of an individual electric match can significantly alter the all-fire current value. For example, the type of elec-

trostatic discharges commonly produced by individuals as they work, may produce electric currents many times greater than the all-fire current. Yet very few, if any, standard electric matches will fire from such an electrostatic discharge pulse passing through the bridgewire. This is because the duration of the current pulse is very short, typically less than a few microseconds in duration, and so has little total energy.

Because it cannot be absolutely assured that all electric matches of a given type will always ignite if a current equal to their all-fire current were applied, the recommended individual electric match firing current is typically about 40% above the all-fire current stated by the manufacturer, and the recommended series firing current is typically about double the all-fire current. (Note that this corresponds to supplying electric power at a rate that is two and four times that at the all-fire current, respectively, see equation 5.)

Additional Considerations

The shaded area in Figure 3, between the no-fire and all-fire currents, is a region of uncertainty, wherein it cannot be absolutely assured whether or not any individual electric match, of the type being considered, will ignite.

For the purposes of this discussion, a *good* electric match will be defined as one for which the thermal contact between the bridgewire and the pyrogen is completely effective, and a *bad* electric match will be one for which the thermal contact is imperfect or incomplete. Within the context of these definitions, note that a good electric match will require a greater firing energy to function than will a bad device. This is because, at normal firing current levels, the good device will transfer more heat away from the critical interface between the pyrogen and bridgewire, before that pyrogen heats up sufficiently to ignite. Whereas, in the bad device, the voids, cracks, decoupling, etc. serve to impede the heat flow away from the interface. As a result, that portion of the pyrogen still well coupled to the bridgewire will reach its ignition temperature sooner, thus requiring less total energy to function the electric match.

Following the good/bad terminology of the previous paragraph, consider an *extremely bad* electric match, one in which there has been a total decoupling of the pyrogen from the bridgewire. This can, and often does, happen because of applying a somewhat too low (or an intermittent) firing current. In that case, the pyrogen in contact with the bridgewire is raised more slowly than intended toward its ignition temperature, and the pyrogen may decompose without actually igniting. As a result of gas produced in this process, a tiny gap can form between the pyrogen and the bridgewire, thus thermally isolating the bulk of the pyrogen from the heat of the bridgewire. In some cases when this occurs the decoupling may be so severe that the bridgewire may become sufficiently far out of contact with the bridgewire, that the bridgewire may actually heat to its melting temperature and burn out (*fuse*) without transferring sufficient heat to ignite the pyrogen. Nicks in the bridgewire, poor welds, solder voids, and switch chatter are frequent causes of such malfunctions. Nicks in the bridgewire, poor welds and solder voids have the potential for reducing the electric current flowing in the firing circuit because of significantly greater electric match resistance. So called switch chatter can be the result of a physical bouncing of the switch contacts upon closure or because of dirt or oxidation on the surfaces of the switch contacts, either of which has the potential to reduce the intended firing current.

The term "volts to fire" is meaningless unless details of the complete firing system are specified, including all of the wiring and connectors. This is because the resistance of all the firing lead wiring, the connection resistances and the internal resistance of the battery (if used) all affect the voltage required to produce the required firing current through the bridgewire. However, it might be appropriate to speak of "volts to fire" for a bare electric match head, or some other well specified condition.

The term "firing energy" is only meaningful if the rate of delivering that energy (i.e., power) is also specified. Using equation 6, a continuity test current of only 0.02 ampere through a 2 ohm bridgewire for about 20 minutes is found to deliver 1 joule of energy to the bridgewire and pyrogen. By comparison, most electric matches are considered to require a firing energy of approximately 0.02 joule (0.5 ampere through 2 ohms for 0.05 second).

Conclusion

While electric matches are simple devices, like so many other simple devices, they require the user to have some basic knowledge to truly understand and properly use them. It is hoped that this article has provided a reasonable amount of that information.

Possibly Useful Definitions

To make these definitions more user friendly, there is necessarily some redundancy of the information. Those definitions in quotes are taken from the *CRC Handbook of Chemistry and Physics*, 62nd edition, 1981.

adiabatic: "A body is said to undergo an adiabatic change when its condition is altered without gain, or loss, of heat." In the case presented in this article, this does not include the heat generated within the bridgewire by the passage of electric current.

ampere: The unit of electric current, for which the abbreviation A may be used, and the symbol *I* is commonly used in equations. When an electric potential (voltage) of one volt is applied to a circuit with a resistance of one ohm, a current of one ampere will flow.

bridgewire: A small diameter, relatively high resistance, conductor in an electric match. Commonly, bridgewires have a diameter of approximately 0.025 mm and are made of the alloy Nichrome.

calorie: A unit of heat energy, which has fallen into disfavor, is commonly abbreviated cal, and which is equivalent to 4.18 joules (J) (the currently more favored unit).

current (Electric)**:**"The rate of transfer of electricity…." The unit of electric current is an ampere, for which the abbreviation A may be used, and the symbol *I* is commonly used as current in equations.

electric detonator: An electrically actuated device producing a detonation that is used to initiate another detonating explosive. These devices are not usually used with pyrotechnic devices. An electric detonator may contain an electric match.

electric match: A small electrically activated device producing a small ignition pulse (flame) used to ignite pyrotechnic devices. (Note: A "**squib**" is **not** an electric match, but a device having a greater energy output, which may be designed and used for propulsion, actuation, or ignition. While it may contain an electric match, the terms should not be confused or interchanged.)

electric potential: (Also potential difference and related to electromotive force or voltage). The unit of electric potential is the volt, for which the abbreviation V may be used, and the symbol *E* is commonly used as potential difference in equations. When an electric potential (voltage) of one volt is applied to a circuit with a resistance of one ohm, a current of one ampere will flow.

energy: "The capability of doing work." In this article, the symbol for energy is *J*, and the unit of energy may be joules (J) or calories (cal).

heat: "Energy transferred by a thermal process."

heat capacity: "The quantity of heat required to increase the temperature of a system or substance by one degree of temperature. It is usually expressed in calories per degree centigrade or joules per degree Celsius." (See specific heat capacity.)

joule: A unit of energy, including thermal energy, is abbreviated as J. A joule is equal to one watt second, and equals 0.24 calorie.

ohm: The unit of electric resistance is the ohm, for which the abbreviation Ω (Greek capital letter omega) is commonly used, and the symbol *R* is commonly used in equations. When an electric potential (voltage) of one volt is applied to a circuit with a resistance of one ohm, a current of one ampere will flow.

Ohm's Law: Expresses the direct relationship between current (*I*), potential difference *(E),* and resistance (*R*) in an electric circuit. A common form of Ohm's Law is expressed by the equation, $I = \frac{E}{R}$

power: Is the time rate of energy transfer or production. A common unit of power is the watt, which is commonly abbreviated as W, defined as one joule per second, and the symbol *W* may

be used for power in equations. In an electric circuit, the amount of power produced is equal to the product of current (*I*) through the circuit and potential difference (*E*) across the circuit, $W = I \cdot E$, *or* $W = J/t$

pyrogen: An energetic mixture of chemicals used to produce heat, flame, or similar.

resistance: "…is a property of conductors depending on their dimensions, material and temperature which determines the current produced by a given difference of potential." The unit of resistance is the ohm, which is commonly abbreviated as Ω (Greek capital letter omega), and the symbol *R* is commonly used in equations. When an electric potential (voltage) of one volt is applied to a circuit with a resistance of one ohm, a current of one ampere will flow.

specific heat capacity: Heat capacity per gram (g) of material, commonly using the units of joules per gram-degree Celsius (J / g-°C), and the symbol *C* is commonly used in equations.

squib: (Also electric squib) A device containing an electric match plus a pyrotechnic base charge, generally contained in a small metal tube.

temperature: "Temperature may be defined as the condition of a body which determines the transfer of heat to or from other bodies." Note: The units of temperature may be degrees Fahrenheit (°F), degrees Celsius (°C) or Kelvin (K) (by custom, when using K the word degree is not used). Modern technical usage tends toward using either °C or K. The temperature scales may be converted as follows:

$$°\mathrm{F} = 32 + \left(\frac{9}{5}\right) °\mathrm{C}$$

$$°\mathrm{C} = \left(\frac{5}{9}\right) (°\mathrm{F} - 32)$$

$$\mathrm{K} = °\mathrm{C} + 273.15$$

time: Time is usually expressed in seconds, for which the abbreviation s may be used, and the symbol *t* is commonly used as time in equations.

volt: "The unit of electric potential difference…", for which the abbreviation V may be used, and the symbol *E* is commonly used for voltage in equations.

watt: The unit of electric power, which is commonly abbreviated as W, and corresponds to the production or consumption of energy at the rate of one joule per second.

Communications

Brief technical articles, comments on prior articles and book reviews

Comment on: "Review of *Pyrotechnics*"

that appeared in Issue 18, Winter 2003

Ron Lancaster

Kimbolton Fireworks, 7 High Street, Kimbolton, Huntingdon, Cambs., PE18 0HB Great Britain

In the late 1960s there was only Weingart's *Pyrotechnics*, and it was a suggestion of a re-write to the Publisher that led to my own first edition in 1972. As we have grown in experience there have been two further editions. It has been interesting to see how many little bits of new information first published in those times are now taken as commonplace.

However this is what progress is all about. Nevertheless it was never intended to print all the commercial information that had been accrued through hard graft and time and that our competitors in parts of the world with cheaper labour than us are keen to learn. We have also yet to see them publishing what they do.

I found the three reviews of the Hardt book quite interesting, and I am delighted that all three of them gave the deserved praise that was due concerning the quality of the book itself, a tribute to those who spent hours of time on it for very little return on such a specialised work. It is also a tribute to a printing house with a great love for the subject. I can also vouch for the soundness of what was written concerning the practicality of the firework chapter and its formulations.

No doubt the Publisher will now be wondering whether it was worth taking on the publication of the book now that our information has moved on. He will be asking whether the whole thing should have been re-written by various 'experts'. I recall the problem of first receiving the script from Dr Shimizu, being sensitive to his attempts in English and of trying to keep it much as he had written it. In the end was it Hardt's Book or something else. I ought to have converted my book into a PhD thesis and put more into it, but I asked one or two others to make contributions.

Now I do not know Barry Sturman, and I am sure that he is a splendid fellow, but his review has made me feel rather unhappy for all my sympathies are with the people who got the book into production. All the more because I know that like me they are not going to make any money out of it. I note in his final words that it would have been a mammoth task for another editor to put the book into a form that would have been pleasing to him. I shall look forward to his major opus, which will—in the words of the hymn—leave us all 'lost in wonder, love and praise'.

In the meantime we are grateful to those who are making the effort to look into these scientific issues that are of limited interest and value to the practicalities of firework manufacture—or what there is left of it—in the West but even more thanks to the Publisher for a fine piece of work.

Review of: *Ignition Handbook*

Vytenis Babrauskas

Fire Science Publishers

[ISBN 0-9728111-3-3] 2003

K. L. Kosanke

PyroLabs, Inc., Whitewater, CO USA

What an incredible reference text, especially to have been assembled by a single author. The book has 1116 large format pages (8.5 by 11 inches), is printed on high quality paper and sturdily bound, is well indexed (36 pages), is very thoroughly referenced (one chapter has 2154 references) and sells for only US$198 ($140 if purchased directly from the author).[1]

The chapters are titled:

1) Introduction (12 pages)
2) Terminology (11 pages)
3) Fundamentals of combustion (17 pages)
4) Ignition of gases and vapors (100 pages)
5) Ignition of dust clouds (41 pages)
6) Ignition of liquids (52 pages)
7) Ignition of common solids (118 pages)
8) Ignition of elements (15 pages)
9) Self-heating (77 pages)
10) Explosives, pyrotechnics and reactive substances (53 pages)
11) Characteristics of external ignition sources (94 pages)
12) Preventative measures (18 pages)
13) Special topics (28 pages)
14) Color Plates (38 pages)
15) Information on specific materials and devices (347 pages)
16) Tables (59 pages)

Index (36 pages)

In terms of the accuracy of the information relating to pyrotechnics and explosives, a cursory examination by this reviewer, found no errors. However, there were occasionally minor points wherein the author's lack of detailed and current experience with pyrotechnics is somewhat apparent. As an example of this, potassium chlorate is described as being "commonly used in pyrotechnics". While was once quite correct and still today this is not incorrect, it may give the impression that potassium chlorate is currently used somewhat more frequently than it is.

While no more than about 10% of the book explicitly relates to pyrotechnics and explosives, probably another 20% is of relevance to pyrotechnics and explosives. Considering the price of the book, even if one never uses any of the non-pyrotechnic information, this still must make this text one of the most cost effective sources of pyrotechnic data and information available anywhere. This reviewer is most pleased to have this fine volume on his bookshelf.

1) vytob@doctorfire.com.

Events Calendar

Pyrotechnics and Fireworks

2004 Le Mondial SAQ Montreal Fireworks Competiton

June 12 Ampleman Pyrotechnie (Canada)
June 19 Pirotécnia Igual (Spain)
June 26 Marutamaya (Japan)
July 03 IPON (Italy)
July 10 Pirotécnia Vincente Caballer (Spain)
July 14 JNS Pyrotechniek (Holland)
July 17 Sunny International (China)
July 21 Société Lacroix-Ruggieri (France)
July 24 Weco Pyrotechnische (Germany)
July 28 Panzera S.A.S. (Closing)

For more information, visit the web site:
www.montreal-fireworks.com or
www.lemondialsaq.com

Special Topics in Pyrotechnics

June 13–18 2004 Chestertown, MD, USA
Contact: John Conkling
PO Box 213
Chestertown, MD 21620, USA
Phone: +1-410-778-6825
FAX: +1-410-778-5013
email: JConkling2@washcoll.edu
web: www.John.Conkling@washcoll.edu

1st Workshop on Pyrotechnic Combustion Mechanisms

July 10, 2004, Fort Collins, CO, USA

Contact: Dr. Steve Son
Los Alamos National Lab
PO Box 1663
Los Alamos, NM 87545, USA
email: son@lanl.gov
web: http://www.intlpyro.org/pyro-combustion-mechanisms.htm

31st Int'l Pyrotechnics Seminar

July 11–16 2004, Fort Collins, CO, USA

Contact: Linda Reese, Appl. Res. Assoc., Inc.
10720 Bradford Road, Suite 110
Littleton, CO 80127, USA
Phone: +1-303-795-8106
FAX: +1-303-795-8159
email: lreese@ara.com

Chemistry of Pyrotechnics & Explosives

July 25– 30 2004 Chestertown, MD, USA
Contact: John Conkling
PO Box 213
Chestertown, MD 21620, USA
Phone: +1-410-778-6825
FAX: +1-410-778-5013
email: JConkling2@washcoll.edu
web: www.John.Conkling@.washcoll.edu

2004 – Celebration of Light – Vancouver

July 30 Czech Republic
Aug. 2 Canada
Aug. 6 China
Aug. 9 Grand Finale

For more information, visit the web site:
www.celebration-of-light.com

Pyrotechnics Guild Int'l Convention

Aug. 7–13 2004, Fargo, ND, USA
Contact:, Frank Kuberry, Sec. Treas.
304 W Main St
Titusville, PA 16354, USA
Phone: +1-814-827-6804
e-mail: kuberry@earthlink.net
web: www.pgi.org

8th International Symposium on Fireworks

April 18–22 2005 Shiga, Japan

Contact: Fred Wade
Box 100
Grand Pre, NS, B0P 1M0
Canada
Phone: +1-902-542-2292
FAX: +1-902-542-1445
email: symposium@fireworksfx.com
web: www.ISFireworks.com

Energetic Materials

Computational Mech. Assoc. Courses–2004

Contact: Computational Mechanics Associates
PO Box 11314,
Baltimore, MD 21239-0314, USA
Phone: +1-410-532-3260
FAX: +1-410-532-3261
email: 74047.530@compuserve.com
web: www.compmechanics.com

13th Int'l Symp. on Chemical Problems Connected with the Stability of Explosives

June 6–10 2004, Kristianstad, Sweden

Contact: Stig Johansson
Johan Skyttes väg 18, SE 55448
Jönköping, Sweden
Phone/FAX: +46-3616-3734
email: stru.johansson@telia.com

Carl Cranz Gesellschaft Course Waffentechnik / Ballistik [language German]

June 14–17 2004, Braunschweig, Germany

Contact: Dirk Cegiel [course leader]
RWM Schutz & Pyrotechnik, Trittau
Phone: +49-8153-28-24113
email: D.Cegiel@nicopyro.de
anmelden@ccg-ev.de (registration)

35th Int'l Annual Conf. ICT – Energetic Materials – Structure and Properties

June 29–July 2 2004, Karlsruhe, Germany

Contact: Manuella Wolff
Fraunhofer-Inst. für Chem. Technologie (ICT)
P. O. Box 1240
D-76318 Pfinztal (Berghausen), Germany
Phone: +49-(0)721-4640-121
FAX: +49-(0)721-4640-120
email: mw@ict.fhg.de
web: www.ict.fhg.de

Franklin Applied Physics Lectures

July 26–30, 2004, Oaks, PA, USA

Contact: James G. Stuart, Ph.D., Pres.
Franklin Applied Physics, Inc.
98 Highland Ave., PO Box 313
Oaks, PA 19456, USA
Phone: +1-610-666-6645
FAX: +1-610-666-0173
email: JStuartPhD@aol.com

31st Annual Conference on Explosives and Blasting Technique

Feb. 6–9 2005, Walt Disney World, FL, USA

Contact: Lynn Mangol
Phone: 440-349-4400
email: mangol@isee.org

Propulsion

AIAA/ASME/SAE/ASEE Joint Propulsion Conference

July 11–14 2004, Fort Lauderdale, FL, USA

Contact:
Phone: +1-703-264-7500 / 800-639-2422
web: www.aiaa.org

High Power Rocketry

LDRS 2004

Contact: see web site
www.tripoli.org/calendar.htm

Model Rocketry

NARAM 2004

Contact: — see web site for details:
web: www.naram.org
For other launch information visit the NAR Web site: www.nar.org

Future Events Information

If you have information concerning future—explosives, pyrotechnics, or rocketry—meetings, training courses or other events that you would like to have published in the *Journal of Pyrotechnics*, please provide the following information:

Name of Event

Date and Place (City, State, Country) of Event

Contact information — including, if possible, name of contact person, postal address, telephone and fax numbers, email address and web site information.

This information will also be published on the Journal of Pyrotechnics Web Site:
http://www.jpyro.com

Journal Sponsors

Journal of Pyrotechnics **wishes to thank the following Sponsors for their support.**

Individual Sponsors:

Ed Brown
P.O. Box 177
Rockvale, CO 81244, USA
Phone: 719-784-4226
email: edwinde@cs.com

Gerald Laib
17611 Longview Lane
Olney, MD 20832, USA
Phone: 301-744-4358
FAX: 301-744-4784

Corporate Sponsors:

Aerotech & Industrial Solid Propulsion Inc.
Gary Rosenfield
2113 W 850 N St
Cedar City, UT 84720, USA
Phone: 435-867-9998
FAX: 435-865-7120
email: garyr@powernet.net
web: aerotech-rocketry.com

Allied Specialty Insurance
David H. Smith
10451 Gulf Blvd.
Treasure Island, FL 33706, USA
Phone: 800-237-3355
FAX: 727-367-1407
email: info@alliedspecialty.com
web: www.alliedspecialty.com

American Fireworks News
Jack Drewes
HC 67 Box 30
Dingmans Ferry, PA 18328, USA
Phone: 570-828-8417
FAX: 570-828-8695
email: afn@fireworksnews.com
web: www.fireworksnews.com

American Pyrotechnics Association
Julie Heckman
4808 Moorland Lane - Ste 109
Bethesda, MD 20814, USA
Phone: 301-907-8181
email: jheckman@americanpyro.com
web: www.americanpyro.com

Astro Pyrotechnics
Leo Autote
2298 W. Stonehurst
Rialto, CA 92377, USA
Phone: 909-822-6389
FAX: 909-854-4749
web: www.astropyro.com

Australian Soc. of Accredited Pyros.
Chris Larkin
PO Box 606
Mt. Ommaney, QLD 4074, Australia
Phone: 61-7-371-20804
FAX: 61-7-327-90614
email: nitrotech@smartchat.net.au

Brooke Mawhorr, PC
Douglas K Mawhorr
112 East Gilbert StPO Box 1071
Muncie, IN 47305, USA
Phone: 765-741-1375
FAX: 765-288-7763
email: dlmmawhorr@aol.com

Canadian Explosives Research Laboratory
Dr. Phil Lightfoot, Manager
CANMET - 555 Booth St.
Ottawa, ON K1A 0G1, Canada
Phone: 613-947-7534
FAX: 613-995-1230
email: plightfo@nrcan.gc.ca
web: www.nrcan.gc.ca/mms/cerl

Combined Specialties Int'l. Inc.
John and Alice Allen
8362 Tamarack Village, Ste. 119
Woodbury, MN 55125, USA
Phone: 651-855-0091
FAX: 651-855-0088
email: jallen@combinedspecialties.com

Daveyfire, Inc.
Alan Broca
2121 N California Blvd. Ste. 290
Walnut Creek, CA 94596, USA
Phone: 925-926-6414
FAX: 925-926-6439
email: info@daveyfire.com

Delcor Industries Inc.
Sam Bases
19 Standish Ave.
Yonkers, NY 10710, USA
Phone: 914-779-6425
FAX: 914-779-6463
email: delcor@hotmail.com
web: www.delcorind.com

European Pyrotechnic Arts Newsletter
Rob Driessen
Grenadiersweg 55
Riemst, B 3770, Belgium
Phone: 32-12-210-630
FAX: 32-12-210-630
email: epan@pandora.be
web: http://users.pandora.be/epan

Fawkes Fireworks
Tony Cardell and David Watts
89 Lingfield Road
Edenbridge, Kent TN8 5DY, UK
Phone: 44-1732-862-862
FAX: 44-1342-317-818
email: Tony@fawkes.co.uk

Fire One
Dan Barker
863 Benner Pike
State College, PA 16801, USA
Phone: 814-238-5334
FAX: 814-231-0799
email: info@fireone.com
web: www.fireone.com

Firefox Enterprises Inc.
Gary Purrington
11612 N. Nelson
Pocatello, ID 83202, USA
Phone: 208-237-1976
FAX: 208-237-1976
email: custserv@firefox-fx.com
web: www.firefox-fx.com

Firework Professionals
Anthony Lealand
PO Box 19-912
Christchurch, 8030, New Zealand
Phone: 64-3-982-3473
FAX: 64-3-982-3474
email: firework@firework.co.nz
web: www.firework.co.nz

Fireworks
PO Box 40
Bexhill, TN40 1GX, England
Phone: 44-1424-733-050
FAX: 44-1424-733-050
email: editor@fireworks-mag.org
web: www.fireworks-mag.org

Fireworks and Stage FX America
Kevin Brueckner
P.O. Box 488
Lakeside, CA 92040-0488, USA
Phone: 619-938-8277
FAX: 619-938-8273
email: info@fireworksamerica.com
web: www.fireworksamerica.com

Fireworks Business
Jack Drewes
HC 67 Box 30
Dingmans Ferry, PA 18328, USA
Phone: 717-828-8417
FAX: 717-828-8695
email: afn@fireworksnews.com
web: www.fireworksnews.com

Fullam's Fireworks, Inc.
Rick Fullam
P.O. Box 1808 CVSR
Moab, UT 84532, USA
Phone: 435-259-2666
email: RFullam_3@yahoo.com

Goex, Inc.
Mick Fahringer
PO Box 659
Doyline, LA 71023, USA
Phone: 318-382-9300
FAX: 318-382-9303
email: email@goexpowder.com
web: www.goexpowder.com

High Power Rocketry
Bruce Kelly
PO BOX 970009
Orem, UT 84097-0009, USA
Phone: 801-225-3250
FAX: 801-225-9307
email: 71161.2351@compuserve.com
web: www.tripoli.org

IPON srl
Pagano Benito
Via Trofa
Ottaviano, Napoli 80044, Italy
Phone: 39-81-827-0934
FAX: 39-81-827-0026
email: info@ipon.it
web: www.ipon.it

Island Fireworks Co. Inc.
Charles Gardas
N735 825th St.
Hager City, WI 54014, USA
Phone: 715-792-2283
FAX: 715-792-2640
email: islndfwk@pressenter.com
web: www.pyro-pages.com/island

Lantis Fireworks & Lasers
Ken Lantis
PO Box 491
Draper, UT 84020, USA
Phone: 801-768-2255
FAX: 801-768-2433
email: info@fireworks-lasers.com
web: www.fireworks-lasers.com

MagicFire, Inc.
Paul McKinley
PO Box 896
Natick, MA 01760-0896, USA
Phone: 508-647-9645
FAX: 508-647-9646
email: pyrotech@magicfire.com
web: www.magicfire.com

Marutamaya Ogatsu Fireworks Co., Ltd.
1-35-35 Oshitate Fuchu
Tokyo, 183-0012, Japan
Phone: 81-42-363-6251
FAX: 81-42-363-6252
email: hanabi@mof.co.jp
web: www.mof.co.jp

Mighty Mite Marketing
Charlie Weeth
122 S. 17th St.
LaCrosse, WI 54601-4208, USA
Phone: 608-784-3212
FAX: 608-782-2822
email: chzweeth@pyro-pages.com
web: www.pyro-pages.com

MP Associates Inc.
P.O. Box 546
Ione, CA 94640, USA
Phone: 209-274-4715
FAX: 209-274-4843

Precocious Pyrotechnics, Inc.
Garry Hanson
4420 278th Ave. N.W.
Belgrade, MN 56312, USA
Phone: 320-346-2201
FAX: 320-346-2403
email: ppinc@tds.net
web: www.pyro-pro.com

Pyro Shows, Inc.
Lansden Hill
P.O. Box 1406
LaFollette, TN 37766, USA
Phone: 800-662-1331
FAX: 423-562-9171
email: info@pyroshowsusa.com
web: www.pyroshowsusa.com

Pyrodigital Consultants
Ken Nixon
1074 Wranglers Trail
Pebble Beach, CA 93953, USA
Phone: 831-375-9489
FAX: 831-375-5225
email: pyrodig@aol.com
web: www.infinityvisions.com/pyrodigital

PyroLabs, Inc.
Ken Kosanke
1775 Blair Road
Whitewater, CO 81527, USA
Phone: 970-245-0692
FAX: 970-245-0692
email: ken@jpyro.com

Pyrotechnics Guild Int'l., Inc.
Frank Kuberry, Sec.-Treas.
304 W Main St
Titusville, PA 16354, USA
Phone: 1-814-827-6804
email: kuberry@earthlink.net
web: www.pgi.org

RES Specialty Pyrotechnics
Steve Coman
21595 286th St.
Belle Plaine, MN 56011, USA
Phone: 952-873-3113
FAX: 952-873-2859
email: respyro@earthlink.net
web: www.respyro.com

Rozzi Famous Fireworks
Arthur Rozzi
PO Box 5
Loveland, OH 45140, USA
Phone: 513-683-0620
FAX: 513-683-2043
email: art@rozzifireworks.com
web: rozzifireworks.com

Service Chemical, Inc.
Ben Cutler
2651 Penn Avenue
Hatfield, PA 19440, USA
Phone: 215-362-0411
FAX: 215-362-2578
email: ben@servicechemical.com
web: www.servicechemical.com

Skylighter, Inc.
Harry Gilliam
PO Box 480
Round Hill, VA 20142, USA
Phone: 540-338-3877
FAX: 540-338-0968
email: orders@skylighter.com
web: www.skylighter.com

Starburst Pyrotechnics & Fireworks Displays Ltd
Bonnie Pon
2nd Fl-Sui Hing Hong Bldg
17 Commissioner St
Johannesburg, Gauteng 2000,
South Africa
Phone: 27-11-838-7704
FAX: 27-11-836-6839
email: info@starburstpyro.co.za
web: www.starburstpyro.co.za

Western Pyrotechnics, Inc.
Rudy Schaffner
2796 Casey Road
Holtville, CA 92250, USA
Phone: 760-356-5426
FAX: 760-356-2051
email: rudys@holtville.net

Sponsorships

No advertising as such is printed in the *Journal of Pyrotechnics*. However, a limited number of sponsors have been sought so that the selling price of the Journal can be reduced from the listed cover price. The cost of helping sponsor an issue of the *Journal of Pyrotechnics* is $70 per issue for business and organizations [$35 for individuals]. In addition to a listing in the Sponsor section of the Journal, full sponsors receive two free copies of the sponsored Journal [one copy for individual sponsors] and a brief listing on a flyer inserted under the transparent cover of the Journal.

Additionally, if you so desire, we will provide a link from the Journal of Pyrotechnics Web Site to sponsors' web site, e-mail address or simply a company name, address and phone information listing. If you would like to be a sponsor contact the publisher.

Guide for Authors

Style Guide

The *Journal of Pyrotechnics* has adopted the *ACS Style Guide* [ISBN 0-8412-3462-0]. It is not necessary that authors have a copy; however, a copy can be ordered through a local bookstore.

Subject Areas

Fireworks, Pyrotechnic Special Effects, Propellants, Rocketry and Civilian Pyrotechnics

Manner of Submission

Submissions should be made directly to the publisher at the address at bottom of page. Upon receipt of an article, the author will be sent an acknowledgment and a tentative publication date. For specific requests regarding editors, etc. please include a note with that information. Preferably the text and graphics will be submitted electronically or on a 3-1/2" diskette or CD in IBM format with a print copy as backup. The Journal is currently using Microsoft Word 2002, which allows for the import of several text formats. Graphics can also be accepted in several formats. Please also inform us if any materials need to be returned to the author.

General Writing Style

- The first time a symbol is used, it is preferred to write it out in full to define it [e.g., heat of reaction (ΔH_r) or potassium nitrate (KNO_3)].
- Avoid slang, jargon, and contractions.
- Use the active voice whenever possible.
- The use of third person is required; first person is only acceptable where it is absolutely necessary to keep the meaning clear.

Format

In addition to the authors' names, please include an affiliation for each author and an address for at least the first author.

A short abstract is needed. (An abstract is a brief summary of the article, not a listing of areas to be addressed.)

Include 3 to 7 keywords to be used in a reference database: However, multi-word names and phrases constitute only one keyword (e.g., potassium nitrate and heat of reaction are each one word).

Use of SI units is preferred. If English units are used, please provide conversions to SI units.

Figures, Photos, and Tables are numbered consecutively. For submission, place them at the end of the text or as separate files. During page composition, they will be inserted into the text as appropriate. For graphs, please also submit "raw" X–Y data.

References cited in the text are referred to by number (i.e., "Smith[1] states"; or "the research[2,3] shows ..."). In the reference section, they will be ordered by usage and not alphabetically. It is preferred that a full citation, including author, title, book or journal, publisher for books, and volume and pages for journals, etc. be provided. Examples:

1) A. E. Smith, *Pyrotechnic Book of Chemistry*, XYZ Publishers (1993) [p nn–nn (optional)].
2) A. E. Smith, R. R. Jones, "An Important Pyrotechnic Article," *Pyrotechnic Periodical*, Vol. 22, No. 3 (1994) [p n–n, (optional)].

Editing

The *Journal of Pyrotechnics* is refereed. However, the editing style is friendly, and the author makes the final decision regarding what editing suggestions are accepted.

More Information

Contact Bonnie Kosanke, Publisher, the Journal of Pyrotechnics, Inc., 1775 Blair Road, Whitewater, CO 81527, USA.
or
email bonnie@jpyro.com